

**Triplet combination of palbociclib,
taselisib and fulvestrant and biomarkers
for CDK4/6 and PI3-kinase inhibition in
breast cancer**

Dr. Francisco Javier Pascual López

Molecular Oncology Team, Division of Breast Cancer Research

The Institute of Cancer Research

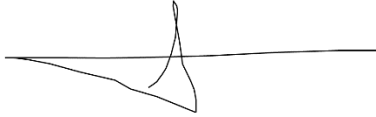
University of London

Submitted for the degree of Doctor of Medicine (Research) - MD(Res)

April 2021

Declaration of originality

I declare that the work presented in this thesis is my own and that any work that is not mine has been referenced. In addition, any data originating from collaborative work has been clearly acknowledged.

A handwritten signature in black ink, consisting of a horizontal line with a stylized, looped flourish above it.

Javier Pascual

Abstract

Targeting the commonly upregulated cell-cycle and PI3-kinase pathway in breast cancer are two of the most novel approaches to tackle the disease, with both strategies having led to clinically meaningful results and licensed drugs to use in the clinic. However, resistance to drugs inhibiting these pathways inevitably occurs and alternative strategies to delay this resistance and prolong survival are needed. CDK4/6 and PI3-kinase inhibitors synergise in *PIK3CA* mutant ER-positive and negative breast cancer pre-clinical models. A two-stage phase Ib trial was conducted to investigate safety and preliminary efficacy for the doublet CDK4/6 inhibitor palbociclib plus selective PI3-kinase inhibitor taselisib in solid tumours and the triplet palbociclib plus taselisib plus fulvestrant in patients with *PIK3CA* mutant ER positive HER2 negative advanced breast cancer. The escalation phase defined the recommended dose for phase 2 (RDP2) and subsequent patients were enrolled in the expansion phase and treated with the RDP2, which required a dose reduction in taselisib (from the 4mg to 2mg dose PO QD). There was evidence of AKT pathway modulation in pharmacodynamics studies conducted in platelet rich plasma, suggesting inhibition of PI3K by taselisib at this dose. However, increased AKT phosphorylation 24h post-dose suggested rebound of PI3K pathway activation. Most reported all-grade AEs across expansion cohorts were neutropenia (88%), thrombocytopenia (57%), anaemia (48%), fatigue (45%), leukopenia (36%) and diarrhoea (34%). Most common grade 3/4 AEs in expansion phase were neutropenia (53%) and leukopenia (19%). The study recruited 25 patients with ER positive HER2 negative *PIK3CA* mutant advanced breast cancer with an objective response rate of 37.5% (95% CI 18.8-59.4) and clinical benefit rate of 58.3% (95% CI 36.6-77.9). In addition, there was durable disease control for some *PIK3CA* mutant ER negative patients and other solid tumours with the doublet taselisib plus palbociclib, with particularly long-lasting stabilizations in TNBC with high expression of androgen receptor. In the biomarker analysis in *PIK3CA* mutant triplet arm, high baseline cyclin E1 expression levels were associated with short progression free survival (PFS) (HR 4.16, 95% CI 1.32-13.11, p=0.02), and early ctDNA dynamics were associated with PFS (high

on treatment ctDNA HR 5.23, 95% CI 1.41-19.42, $p=0.04$). High-depth error-corrected paired plasma ctDNA sequencing provided evidence of ongoing cancer genomic evolution through triplet therapy, with evidence of *ESR1* and *FAT1* mutation acquisition under therapy. In conclusion, the triplet of palbociclib, taselisib, and fulvestrant has promising efficacy in patients with heavily pretreated *PIK3CA*-mutant ER-positive HER2-negative advanced breast cancer. A subset of patients with *PIK3CA*-mutant triple-negative breast cancer derived clinical benefit from palbociclib and taselisib doublet, suggesting a potential nonchemotherapy targeted approach for this population. Our study further supports high expression of cyclin E1 as a poor prognostic marker on palbociclib combinations and reinforces the evidence of early ctDNA changes predicting treatment efficacy. These findings provide preliminary proof-of-concept that supports future combination approaches involving both PI3K and cyclin-dependent pathway.

Publications related to this thesis

J Pascual and NC Turner. Targeting the PI3-kinase pathway in triple negative breast cancer. *Annals of Oncology*. 2019.

J Pascual, Joline S. J. Lim, Iain R. Macpherson *et al.* Triplet therapy with palbociclib, taselesib and fulvestrant in PIK3CA mutant breast cancer and doublet palbociclib and taselesib in pathway mutant solid cancers. *Cancer Discovery*. 2020.

Abstracts to conferences related to this thesis

Javier Pascual, Iain R. MacPherson, Anne Caroline Armstrong, Sarah Emily Ward, Mona Parmar, Alison Joanne Turner, Hannah Bye, Paula Proszek, Andrew Dodson, Isaac Garcia-Murillas, Jenny King, Emma Hall, Laura Finneran, Juanita Suzanne Lopez, Alicia Frances Clare Okines, Alistair E. Ring, Nicholas C. Turner. PIPA: A phase Ib study of β -isoform sparing phosphatidylinositol 3-kinase (PI3K) inhibitor Taselesib (T) plus Palbociclib (P) and fulvestrant (FUL) in PIK3CA-mutant (mt) ER positive and Taselesib (T) plus Palbociclib (P) in PIK3CA-mutant (mt) ER negative advanced breast cancer. 2019 ASCO Annual Meeting.

Juanita Suzanne Lopez, Manuel SelviMiralles, Malaka Ameratunga, Anna Minchom, **Javier Pascual**, Udai Banerji, Hannah Bye, Florence I. Raynaud, Karen E Swales, Jason Malia, Michael Hubank, Isaac Garcia-Murillas, Mona Parmar, Sarah Emily Ward, Laura Finneran, Emma Hall, Alison Joanne Turner, Johann S. De Bono, Timothy A Yap, Nicholas C. Turner. PIPA: A phase Ib study of selective β -isoform sparing phosphatidylinositol 3-kinase (PI3K) inhibitor taselesib (T) plus palbociclib (P) in patients (pts) with advanced solid cancers—Safety, tolerability,

pharmacokinetic (PK), and pharmacodynamic (PD) analysis of the doublet combination. 2019 ASCO Annual Meeting.

Acknowledgements

Nick Turner – Group Leader in the Molecular Oncology Team at The Institute of Cancer Research and Consultant Medical Oncologist at The Royal Marsden Hospital, London.

Nick was the primary supervisor of this project and provided his guidance and expertise throughout the different phases of this work. He was chief investigator of the PIPA trial and designed the original outline of both the clinical and translational goals derived from it, alongside further strategic direction and review of both analyses and writing.

Maria Herrera Abreu- Senior Scientific Officer, Molecular Oncology Team, The Institute of Cancer Research.

Maite was the associate supervisor of this project, providing both guidance and support over the analysis phase. She also carried most of the pre-clinical work in cell lines testing CDK4/6 and PI3K inhibitor combinations, a contribution that ultimately led to the design of this clinical trial.

Ros Cutts – Senior Bioinformatician, Molecular Oncology Group, The Institute of Cancer Research.

Ros performed the copy number and variant calling for all the sequencing data together with the Centre for Molecular Pathology, including refinement of the UMI error-corrected sequencing-calling pipeline. She was also very helpful in designing the CNV graphs encapsulating the findings.

Isaac García Murillas- Staff Scientist, Molecular Oncology Team, The Institute of Cancer Research.

Isaac provided strategic guidance regarding both ctDNA ratio work and plasma ctDNA sequencing. He helped with the refinement of final sequencing analysis, designed some of the ddPCR assays used for

validation and provided with crucial education regarding the use of liquid biopsies.

Alex Pearson- Senior Scientific Officer, Molecular Oncology Team, The Institute of Cancer Research.

Alex provided overall scientific education on the biology of cancer, particularly regarding functional implication of different molecular pathways and experiment design methodology. He also helped with tissue imaging and scanning.

Sarah Hrebien- Higher Scientific Officer, Molecular Oncology Team, The Institute of Cancer Research.

Sarah provided overall scientific education on the biology of cancer, particularly regarding different sequencing technologies and how to apply them. She also helped and instructed with the library preparation of tissue DNA for whole-genome sequencing.

Molecular Oncology Team, The Institute of Cancer Research.

As a whole group, the Molecular Oncology Team provided excellent regular review of the different analysis carried on for this project, making valuable contributions that ultimately improved the overall quality of this work.

Further contributions.

Paula Proszek performed both baseline tissue whole-genome and targeted plasma ctDNA sequencing in the Centre for Molecular Pathology at the Institute of Cancer Research.

Karen Swales and Jason Malia performed the pharmacodynamics assessments as part of the Clinical Pharmacodynamic Biomarker Group at

the Institute of Cancer Research. They have also provided the figures representing PD analysis included in this thesis.

Ruth Ruddle and Florence Raynaud supervised the pharmacokinetic assessments which were analysed at Covance Bioanalytical Laboratories. They also generated all PK data and provided with the figures and tables representing PK included in this thesis.

The Institute of Cancer Research Clinical Studies Division and its Clinical Trials & Stats Unit wrote the statistical analysis report summarizing the clinical findings and provided with some of the tables included in this thesis. I helped supervising and reviewing the final version of it.

Margaret Hills performed immunohistochemistry staining and scoring in the Ralph Lauren Centre for Breast Cancer Research at The Royal Marsden Hospital.

Farzana Noor and the rest of the team in Core Facilities cut the FFPE blocks into slides and stained them with nuclear fast red (NFR) prior to nucleic acid extraction.

Heidi Gevensleben externally reviewed the H&E scans to provide optimal invasive area assessment for further nuclei acid extraction.

Funding.

This project represents independent research supported by the National Institute for Health Research (NIHR) Biomedical Research Centre at The Royal Marsden NHS Foundation Trust and the Institute of Cancer Research, London. Funding for the PIPA trial was also provided by Roche and Pfizer. The views expressed are those of the author(s) and not necessarily those of the NIHR or the Department of Health and Social Care. This work was also partially funded by the Spanish Society for Medical Oncology (SEOM) through a translational research grant that covered my salary during the first two years of this project.

Abbreviations

µl – Microlitre

AE – Adverse event

AI – Aromatase inhibitor

AR – Androgen receptor

AutoDG – Automated droplet generator

C1D1 – Cycle 1-Day 1

C2D1 – Cycle 2-Day1

CDK – Cyclin-dependent kinase

CDR28 – ctDNA ratio between C2D1 and C1D1 (28 days on average)

cfDNA – Cell-free DNA

ctDNA – Circulating tumour DNA

CNV – Copy number variation

CTCAE – Common terminology criteria for adverse events

ddPCR – Droplet digital PCR

DNA – Deoxyribonucleic acid

ECL – Electrochemiluminescence

EMA – European medicines agency

EOT – End of treatment

ER+ve – Oestrogen receptor positive

FAM – 6-carboxyfluorescein

FDA – Food and drug administration

FFPE - Formalin-fixed paraffin-embedded

FISH - Fluorescence in situ hybridization

HER2 - Human epidermal growth factor receptor 2

HEX – 5' hexachloro-fluorescein

HR+ve – Hormone receptor positive

IHC – Immunohistochemistry

LBD – Ligand-binding domain

MHRA – Medicines and healthcare products regulatory agency

MRD – Minimal residual disease

MTD – Maximum tolerated dose

mTOR – Mammalian target of rapamycin

NGS – Next generation sequencing

NTC – No template control

PCR – Polymerase chain reaction

qPCR – Quantitative PCR

PD – Pharmacodynamics

PI3K – Phosphatidylinositol 3-kinase

PK - Pharmacokinetics

pRB – Retinoblastoma protein

PRP – Platelet-rich plasma

RECIST – Response evaluation criteria in solid tumours

RP2D – Recommended phase 2 dose

SAE – Serious adverse event

SNP – Single nucleotide polymorphism

SUSAR – Suspected unexpected serious adverse reaction

TNBC – Triple negative breast cancer

UMI – Unique molecular identifier

VIC – VIC dye for probes

Table of contents

Abstract	3
Publications related to this thesis.....	5
Abstracts to conferences related to this thesis	5
Acknowledgements	7
Abbreviations	10
List of figures	15
List of tables.....	18
Chapter 1. Introduction	19
1.1 Cell cycle biology basics.....	19
1.2 CDK4/6 inhibitors in metastatic breast cancer.....	20
1.3 PI3K pathway.....	21
1.4 PI3K inhibitors in metastatic breast cancer.....	23
1.5 Synergy of CDK4/6 and PI3K inhibitors in pre-clinical models.....	25
1.6 Circulating tumour DNA	27
1.7 Current knowledge of biomarkers of sensitivity and resistance for CDK4/6 inhibition	29
1.8 Current knowledge on biomarkers of sensitivity and resistance for PI3K inhibition.....	30
1.9 Aims of the present study.....	32
Chapter 2. Patients and methods	33
2.1 PIPA clinical trial design and patients.....	33
2.2 Dose modifications	35
2.3 Safety analysis plan.....	36
2.4 Pharmacokinetic analysis	36
2.5 Pharmacodynamic analysis.....	38
2.6 Efficacy analysis.....	41
2.7 Translational cohort patients	42
2.8 Samples for translational biomarker research	43
2.9 FFPE biopsies processing	44
<i>Scanning FFPE biopsies slides with the Hamamatsu Nanozoomer and uploading onto PathXL.....</i>	44
<i>Cyclin D1, cyclin E1 and androgen receptor (AR) expression assessment</i>	45
<i>DNA and RNA extraction for genomic interrogation.....</i>	46
2.10 Blood processing.....	47
<i>Plasma DNA extraction using automated method.....</i>	47

<i>Buffy coat DNA extraction using columns method</i>	47
<i>Quantification of extracted DNA by droplet digital PCR (ddPCR)</i>	48
2.11 Whole-genome sequencing of baseline tissue	51
2.12 Targeted sequencing of paired plasma samples	51
2.13 <i>PIK3CA</i> mutations validation and ctDNA ratio	53
2.14 Statistics	54
Chapter 3. Clinical findings	55
3.1 Introduction	55
3.2 Patient demographics and characteristics	57
3.3 Pharmacokinetics	60
3.4 Pharmacodynamics	66
3.5 Safety and RDP2	68
3.6 Response analysis	73
3.7 Exploratory survival	76
3.8 Discussion	78
Chapter 4. Baseline prognostic and predictive biomarkers	81
4.1 Introduction	81
4.2 Samples analysed for baseline biomarker work	83
4.3 Baseline tissue whole-genome sequencing for CNV analysis	83
4.4 Baseline tissue IHC and FISH analysis	88
<i>Cyclin D1 expression assessment by immunohistochemistry</i>	88
<i>Cyclin D1 amplification assessment by immunofluorescence</i>	91
<i>Cyclin E1 expression assessment by immunohistochemistry</i>	92
<i>Androgen receptor expression assessment in TNBC by immunohistochemistry</i>	94
4.5 Discussion	98
Chapter 5. Longitudinal predictive biomarkers	100
5.1 Introduction	100
5.2 Early changes in <i>PIK3CA</i> mutations in ctDNA for predicting treatment benefit	101
5.3 Paired baseline and end-of-treatment plasma ctDNA analysis to study genomic evolution through treatment	107
5.4 Discussion	115
Chapter 6. Conclusions	117
References	123
Appendix 1. RMH200 panel design	132
Thanks to	135

List of figures

Figure 1. Simplified diagram of the cell-cycle.....	20
Figure 2. PIK3CA protein domains and somatic variants as per COSMIC catalogue.	22
Figure 3. Simplified diagram of the PI3K-pathway	23
Figure 4. Study overview and samples for translational research.	44
Figure 5. Consort diagram for clinical trial with final number of recruited patients.	59
Figure 6. Pharmacokinetic analysis in the escalation phase (part A).	63
Figure 7. Pharmacodynamic (PD) analysis in platelet-rich plasma (PRP) ...	66
Figure 8. Pharmacodynamic (PD) analysis of pSer780 Rb: total Rb ratio in tumour samples for all dose levels grouped.....	67
Figure 9. Pharmacodynamic (PD) analysis of pSer473-AKT: total AKT, pSer9-GSK3 β : total GSK3 β and pThr421/Ser424-P70S6K: total P70S6K in tumour samples for all dose levels grouped.....	68
Figure 10. Part A (escalation phase) final patient recruitment and dose-limiting toxicities observed in each dose level.....	69
Figure 11. Waterfall plot with best percentage of tumour change from baseline sum of the longest diameter in target lesions and best confirmed overall response for evaluable patients in part B1 (N=24).	74
Figure 12. Waterfall plot with percentage of tumour change and best overall response for evaluable ER-ve breast patients in part B2 (N=10) [89].	75
Figure 13. Waterfall plot with percentage of tumour change and best overall response for evaluable solid tumours patients in part B2 with follow-up to assess confirmed response (N=11)	76
Figure 14. PFS for patients in part B1 (treated with the triplet palbociclib, taselisib and fulvestrant).	77
Figure 15. PFS for ER-ve breast patients enrolled in part B2 (treated with the doublet palbociclib and taselisib).	77
Figure 16. PFS for solid tumour patients enrolled in part B2 (treated with the doublet palbociclib and taselisib).	78
Figure 17. Quality control for the ultra-low whole-genome sequencing experiment showing mean coverage and purity per sample sequenced.....	85
Figure 18. Ultra-low whole genome sequencing (ulWGS) for baseline CNV in the sequenced <i>PIK3CA</i> -mt ER+ve/HER2-ve breast patients treated with the triplet in part B1 (N=17), reported as thresholded adjusted copy number call (amplification/gain/neutral/heterozygous deletion/homozygous deletion)	86
Figure 19. Ultra-low whole genome sequencing (ulWGS) for baseline CNV in the sequenced <i>PIK3CA</i> -mt ER-ve breast patients treated with the doublet in part B2 (N=7), reported as thresholded adjusted copy number call (amplification/gain/neutral/heterozygous deletion/homozygous deletion). ...	87
Figure 20. Ultra-low whole genome sequencing (ulWGS) for baseline CNV in the sequenced PI3K hyperactivated solid tumour patients treated with the doublet in part B2 (N=8), reported as thresholded adjusted copy number call (amplification/gain/neutral/heterozygous deletion/homozygous deletion). ...	87

Figure 21. Ultra-low whole genome sequencing (ulWGS) for paired baseline/progression CNV in available patients treated with the doublet (N=2), reported as thresholded adjusted copy number call (amplification/gain/neutral/heterozygous deletion/homozygous deletion). ...	88
Figure 22. Examples of cyclin D1 IHC staining	89
Figure 23. Histogram of cyclin D1 IHC H-score frequency distribution	89
Figure 24. PFS for B1 cohort stratified above/below median cyclin D1 H-score (N=21).....	90
Figure 25. PFS for available ER-ve breast patients in part B2 stratified above/below median cyclin D1 H-score (N=8).	91
Figure 26. Examples of FISH amplification for cyclin D1 for the two patients considered amplified.	92
Figure 27. Contingency table representing predictive positive and negative values for copy number gain vs FISH amplification for <i>CCND1</i>	92
Figure 28. Examples of cyclin E1 IHC staining.	93
Figure 29. Histogram of cyclin E1 IHC % staining frequency distribution.	93
Figure 30. PFS for part B1 stratified by above/below median cyclin E percentage of invasive nuclei stained.	94
Figure 31. PFS for ER-ve breast in part B2 stratified by above/below median cyclin E percentage of invasive nuclei stained.	94
Figure 32. Examples of AR IHC staining.	95
Figure 33. Histogram of % staining (above) and AR IHC H-score (below) showing frequency distribution in 8 TNBC patients.	96
Figure 34. PFS for TNBC in part B2 stratified by above/below median AR H-score (N=7).	97
Figure 35. H-score for androgen receptor (AR) expression distribution in available baseline tumours of TNBC patients available (N=7).	97
Figure 36. Early <i>PIK3CA</i> mutation dynamics comparing C1D1 to C2D1 allele frequency for the whole population analysed passing predefined quality control for longitudinal analysis (N=30) and same analysis represented as change per patient.	102
Figure 37. Early <i>PIK3CA</i> mutation dynamics comparing C1D1 to C2D1 allele frequency for evaluable <i>PIK3CA</i> -mt ER+/HER2-ve breast cancer patients enrolled in part B1 (N=16) and same analysis represented as change per patient.	103
Figure 38. Kaplan-Meier curve representing progression-free survival (PFS) for patients in part B1 stratified above/below 0.1 CDR ₂₈ derived from allele frequency and same analysis for patients in part B1 stratified for incomplete/complete ctDNA suppression.	104
Figure 39. Early <i>PIK3CA</i> mutation dynamics comparing C1D1 to C2D1 mutant copies/ml for the whole population analysed passing predefined quality control for longitudinal analysis (N=30) and same analysis represented as change per patient.	105
Figure 40. Early <i>PIK3CA</i> mutation dynamics comparing C1D1 to C2D1 mutant copies/ml for evaluable <i>PIK3CA</i> -mt ER+/HER2-ve breast cancer	

patients enrolled in part B1 (N=16) and same analysis represented as change per patient.	106
Figure 41. Kaplan-Meier curve representing progression-free survival (PFS) for patients in part B1 stratified above/below 0.1 CDR ₂₈ using mutant copies/ml.....	106
Figure 42. <i>PIK3CA</i> mutations identified at baseline (N=23) with the RMH200 panel.	109
Figure 43. Double <i>PIK3CA</i> mutation allele frequencies dynamics for patients with at least 1 read in any both timepoints (N=4) represented in a log ₂ scale.	110
Figure 44. Kaplan-Meier curves for patients in part B1 stratified as double vs single <i>PIK3CA</i> -mutant (N=16).....	110
Figure 45. <i>ESR1</i> status at baseline (N=23) using RMH200 panel.	111
Figure 46. <i>ESR1</i> mutation allele frequencies dynamics with frequent acquisition and loss of <i>ESR1</i> mutations. Evidence of a second Y537S and Y537C acquisition, loss of T182P in a double mutant patient and loss of E380Q in a single mutant patient.	112
Figure 47. Kaplan-Meier curve representing progression-free survival (PFS) for patients in part B1 stratified as <i>ESR1</i> mutant/wild-type	112
Figure 48. Lollipop diagram for predicted truncating <i>FAT1</i> mutations.....	113
Figure 49. <i>FAT1</i> mutation allele frequencies dynamics represented in a log ₂ scale. PIPA20 had an acquisition.....	114

List of tables

Table 1. Dose reduction schedule for palbociclib and taselesib depending on starting dose.	35
Table 2. Triplex in-house design for quantification of plasma DNA.	49
Table 3. PCR reaction reagents for quantification using in-house triplex.	50
Table 4. Part A (escalation phase) dose levels with combination doses schedules and estimated number of patients to be treated per level.	58
Table 5. Demographic characteristics of enrolled patients and mutation distribution as per enrolment screening.	60
Table 6. PK parameters for taselesib and palbociclib in the escalation phase (part A).	62
Table 7. Pharmacokinetic (PK) analysis of taselesib and palbociclib concentrations in both triplet (with fulvestrant added) and doublet combination in the expansion phase (part B1 and B2). PK data from escalation phase also provided for comparison.	65
Table 8. All adverse events reported for >10% patients with grading.	70
Table 9. Serious adverse events (SAEs), serious adverse reactions (SARs) and suspected unexpected serious adverse reactions (SUSARs) in the different cohorts of the study.	71
Table 10. Treatment administration in the different cohorts of the study.	73
Table 11. Percentage on target, mean and median coverage for 23 patients undergoing paired cycle 1-day 1 (C1D1) - end of treatment (EOT) plasma sequencing.	108

Chapter 1. Introduction

1.1 Cell cycle biology basics

Uncontrolled cell cycling is one of the common hallmarks in cancer [1], leading ultimately to increased proliferation, growth and survival of tumour cells. Cyclins and cyclin dependent kinases (CDK) are a family of proteins that regulate cell cycle by promoting transition through different phases of the cycle. These phases consist in a quiescence phase (G0), first growth phase (G1), DNA synthesis phase (S) where DNA is replicated, second growth phase (G2), and lastly mitosis phase (M) where the original cell divides its replicated DNA and cytoplasm into two new daughter cells. A simplified diagram of the cell-cycle can be found in **figure 1**. The transition through G1 phase is regulated by the axis formed by cyclin D-CDK4/6, in what is called a restriction point [2-4]. The binding of cyclin D leads to CDK4/6 activation that phosphorylates the retinoblastoma protein (pRB). Phosphorylated pRB reduces binding and inhibition of the E2F family of transcription factors. The resulting activated E2F proteins upregulate cyclin E, which turns in additional phosphorylation of pRB, activation of S phase program and consequently commitment of the cell to complete mitosis. In oestrogen receptor positive (ER+ve) breast cancer, cyclin D is a common downstream effector of different driver pathways and thus overexpression of cyclin D leads to enhanced cyclin D-CDK4/6 axis and increased G1-S phase transition as a result.

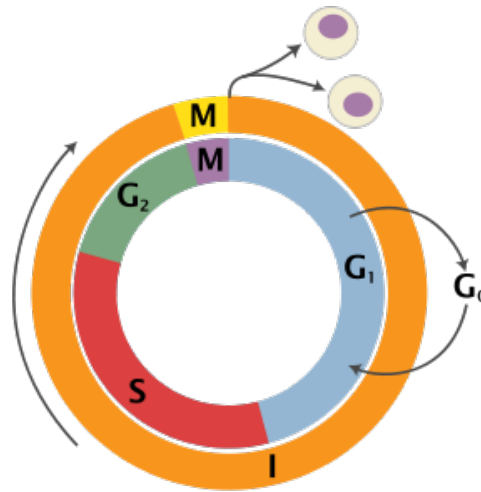


Figure 1. Simplified diagram of the cell-cycle. I= interphase, M=mitosis, G0= gap0/quiescent phase, G1= gap1, G2= gap2, S= synthesis. Image from: Cooper GM (2000). Chapter 14: The Eukaryotic Cell Cycle. The cell: a molecular approach (2nd ed.). Washington, D.C: ASM Press. ISBN 978-0-87893-106-4.

This rationale led to early attempts to target the cell cycle in solid tumours in a non-specific fashion using broad CDK inhibitors like flavopiridol and seliciclib [5-8], but this strategy was limited by side effects in the clinic, leading to more specific inhibitors that concentrate in targeting important specific events such as the G1 to S transition through CDKs inhibition [9].

1.2 CDK4/6 inhibitors in metastatic breast cancer

A deeper understanding of the cell cycle has provided the basis for the development and license of molecules capable of selectively inhibiting CDK4 and 6 by competitive binding to their ATP binding pocket, namely palbociclib, ribociclib and abemaciclib. CDK4/6 inhibitors ultimately tackle the increased cell-cycle transition of tumour cells, leading to cytostasis or cell cycle arrest. All three drugs are currently standard of care in combination with endocrine therapy (ET) for metastatic ER+ve breast cancer and widely share their toxic profile, although lower neutropenia and higher gastrointestinal adverse event rates have been noted for abemaciclib [10].

Palbociclib is a highly selective oral inhibitor of CDK4 and 6 at the nanomolar level, which only inhibits other CDKs (i.e., CDK1, CDK2 and CDK5) at

micromolar concentrations, thus providing a therapeutic window that has been successfully exploited. An anti-proliferative effect through G1 phase cell-cycle arrest was initially demonstrated *in vitro*, tumour xenografts and *ex vivo* analysis of human tumours [11, 12]. Large clinical trials showing survival benefit have been carried in ER+ve, human epidermal growth factor receptor 2 negative (HER2-ve) metastatic breast cancer for palbociclib in combination with ET, whether fulvestrant or letrozole [13, 14], demonstrating better survival outcomes with the combination and leading to regulatory agencies approval for its use in both untreated and previously treated patients. Nowadays, a combination of a CDK4/6 inhibitor (either palbociclib, ribociclib or abemaciclib) plus endocrine therapy is considered the preferred first-line treatment for most ER+ve HER2-ve advanced breast cancer patients.

1.3 PI3K pathway

The phosphoinositide-3 kinase (PI3K) pathway is a canonical intracellular signalling mechanism commonly dysregulated in cancer which upregulation ultimately leads to enhanced cancer cell growth and survival. The phosphoinositide-3 kinases (PI3Ks) are enzymes that phosphorylate the free 3- hydroxyl of the phosphoinositide in the cell membrane, resulting in downstream activation of other pathway nodes like AKT (protein kinase B) and mTOR (mammalian target of rapamycin). The different PI3Ks are commonly grouped in different classes, with class I PI3K being the most commonly altered in cancer, formed of a heterodimer composed by a regulatory (p85) and a catalytic (p110) subunit. There are multiple paralogs of the regulatory subunits (p85 α and p85 β) and the catalytic subunits (p110 α , β , γ and δ) [15]. The vast majority of activating mutations leading to hyperactivation of the pathway occur in the p110 α (alpha subunit) encoded by the gene *PIK3CA*, occurring in around 40% of ER+ve breast cancer [16]. *PIK3CA* gene is located in chromosome 3 and the vast majority of those mutations appear in hotspot regions located in the helicase domain encoded by exon 9 (E542K and E545K) and in the catalytic domain encoded by exon

20 (H1047L and H1047R). A complete record of somatic variants appearing in the COSMIC catalogue can be found in **figure 2**.

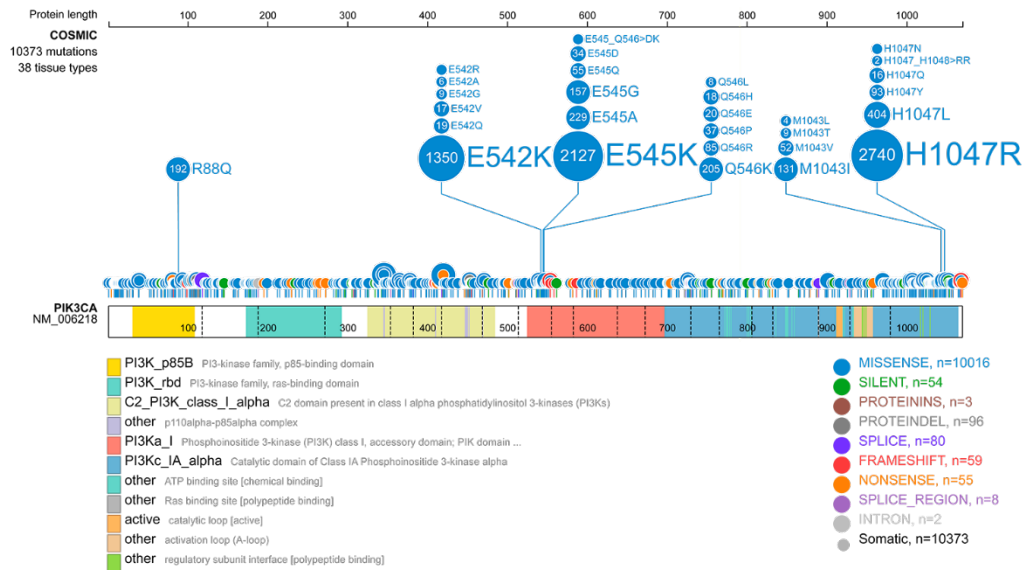


Figure 2. PIK3CA protein domains and somatic variants as per COSMIC catalogue [17].

The model is negatively regulated by PTEN (phosphatase and tensin homolog) protein, which serves as a tumour suppressor through its phosphatase action dephosphorylating phosphatidylinositol (3,4,5)-trisphosphate (PIP3) resulting in an inhibition of AKT and hence the rest of the signalling cascade. PTEN loss of function has been associated with increased PI3K activity and sensitivity to PI3K inhibitors [18]. Inositol polyphosphate 4-phosphatase type II (INPP4B) is a second phosphatase in the PI3 kinase pathway, acting sequentially after dephosphorylation of phosphatidylinositol (3,4,5) triphosphate (PIP3) into phosphatidylinositol (3,4)-bisphosphate (PIP2) by the SH2-domain containing inositol phosphatases 1 and 2 (SHIP1 and 2). INPP4B then dephosphorylates phosphatidylinositol (3,4)-bisphosphate (PIP2) generating precursors phosphatidylinositol (3)-phosphate (PI3P) and phosphatidylinositol (4)-phosphate (PI4P). Additionally, in situations of PTEN deficiency INPP4B also may be involved in direct PIP3 dephosphorylation [19]. INPP4B loss of function has been mainly described in triple negative

breast cancer (TNBC), where it can be found in up to 80% of cases [20, 21], being a main feature in the basal-like intrinsic subgroup [22]. Recently, *in vivo* work has demonstrated that INPP4B knockdown results in increased PI3K and ERK activation and increased sensitivity to PI3K and MEK inhibitors in TNBC [23]. Interestingly, in ER+ve breast cancer INPP4B can function not as a tumor-suppressor, but as an oncogene through activation of the serum and glucocorticoid-regulated kinase 3 (SGK3) [24, 25]. A simplified diagram of the PI3K pathway can be found in **figure 3**.

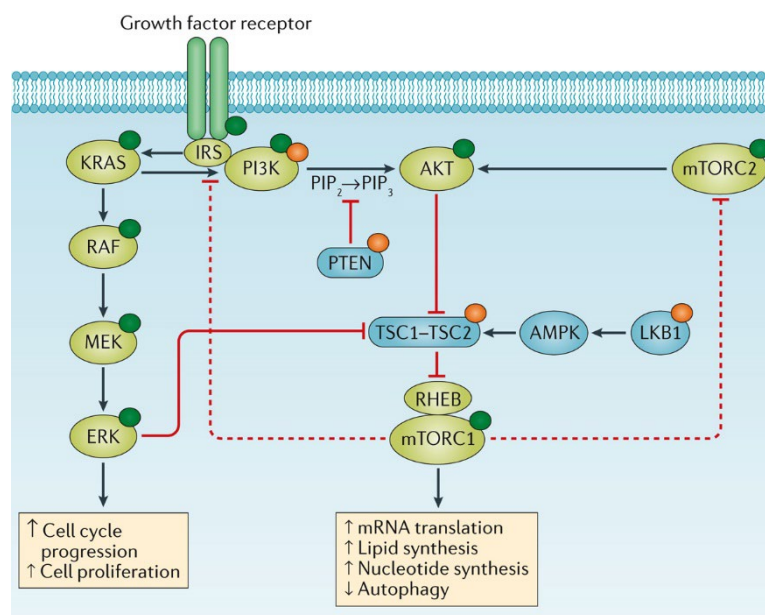


Figure 3. Simplified diagram of the PI3K-pathway [26].

1.4 PI3K inhibitors in metastatic breast cancer

Clinical development of PI3K/AKT/mTOR-pathway inhibitors for breast cancer has evolved since the mTOR inhibitor everolimus was first approved in combination with exemestane [27] for pre-treated metastatic ER+/HER2-ve breast cancer. Later, the PI3K pan-inhibitor buparlisib was tested in advanced breast cancer patients demonstrating a modest survival improvement at the expense of substantial increase in toxicity, mainly liver function disorders and also an increase in mood disorders like depression

and anxiety [28]. This led to the design of more selective PI3K inhibitors in order to minimize toxicity whilst improving efficacy.

Taselisib is an oral β -sparing PI3K inhibitor that exhibits potent inhibition of p110 α , γ and δ forms but has a 30-fold lesser inhibition of the p110 β form and therefore was predicted to have improved efficacy in *PIK3CA*-mutant tumours (predicted to have a hyperactive p110 α subunit leading to enhanced activity) with a more favourable toxicity profile by reducing toxicity coming from p110 β inhibition. Taselisib was first found active in *PIK3CA*-mutant solid tumours including breast cancer patients with doses ranging from 3-16mg daily, with frequent dose-dependent toxicities like diarrhoea, fatigue, decreased appetite, hyperglycaemia, nausea and stomatitis [29]. In the phase 2 trial of taselisib in combination with fulvestrant for previously treated HR+ve/HER2-ve breast cancer patients, taselisib was given at the 6mg daily dose and the combination was found to be active particularly in the *PIK3CA*-mutant population (confirmed response rate 38,5%, clinical benefit rate 38.5%) without new safety issues [30]. Unfortunately, the primary analysis of the subsequent confirmatory phase III trial (SANDPIPER) for taselisib + fulvestrant combination versus placebo + fulvestrant was able to show only a modest 2-month improvement in PFS (7.4 vs 5.4 months respectively) albeit still with significant toxicity increase leading to higher rates of discontinuations and dose reductions in the taselisib arm [31]. There was also an overall increase in objective responses and clinical benefit rate in patients with measurable disease. Of note, the study was designed with a further reduction in the dose of taselisib compared with the preceding phase 2, with taselisib given at 4mg daily dose. Following these findings, the combination of taselisib plus fulvestrant is no longer under clinical investigation given its safety profile and modest clinical benefit.

Other drugs have been safely combined with taselisib. Recently, a phase Ib trial has shown preliminary activity of taselisib combined with tamoxifen in pre-treated ER+ve metastatic breast cancer patients [32], with an ORR of 24%. Adverse event profile was consistent with expected class-toxicity like diarrhoea, mucositis and hyperglycaemia. Also, its use in combination with letrozole has been explored in early breast cancer for the neoadjuvant

setting in the randomized phase II trial LORELEI [33]. In this study, there was higher objective response rates in patients receiving taselisib in combination with endocrine therapy vs placebo, both in all randomized patients and in particular in *PIK3CA*-mt, consistent with the benefit observed for taselisib in the metastatic setting.

The most selective and clinically licensed PI3K inhibitor is alpelisib. With a parallel clinical development, the alpha selective PI3K inhibitor alpelisib in combination with fulvestrant for *PIK3CA*-mutant HR+ve/HER2-ve cancers has become a standard of care after favourable results in the confirmatory phase III SOLAR-1 trial [34]. PFS was 11 vs 5.7 months in the alpelisib in combination with fulvestrant vs placebo group, also with higher overall response rates. Alpelisib is now under research to better determine its most suitable indication in the range of available effective drugs for metastatic ER+ve breast cancer, with some trials being conducted after prior exposure to CDK4/6 inhibitors and suggesting meaningful efficacy in this context [35].

1.5 Synergy of CDK4/6 and PI3K inhibitors in pre-clinical models

After confirmation of clinical activity for both CDK4/6 and PI3K inhibitors, a growing interest in potential combinations between both approaches followed. CDK4/6 inhibition was found to sensitize breast cancer cells to PI3K inhibition [36], and PI3K inhibition increases ER-dependence through increased transcriptional activity in ER+ve breast cancer cell models [37]. Additional work carried on in MCF7 and T47D breast cancer cell models and patient-derived tumour xenograft models (PDX), showed that the doublet combination of a CDK4/6 and a PI3K inhibitor prevents early resistance to CDK4/6 inhibitors, and triggered cell apoptosis in addition to the classical cytostatic effect often seen with CDK4/6 alone [38]. This synergy was particularly effective in ER+ve cells harbouring mutations in the PI3K pathway. In addition, it was shown that the triplet combination of palbociclib, pictilisib (a pan-PI3K inhibitor) and fulvestrant ablates growth in clonogenic assays to a greater extent than doublet combinations, with decreased expression levels of phospho-Rb, cyclin D1, cyclin E2, active CDK2, and

increase on PARP cleavage as a marker of cell apoptosis. These findings offered a potential new strategy for ER+ve breast cancer treatment to test and prompted the rationale for the main hypothesis of this project, which is the expected synergy of palbociclib and a PI3K inhibitor in particular for *PIK3CA*-mt ER+ve/HER2-ve breast cancer.

Moreover, *in vitro* experiments showed that PI3K inhibition decreases post-mitotic CDK2 activity in *PIK3CA*-mutant triple-negative breast cancer (TNBC) leading to potential sensitization to CDK4/6 inhibitors [39]. These findings suggest a rationale for testing the doublet combination of a CDK4/6 and a PI3K inhibitor in TNBC, a subset of breast cancer characterized by poor outcome and limited treatment options currently available. Lehmann *et al.*, using gene expression classifiers, identified distinctive intrinsic TNBC subtypes that has enabled better understanding of the wide variety of biological subtypes within TNBC. These are composed of a basal-like 1 and 2 subtypes (BL1 and BL2), mesenchymal subtype (M), a mesenchymal stem-like (MSL) subtype that has overlap with claudin-low subtypes, a TNBC luminal androgen receptor (LAR) subtype which resembles genomically ER+ve (luminal) breast cancer, and a further immunomodulatory (IM) subtype that reflects tumours with high lymphocytic infiltration [40]. The LAR subtype has already been shown to be sensitive to different endocrine-deprivation therapy. A phase II clinical trial exploring enzalutamide (an AR inhibitor) in this population showed clinical activity [41], so did the parallel phase II trial for abiraterone acetate (CYP17 inhibitor) plus prednisone [42].

Palbociclib has shown activity both *in vitro* and *in vivo* experiments also conducted in this population [39], and thus TNBC LAR breast cancer patients (or AR-expressing as a surrogate) may have increased sensitivity to a combination of CDK4/6 and PI3K inhibitors, providing rationale for also exploring this combination in *PIK3CA*-mt ER-ve breast cancer patients. Of note, other combination strategies involving palbociclib combinations in AR positive TNBC also warrant further clinical research, as illustrated by the *in vitro* activity shown for the combination of palbociclib and enzalutamide [43].

There is also additional evidence in other solid tumour types for combined CDK4/6 and PI3K inhibition [44, 45], also providing rationale for clinical testing the combination in well-designed clinical trials for solid tumours with pathway activation.

1.6 Circulating tumour DNA

Circulating tumour DNA (ctDNA) is the fraction of DNA fragments shed into physiological fluids (e.g., circulation) by tumour cells and can be found within the plasma cell-free DNA (cfDNA) fraction of the blood. cfDNA is found highly fragmented in the circulation as a result of enzymatic processing of DNA fragments associated with nucleosomes, with an average size around 166 base pairs (bp), representing 146bp of a nucleosome plus 2x10 bp from H1 linkers, characteristic of apoptotic cell death [46], although high-molecular-weight DNA fragments larger than 10,000bp coming from necrosis can also be found. However, cfDNA is composed largely by non-tumour-derived DNA resulting from tissue cell turnover, cell injury, and hematopoietic cells, being the latter the main source of cfDNA [47]. The proportion of ctDNA in the whole cfDNA is often referred as tumour purity. Improvements in DNA sequencing technology has led to refined resolution of cfDNA fragments and demonstrated that selecting fragments 90-150bp in cancer patient circulation improves detection of ctDNA [48], allowing for more effective sequencing.

ctDNA has been found to often contain tumour-specific somatic mutations and additionally it has a quick turnover in circulation with a short half-life ranging from minutes to few hours [49], making its interrogation an excellent candidate tool for the assessment of tumour dynamics [50]. This is often referred to as a “liquid biopsy” and represents an alternative to classic tumour biopsies, as it can avoid invasive procedures, partially avoids inevitable heterogeneity, and allows prospective serial sampling during treatment [51-53].

ctDNA can be detected with a number of different methodologies ranging from whole-genome sequencing to digital polymerase chain reaction (dPCR),

the former being capable of interrogating the entire genome for previously unknown aberrations, and the latter being highly sensitive and capable of detecting allele fractions down to 0.01%, although at a narrower level requiring prior knowledge of mutations to be identified. ctDNA can be therefore used for tumour genomic profiling and tailoring of targeted therapies, as it has already been demonstrated in the plasmaMATCH trial [54]. ctDNA has also been used for the detection of minimal residual disease (MRD) after breast cancer surgery that can anticipate clinic relapse by months [53, 55]. Moreover, early dynamics measured as a ratio between both mutant copies/ml and allele frequency from different early timepoints during therapy has been found to predict efficacy in patients treated both with palbociclib [56] and the AKT inhibitor capivasertib [57]. This represents a novel early on-treatment, non-invasive tool for assessing response to targeted therapies, with the potential to be introduced in future clinical trial design [58].

An important limitation for plasma ctDNA analysis is differentiating the germline DNA fraction coming from white-blood cells from the actual ctDNA coming from tumour cells. Germline DNA can display mutations that do not represent true tumour biology and thus potential for targeting. This can be partially addressed in the pre-analytical phase by using preservative tubes for the collection of blood samples that minimize degradation of cfDNA by DNAses and stabilize white blood cells preventing lysis [59], and during the analysis by sequencing paired tumour-normal (plasma-buffy coat in the case of blood samples) to detract variants found in the normal sample from the final analysis. Also, hematopoietic cells are the source of clonal hematopoiesis, somatic mutations developing with age that can lead to clonal expansion in the absence of dysplasia, which act as a confounding factor when analyzing true tumour-driver somatic mutations [60].

1.7 Current knowledge of biomarkers of sensitivity and resistance for CDK4/6 inhibition

Although the inclusion of CDK4/6 inhibitors into the breast cancer treatment armamentarium has been a major step forward, our knowledge of which patients may derive greater benefit from these drugs or may on the other hand be intrinsically resistant or develop early resistance is very limited. Cyclin D1 overexpression has long been proposed as a possible biomarker of sensitivity to CDK4/6 inhibition as it binds to CDK4 and 6 to promote RB phosphorylation, which releases E2F, and leads to cyclin E-CDK2 activation and commitment to S-phase entry. Prior work found discordant evidence on its implication in breast cancer prognosis with both favourable OS and shorter DFS reported [61, 62]. Previous work suggests that early resistance to CDK4/6 inhibitors may be achieved by accumulation of cyclin D1 that elicit entry into S-phase through CDK2 activation. Cyclin D1 was found to be downregulated by the addition of a PI3K inhibitor [38].

The same study found cyclin E1 amplification as a potential acquired resistance-mechanism in breast cancer cells treated with palbociclib for a long period [38]. Recently, tumour tissue analysis in patients enrolled in the PALOMA-3 trial, the confirmatory phase 3 clinical trial comparing the combination of palbociclib plus fulvestrant versus placebo plus fulvestrant in pre-treated patients with metastatic ER+ve/HER2-ve breast cancer, demonstrated high levels of cyclin E mRNA measured via EdgeSeq Oncology BM Panel (HTG Molecular Diagnostics) confer lower efficacy on palbociclib [63], supporting previous pre-clinical findings.

Loss of RB1 tumour-suppression function has long been proposed as a plausible acquired mechanism of resistance arising under CDK4/6, which allows overpassing CDK4/6 dependence to activate the family of transcription factors E2F [64-67]. Recent work using paired plasma ctDNA sequencing demonstrated emerging of *RB1* mutations in patients treated with a combination of palbociclib and fulvestrant, although at a very low rate suggesting this mechanism of resistance is rather uncommon [68].

Loss of FAT1 tumour-suppressor function and increased CDK6 expression via Hippo pathway have also been recently found to confer resistance to CDK4/6 inhibitors [69], with a study of 348 patients with ER+ve/HER2-ve breast cancer previously treated with CDK4/6 inhibitors sequenced at the Memorial Sloan-Kettering Cancer Center showing that those with *FAT1* truncating mutations had significantly lower PFS compared to non-mutants (2.4 vs 10.1m, respectively). However, there is still a need to further confirm and validate these observations clinically.

Mutations arising in the ligand-binding domain of *ESR1*, the gene encoding for the oestrogen receptor have been found to confer resistance to AI in breast cancer [70, 71]. These mutations can be detected in plasma and could be potentially targeted by the ER degrader fulvestrant [72]. Paired ctDNA sequencing in PALOMA-3 patients has shown that new *ESR1* mutations can be acquired through treatment, particularly *ESR1* Y537S, although this seems to be independent of CDK4/6 treatment and rather a result of long-term fulvestrant exposure [68]. These mutations tend to be polyclonal and are often found subclonally in the cancer.

As described previously, high levels of androgen receptor (AR) had long been proposed as a plausible biomarker of sensitivity to androgen deprivation for TNBC LAR subtype, as illustrated by the clinical efficacy found for both enzalutamide [41] and abiraterone [42]. Similarly, AR expression could also be used as a biomarker of sensitivity to palbociclib combinations.

1.8 Current knowledge on biomarkers of sensitivity and resistance for PI3K inhibition

The vast majority of PI3K activating mutations occur in the p110 α (alpha subunit encoded by *PIK3CA*) [73, 74] overall mutated in up to 40% of ER+ breast cancer [75, 76] representing the single most common event in breast cancer. In addition, it is mutated in 9% of primary TNBC, being the second most frequent mutated gene after *TP53* [75, 77]. The majority of the

mutations occurring in this gene are located in four specific hotspots on exon 9 (E545K and E542K, helical domain) and 20 (H1047R and H1047L, kinase domain).

Preclinical work showed that the presence of an activating mutation in *PIK3CA* in cancer cells conferred improved sensitivity to both α -selective and β -sparing PI3K inhibitors, and clinical trials have already confirmed this finding [78, 79].

Deletions in the C2 domain of the *PIK3CA* gene have also been found to be a biomarker of enhanced dependence on the pathway and therefore possible markers of sensitivity to PI3K inhibition [80].

PTEN is a tumour suppressor gene that has been long demonstrated to negatively regulate the PI3K pathway [81] and its loss of function increases the cell dependence on p110 β isoform rather than p110 α [82], therefore it has been suggested as a potential mechanism of resistance to α -selective PI3K inhibitors. This has been further confirmed in breast cancer patients with an interesting study where the authors performed a genetic profiling on an index patient harbouring a *PIK3CA* mutation treated with an α -selective PI3K inhibitor [18]. Metastatic lesions upon progression on this drug clearly revealed loss of a *PTEN* copy with additional *PTEN* genomic alterations leading to *PTEN* loss of expression and suggesting this as a mechanism of resistance to α -selective PI3K inhibition. Strikingly, functional work carried on *PTEN*-null cell lines found that p110 β blockade reverted this resistance phenotype, suggesting a potential strategy to revert this resistance.

The AKT family of three different isoforms (AKT1, AKT2 and AKT3) forms a node downstream of PI3K [83]. *AKT1* mutations are found in multiple tumour types including breast cancer, with around 2.5% breast cancer having a mutation resulting in a single amino acid substitution E17K first described by Carpten et al [84], showing that *AKT1* E17K mutations increase AKT1 binding to the PIP3 ligand, accelerating transfer of AKT from cytoplasm to cell membrane, where further phosphorylation enhances the PI3K signalling pathway. Mutations arising in *AKT1* could represent a potential biomarker for selecting PI3K/AKT inhibition therapies.

mTOR is a serine-threonine kinase that can form two complexes mTORC1 and mTORC2, defined by binding to RAPTOR and RICTOR, respectively, which are activated both downstream of AKT (mTORC1) and phosphorylate AKT (mTORC2). Mutations in *MTOR* gene are rare and only found in 1.8% cases in TCGA primary breast cancer, with only a small minority recognised as putative drivers. Although infrequent, these mutations might represent a resistance mechanism, as it would overpass any possible inhibition of PI3K by downstream hyperactivation.

Moreover, there is intense crosstalk between the PI3K and the RAS/RAF/MAPK pathway, with RAS activation being a predictor of resistance to PI3K inhibitor [85].

1.9 Aims of the present study

The present study goal was to assess safety for the combination of the CDK4/6 inhibitor palbociclib and the β -sparing PI3K inhibitor taselisib with or without addition of endocrine therapy (fulvestrant as the main companion to explore in a triplet combination or letrozole as part of a small cohort to explore an alternative endocrine therapy potentially showing differences in the toxicity profile) and expand on exploratory efficacy in different cohorts mainly focusing in *PIK3CA*-mutant ER+ve HER2-ve advanced breast cancer patients treated with the triplet of palbociclib, taselisib and fulvestrant. Also, to enrich understanding of the metabolism and efficacy of the combination schedule, the study includes pharmacokinetic (PK) and pharmacodynamic (PD) assessments carried on as part of the initial clinical trial design. Biological samples provided by the patients enrolled in the trial are further used to build on translational research by providing knowledge of potential baseline and longitudinal biomarkers of sensitivity and resistance to the combination tested in both tissue and plasma ctDNA.

Chapter 2. Patients and methods

2.1 PIPA clinical trial design and patients

A total of 78 patients were enrolled in the PIPA trial (NCT02389842), an open-label non-randomized multi-centre phase Ib clinical trial sponsored by the Royal Marsden NHS Foundation Trust & The Institute of Cancer Research (London, UK) assessing safety of palbociclib and taselisib combination with or without fulvestrant or letrozole. The study was conducted across different breast units in the UK: The Royal Marsden Hospital NHS Foundation Trust (both at Chelsea and London sites), The Christie NHS Foundation Trust (Manchester) and The Beatson Cancer Centre (Glasgow).

Primary objectives were to propose a recommended phase 2 dose (RP2D) by establishing the maximum tolerated doses (MTD) for palbociclib with taselisib, to assess toxicity profile for the combination with or without fulvestrant or letrozole and to obtain preliminary efficacy of the triplet palbociclib, taselisib and fulvestrant in the cohort of *PIK3CA*-mutant ER+ve HER2-ve advanced breast cancer patients. Secondary objectives were to determine pharmacokinetics (PK) of the investigational drugs in different combination regimes. Tertiary objectives included exploratory efficacy in other cohorts of patients (palbociclib and taselisib in advanced solid tumours, palbociclib and taselisib in ER-ve breast cancer with a representation of both HER2+ve and TNBC, and palbociclib, taselisib and letrozole combination in ER+ve HER2-ve breast cancer patients), pharmacodynamics (PD) characterization in tumour biopsies and platelet-rich plasma and exploring mechanisms of sensitivity and resistance by sequencing of tumour tissue and circulating tumour DNA (ctDNA) samples.

Twenty patients with pre-treated advanced solid tumours enriched with PI3-kinase activating mutations were included in part A (escalation phase) and treated at different dose levels following a 3+3 dose escalation design.

Following patients were included in part B (expansion phase) allocated in different cohorts. Part B1 enrolled patients with *PIK3CA*-mutant, ER+ve

HER2-ve advanced breast cancer that had received at least one prior line of endocrine therapy and originally allowing up to two lines of chemotherapy (the protocol was amended to allow any number of prior chemotherapy). They were treated with the RP2D for the doublet combination established in part A (escalation) plus fulvestrant at the standard dose of two intramuscular injections of 250mg every cycle of 28 days plus additional dose given in the first cycle 14 days after the first dose. Part B2 enrolled patients with *PIK3CA*-mutant, ER-ve (whether HER2+ve or-ve) advanced breast cancer or any advanced solid tumour with mutations leading to a hyperactivated PI3K-AKT pathway or other relevant genetic aberrations (ER+ve breast cancer patients could also be included in this solid tumours subcohort) and treated with the RP2D for the doublet of palbocicib and taselisib only. ER-ve HER2+ve breast cancer patients had a minimum of 2 prior anti-HER2 therapy (or one prior therapy where no further HER2 directed therapy was available locally) and triple negative breast cancer and solid tumour patients a minimum of 1 prior chemotherapy. Part B3 was a small cohort which enrolled ER+ve HER2-ve advanced breast cancer patients without regard for *PIK3CA* status, with a minimum of one prior line of endocrine therapy and up to two lines of chemotherapy. These patients were treated with the RP2D for the doublet plus letrozole at the standard dose of 2.5mg daily, with a view to explore potential differences in the adverse event profile that could be determined by using a different endocrine therapy as part of a triplet combination.

Women enrolled into parts B1 and B3 had to be post-menopausal or pre-/peri-menopausal if they had ovarian suppression with the LHRH agonist goserelin. Prior exposure to fulvestrant and/or everolimus was allowed, but prior treatment with a CDK4/6 inhibitor was not. *PIK3CA* mutations must have been documented by an accredited laboratory in archival tumour samples, fresh tumour samples or ctDNA extracted from plasma or serum. Patients in parts A, B2 and B3 had to have measurable disease as assessed by RECIST 1.1 or evaluable disease and for patients in part B1 measurable disease was mandatory.

2.2 Dose modifications

In the event of a significant toxicity that was considered drug-related to either palbociclib or taselesib the dosing could be interrupted within a cycle or there could be a delay in the start of the next cycle of treatment. A significant toxicity was defined as grade ≥ 3 toxicity or grade 2 toxicity lasting >3 weeks despite appropriate supportive treatment, with the exception of uncomplicated grade 3 neutropenia for taselesib interruptions. If toxicity persisted despite these measurements, then dose reductions for either palbociclib or taselesib were permitted depending on their respective starting dose (dose levels further discussed in section 3.2) and following a pre-specified schedule.

For palbociclib and taselesib, dose reductions that were permitted are described in **table 1** below:

Palbociclib starting dose	Reduced dose
125mg/d (21/7)	100mg/d (21/7)
100mg/d (21/7)	75mg/d (21/7)
75mg/d (21/7)	75mg/d (14/14)* *Palbociclib dose de-escalation below 75 mg/d was not allowed, but the schedule was allowed to be changed to 75mg/day 14-days-on and 14-days-off (14/14d).
Taselesib starting dose	Reduced dose
4mg/d (21/7)	2mg/d (21/7)
2mg/d (28/28)	2mg/d (21/7)
2mg/d (21/7)	2mg/d every other day (21/7)

Table 1. Dose reduction schedule for palbociclib and taselesib depending on starting dose.

Dose reductions for fulvestrant in part B1 or letrozole in part B3 were not allowed.

2.3 Safety analysis plan

Adverse events (AEs) and serious adverse events (SAEs) were collected for all enrolled patients and monitored according to CTCAE v4.0 definitions commencing from the time patient gave written consent to participate up to 28 days after the last administration of any of the drugs in the trial. AEs considered of special interest were drug-induced liver injury and pneumonitis of any grade. Event causality for any AE was determined as highly probable, probable, possible, unlikely, and not related with the investigational medicinal product. Follow-up of AEs with a drug-related causality of possible, probable, or highly probable continued until the events resolve, stabilised or the patient started another anti-cancer therapy.

2.4 Pharmacokinetic analysis

PK analyses were performed in part A, B1 and B2. For PK samples in part A, two whole blood samples of 4ml and 6ml (i.e., 10ml in total) were collected. Collection of blood sample for PK analysis in part A was on Cycle 1 Day 1 (pre-dose and post dose at 2 and 4 hours), Cycle 1 Day 8 (pre-dose), Cycle 1 Day 15 (pre-dose and post dose at 2, 4, 6, 8 and 24 hours) and Cycle 2 Day 15 (pre-dose and post dose at 2 hours). For Part B1 three blood samples of 4 mL, 6 mL and 6 mL (i.e., 16 mL in total) were collected and for part B2 two blood samples of 4 mL and 6 mL (i.e. 10 mL in total). These were taken on Cycle 1 Day 15 (pre-dose and post dose 4 hours) and Cycle 2 Day 15 (pre-dose and post dose 4 hours). No PK analysis was required for part B3.

Whole blood samples were collected in 4mL BD (lavender top) Vacutainer® tubes containing K2EDTA as anti-coagulant for the analysis of Palbociclib and in 6mL BD (lavender top) Vacutainer® tubes containing K2EDTA as anti-coagulant for the analysis of taselisib and for the analysis of fulvestrant in part B1.

Blood samples had to be immediately placed into an ice bath so that they were kept at 2 - 8°C during harvesting. Within 30 minutes of blood collection samples were centrifuged at 2000 x g for 15 minutes preferentially in a refrigerated centrifuge present at approximately 2 - 8°C.

For the taselesib PK samples, from the 6mL blood collection tubes roughly equal volumes of plasma supernatant were transferred into 1.8 mL NUNC™ polypropylene storage tubes labelled “Taselesib PK Plasma Aliquot 1” (primary) and “Taselesib PK Plasma Aliquot 2” (back-up). For the palbociclib PK samples, from the 4 mL blood collection tubes the supernatant was transferred into a 4 mL polypropylene cryovial labelled “Palbociclib PK Plasma Aliquot 3”. For the fulvestrant PK samples in Part B1, from the 6mL blood collection tubes roughly equal volumes of plasma supernatant were transferred into 1.8 mL NUNC™ polypropylene storage tubes labelled “Fulvestrant PK Plasma Aliquot 1” (primary) and “Fulvestrant PK Plasma Aliquot 2”.

Plasma samples for PK analysis were all stored at -70°C in an upright position within 30 minutes of plasma preparation and were kept frozen at this temperature until and during shipment to Covance Bioanalytical Laboratories, where they were analysed. If a -70°C freezer was not available, then samples could be stored at -20°C for up to one week. PK analyses were performed with fully validated analytic methods and pharmacokinetic parameters were derived from non-compartmental analysis using the Phoenix® platform. PK findings were audited before final report was made available.

In part A, plasma concentrations for palbociclib and taselesib were listed and summarized by nominal time point, and dose level. PK parameters such as the maximum observed plasma concentration (C_{max}), time to reach C_{max} (T_{max}), the area under the plasma concentration time curve, and the minimum observed plasma concentration (C_{min}) were estimated for palbociclib and taselesib as appropriate, by dose level. For part B, plasma concentrations for palbociclib, taselesib and fulvestrant (part B1) were listed

and summarized by nominal time point, dose level and sub-cohort (B1 or B2).

2.5 Pharmacodynamic analysis

Collection of platelet-rich plasma (PRP) for PD analysis was taken for part A on Cycle 1 Day 1 (pre-dose and post dose at 4 hours), Cycle 1 Day 8 (pre-dose), Cycle 1 Day 15 (post-dose at 6 and 8 hours), Cycle 2 Day 15 (post-dose 2 hours). In part B, PD analyses were performed only in patients consenting to an optional tumour biopsy, and samples were taken on Cycle 1 Day 1 (pre-dose), Cycle 1 Day 15 (post-dose at 4 hours), Cycle 2 Day 15 (post-dose at 4 hours).

Blood samples for PRP-derived PD analysis used colour-coded reagents provided by the ICR (red, blue, and green-labelled). The bench top centrifuge was pre-chilled to 4°C and reagents were thawed prior to use. Blood samples were collected into three different 2.7 mL BD Vacutainer Sodium Citrate coagulation tubes and labelled with required information. Each tube was immediately stored at 4°C for transportation from the patient's bedside to the laboratory for further processing. The three blood tubes were centrifuged at 200g at 4°C for 15 minutes. Following this process, the blood separates into 2 distinct layers: an upper PRP layer and a lower red blood cell layer. The isolated PRP layer was incubated with PhosSTOP (Roche) to stabilize the phosphorylation signals and then lysed using Cell Lysis Buffer (Cell Signaling Technology) containing Phenylmethane sulfonyl fluoride (Sigma-Aldrich). Immediately at the end of processing the PRP samples were snap frozen on dry ice and stored at -80°C prior to transportation to the Clinical PD Biomarker Group at The Institute of Cancer Research for analyses.

PD analysis used pSer473 & total AKT and pSer9 & total GSK3 β counts, and was performed in platelet-rich plasma (PRP) taken in part A on Cycle 1 Day 1 (pre-dose and 4 hours post dose), Cycle 1 Day 8 (pre-dose), Cycle 1 Day 15 (6 and 8 hours post-dose) and Cycle 2 Day 15 (2 hours post-dose), as

previously reported [86]. Ratios of phosphorylated biomarker as percentage of C1D1 pre-dose normalised to total biomarker as percentage of C1D1 pre-dose and platelet counts were performed.

Meso Scale Discovery (MSD[®]) provides a multiplex 96 well plate to assess the phosphorylation status of AKT, GSK3 β and p70S6K [87]. The samples, followed by a solution containing the MSD SULFO-TAG[™] labelled detection antibodies for AKT, GSK3 β and p70S6K were added to the plate. Finally, MSD Read Buffer was added, which provided the appropriate chemical environment for electrochemiluminescence (ECL) to occur. The plate was then analysed on the MSD SECTOR[™] Imager 6000. Inside the SECTOR Imager, a voltage applied to the plate electrodes caused the labels bound to the electrode surface to emit light. The instrument measured the intensity of the emitted light to afford a measure of the amount of phosphorylated proteins present in the sample. A separate multiplex 96 well plate to measure total AKT, GSK3 β and p70S6K proteins was run simultaneously. Of note, no p70S6K data was formally analysed as the levels of this marker are usually close to the assay lower limit of detection when done in PRP samples. The assay was modified into a GCP compliant quantitative assay for AKT by the Clinical PD Biomarker Group by the inclusion of a standard curve of recombinant active AKT protein on every plate. The quality, accuracy and precision of the assays were monitored using quality control (QC) samples created by spiking three known quantities of recombinant AKT into 10% human plasma.

The raw data ECL counts were normalised to platelet count to take into account any drug effect on platelet number, by dividing the ECL counts by the platelet count for each time point. Using these platelet normalised values, the percentage change for phosphorylated biomarker was calculated for each subject by comparing the levels (Platelet count normalised ECL counts) measured at each post-dose time point to pre-dose levels measured on Day 1. The percentage change for total biomarker was calculated for each subject by comparing the levels (Platelet count normalised ECL counts) measured at each post-dose time point to pre-dose levels measured on Day

1. Since the amount of a particular phosphorylated biomarker is a subset of the amount of the same total biomarker, the phosphorylated biomarker levels were normalised to the quantity of total biomarker by calculating the ratio of percentage change in the level of phosphorylated biomarker at a given post-dose time point compared to the pre-dose levels / percentage change in the level of total biomarker at the same post-dose time point. This data was used to evaluate the extent and duration of PD modulation of phosphorylated biomarker.

The following example summarizes these calculations using a hypothetical AKT analysis:

pSer473 AKT	Raw data:	Total AKT	Raw data:
C1D1Pre	535	C1D1 Pre	3001 ECL counts
C1D1 4h	547	C1D1 4h	2793 ECL counts

Platelet count

C1D1 Pre 145

- Platelet normalised raw data = C1D1 Pre raw data / C1D1 Platelet count:

$$\text{pSer473 AKT C1D1 Pre} = 535 / 145 = 3.69$$

$$\text{pSer473 AKT C1D1 4h} = 547 / 145 = 3.77$$

$$\text{Total AKT C1D1 Pre} = 3001 / 145 = 20.70$$

$$\text{Total AKT C1D1 4h} = 2793 / 145 = 19.26$$
- Percentage change for pSer473 AKT = $(\text{C1D1 4h} / \text{C1D1 Pre}) * 100 = (3.77 / 3.69) * 100 = 102\%$
- Percentage change for total AKT = $(\text{C0D12h} / \text{C0D1 Pre}) * 100 = (19.26 / 20.70) * 100 = 93\%$

- Phospho: Total Ratio (at C1D1 4h post-dose) = Percentage change for pSer473 AKT at 4h / Percentage change for total AKT at 4h = $102/93 = 1.10$

Optional snap frozen tumour tissue samples for PD were analysed for phosphorylated and total Rb on C1D1 (pre-dose/baseline), C1D15 (pre-dose) and on disease progression, using ICR validated assays on the Meso Scale Discovery (MSD) technology platform.

Flash frozen tumour biopsies were homogenized using a micro tissue grinder in a CHAPS based lysis buffer containing protease and phosphatase inhibitors (Clinical PD Biomarker Group proprietary recipe). The tumour lysates were centrifuged to remove debris and the protein concentration measured using the BCA assay (Pierce). All lysates were snap frozen and stored at -80°C until analysis.

Meso Scale Discovery (MSD[®]) provides two separate 96 well plates, one that has been pre-coated with the capture antibody for phospho (Ser780) Rb and one pre-coated with total Rb antibody. The samples, followed by a solution containing the MSD SULFO-TAG[™] labelled anti-total Rb detection antibody were added to the plate and the levels of pSer780 and total Rb measured as ECL counts by the process described for the AKT assay above. The assay was modified into a GCP compliant assay by the Clinical PD Biomarker Group by inclusion of a standard curve of MDA-MB-231 cell lysate on every plate. The quality, accuracy and precision of the assays were monitored using quality control (QC) samples created from MCF-7 cell lysates. The raw data was used to calculate the percentage change for pSer780 Rb and total Rb and the phospho total ratio as described for the AKT analysis.

2.6 Efficacy analysis

All patients had a baseline radiological assessment with a computer tomography (CT) scan of thorax, abdomen and pelvis or a magnetic resonance imaging (MRI) scan of abdomen and pelvis plus a chest CT scan.

This baseline imaging had to be performed a maximum of four weeks before receiving the first dose and the interval between the last anti-cancer therapy and measurements in this baseline imaging must have been at least four weeks apart. Radiological assessment had to be repeated every 2 cycles/8 weeks of treatment. After 6 cycles, the frequency of imaging could be reduced to every 3 cycles/12 weeks of treatment at the investigator's discretion.

Disease was measured according to the radiological standards defined in RECIST (response evaluation criteria in solid tumours) version 1.1 [88]. The same methods used to detect evaluable lesions at baseline were used to follow lesions throughout the trial. All lesions measured at baseline must have been measured at every subsequent disease assessment and recorded clearly on the scan reports. All non-measurable lesions noted at baseline must have been noted on the scan report as present or absent.

Objective responses as defined by RECIST version 1.1, overall response rates, progression-free survival (PFS) and duration of response data was analysed. All complete responses (CR) or partial responses (PR) were confirmed by two consecutive observations not less than four weeks apart. Objective response rate (ORR) was defined as CR or PR among subjects with measurable disease. Clinical benefit rate (CBR) was defined as CR, PR, or stable disease (SD) for at least 24 weeks for subjects with measurable disease and as freedom from new lesions or unequivocal progression for at least 24 weeks among subjects with bone metastases only. Best tumour response achieved by each patient while on trial (defined as the best percentage change in the sum of longest dimensions of target lesions) was also recorded and will be presented as a waterfall plot.

2.7 Translational cohort patients

In order to make biomarker analysis derived from study consistent with dosage homogeneity and enriched for breast cancer, a cohort of 62 patients was used for the translational work of this project. This cohort was composed

by all 58 patients enrolled in expansion parts B1, B2 and B3 plus the 4 breast cancer patients included in the escalation phase of the study. Patients enrolled in the expansion phase were all treated with the recommended phase 2 dose (RPD2) of 2mg taselesib PO QD plus 125mg palbociclib PO QD on a three weeks on/1 week off schedule. Out of the 4 breast patients enrolled in the escalation phase 3 of them were also assigned to the same 2mg PO QD continuous taselesib plus 125mg palbociclib PO QD on a three weeks on/1 week off schedule and 1 assigned to the 2mg taselesib PO QD three weeks on/1 week off plus 125mg palbociclib PO QD also three weeks on/1 week off.

2.8 Samples for translational biomarker research

All patients enrolled were requested to provide a mandatory archival formalin-fixed paraffin-embedded (FFPE) sample from either primary or metastatic location. Patients were also offered optional cycle 1 day (C1D1), cycle 1 day 15 (C1D15) and on progression fresh frozen tissue biopsies. Whole blood samples were taken before each cycle of treatment (on average 28 days apart) from C1D1 to end of treatment (EOT).

The plan was to use baseline FFPE samples to perform whole-genome sequencing, immunohistochemistry, and fluorescence in situ (FISH) analysis to explore potential prognostic and predictive baseline biomarkers that could influence the combination therapy efficacy. PRP and fresh frozen tissue samples were used to explore PD analysis of interest. Prospectively collected plasma samples were used to expand on the utility of ctDNA tracking and sequencing as a potential non-invasive tool to predict treatment efficacy and explore potential mechanisms of resistance to the combination drugs.

A schematic representation of every sample and timepoint used for PK, PD and biomarker analysis can be found in **figure 4**.

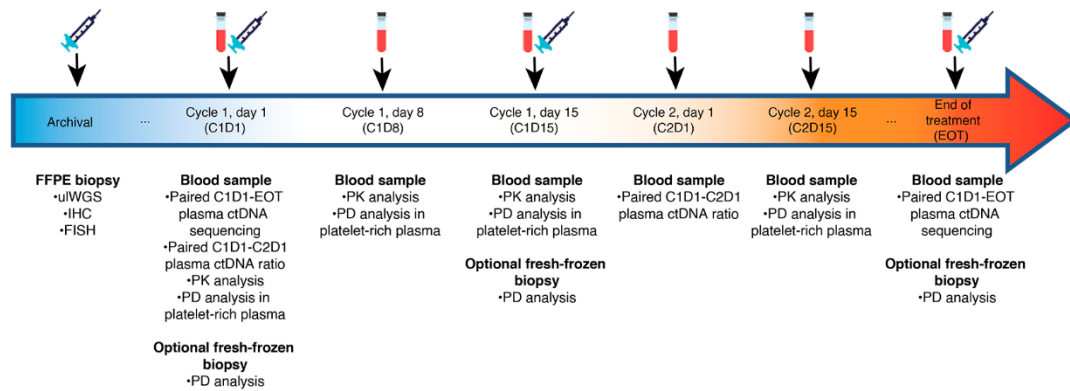


Figure 4. Study overview and samples for translational research. ulWGS= ultra-low whole genome sequencing, IHC= immunohistochemistry, FISH= fluorescence in situ hybridization, PK= pharmacokinetics, PD= pharmacodynamics, ctDNA= circulating tumour DNA [89].

2.9 FFPE biopsies processing

Scanning FFPE biopsies slides with the Hamamatsu Nanozoomer and uploading onto PathXL

A first slide generated from every archival FFPE block was haematoxylin and eosin (H&E) stained by the Breast Cancer Now histopathological core facilities and then scanned using the Hamamatsu Nanozoomer-XR digital slide scanner at 40X magnification with manual focus-points setup. Images generated were uploaded onto PathXL Xplore, an image management system.

Independent external pathology review

The folder with the scans was shared with an external expert pathologist for independent review. Marking of the invasive areas and tumoural content assessment (as an estimated percentage of the tumour content in the respective invasive area) was performed for every scan and scored from 0 to 100%. Genomic content extraction was later on performed using only microdissection (refer to *DNA and RNA extraction for genomic interrogation section*) of areas marked as invasive content by this expert pathologist, to minimize contamination of material coming from areas where no invasive

tumoural cells were detected. Scans shown to have no tumour content at all were discarded for further analyses.

Cyclin D1, cyclin E1 and androgen receptor (AR) expression assessment

Cyclin D1 immunohistochemistry (IHC) staining used specific rabbit monoclonal antibody SP4 clone, performed alongside negative controls and pre-validated positive controls. Only nuclear staining was considered, and all invasive tumour cells were assessed. Samples with poor fixation, preservation, or other causes for which a score could not be obtained like unreliable estimation of invasive nuclei were reported as 'NA' (not assessable). Scoring was reported both as estimated percentage of invasive nuclei stained and intensity scores. H-score was calculated for cyclin D1 by multiplying the percentage of tumour cells stained (0-100) by the intensity grading score (0-3), resulting in a value ranging from 0 to 300.

Cyclin D1 fluorescence in situ hybridization (FISH) staining and scoring as counted ratio of CCND1/CEP11 was performed in all samples available. This analysis was performed alongside positive controls tested in MCF7 cells assessed for the presence of positive CCND1 (red probe) and CEP11 (green probe) signals in the nuclei, prior to scoring of the study specimens. Acceptance criteria was qualitative, and the positive control was classified as accepted or non-accepted based on the presence or absence of CCND1 and CEP11 signals: accepted if there was presence of both CCND1 and CEP11 signals in the majority of the nuclei and non-accepted if absence of either CCND1 or CEP11 signals in the majority of nuclei. In the study samples, 20 representative nuclei were scored, with exclusion of any nuclei where there was only signal present from one of the probes, either only CCND1 (red) or only CEP11 (green). Any nuclei that overlapped and overlaid their neighbours was not counted. If the ratio was <2.0 , CCND1 gene amplification was not called and if the ratio was ≥ 2.0 , CCND1 gene amplification was reported.

Cyclin E1 IHC staining used specific mouse monoclonal antibody HE12 with controls and scoring was reported as estimated percentage of invasive nuclei

stained. For this analysis, H-scores could not be calculated as intensity grading for cyclin E IHC had been previously found to provide too much background signal for reliable quantification and thus the analysis were performed with percentage of nuclei staining data only. Similar to cyclin D1, all invasive tumour cells and only nuclear staining was assessed (including faint staining). Samples with poor fixation, preservation, etc. for which a score could not be obtained were reported as 'NA' (not assessable).

For TNBC patients, an additional androgen receptor (AR) IHC staining using the specific mouse monoclonal antibody AR441 clone was performed, once more with positive and negative controls. Only invasive cells exhibiting brown nuclear staining were included in deriving the score and a minimum of 10-high power fields (HPF) were reviewed and the fields selected must have been representative of the biological heterogeneity observed in AR and the density across the sample regardless of it being a core biopsy or a resection specimen. Scoring was reported as an estimated percentage of invasive nuclei stained.

All IHC and FISH staining and scoring was performed at The Ralph Lauren Centre for Breast Cancer Research at The Royal Marsden Hospital.

DNA and RNA extraction for genomic interrogation

The rest of each FFPE block was cut into 10-micron depth slides for nucleic acid extractions in the Ralph Lauren Centre for Breast Cancer Research and stained with Nuclear Fast Red (NFR) solution in the Breast Cancer Now histopathological core facilities, both at The Royal Marsden Hospital in London. RNA and DNA extraction from archival FFPE 10-micron slides was performed using QIAGEN AllPrep DNA/RNA FFPE Kit using MiniColumns (Catalogue No: 80234) with final elute volume of 30µl for RNA and 50µl for each first and second elution of DNA. Quantification of RNA was performed using Qubit™ 3.0 Fluorometer with Qubit™ RNA HS Assay Kit and quality of the RNA extracted assessed with Bioanalyzer. Quantification of DNA was performed using an RNaseP assay for digital droplet PCR (ddPCR) after manual droplet preparation.

2.10 Blood processing

2x 10ml whole blood samples were collected in EDTA tubes (for London patients) or STRECK tubes (for Manchester and Glasgow patients) and processed for plasma and buffy coat separation at The Institute of Cancer Research Chester Beatty Laboratories. EDTA tubes were processed within 2 hour following venepuncture and STRECK tubes within 48-72 hours. The processed plasma and buffy coat were stored immediately at -80°C until nucleic acids extraction.

Plasma DNA extraction using automated method

Plasma DNA was extracted from 4ml of sample (for C1D1-EOT pairs) or 2ml (for C2D1) using magnetic beads method with the automated Thermo Scientific™ KingFisher™ Flex Purification System and using the MagMax™ Cell-Free DNA Isolation Kit (containing the MagMax™ cell free DNA binding solution, magnetic beads, wash and elution solutions; Thermo Cat # A29319). For samples received in STRECK tubes, 60µl of proteinase K and 200µl of SDS 20% solution were added, incubated for 20 minutes at 60°C on a Eppendorf™ Thermomixer™ and cooled on ice for 5 minutes. The system was loaded with plates containing the sample, MagMax™ cell free DNA binding solution, MagMax™ cell free DNA magnetic beads, MagMax™ cell free wash solution, freshly made 80% ethanol, and a tip comb plate. The Thermo Scientific™ KingFisher™ Flex Purification System was run on programme: MagMAX cfDNA-4mL-Flex-V2-100. DNA was recovered to a total elute volume of 100µl for each first and 50-100µl for second elutions and stored at -20°C prior to quantification.

Buffy coat DNA extraction using columns method

DNA from buffy coat was extracted using QIAGEN QIAamp DNA Mini Kit (Catalogue No: 51304) using columns method. Inputs of 50µL of buffy coat was added to 20µL proteinase K and 4µL of RNase A stock solution

(100mg/ml; Qiagen Cat # 19101) to a 1.5mL microcentrifuge tube and vortexed. This was combined with 200µL buffer AL then briefly vortexed. The sample was incubated at 56°C for 10 minutes, combined with 200µL ethanol (96-100%) and briefly vortexed. This mixture was moved to a QIAmp Mini spin column and centrifuged at >10,000 x g for 1 minute and the filtrate discarded. Subsequently 500µL buffer AW1 was added to the spin column and centrifuged at >10,000 x g for 1 minute and the filtrate discarded. This step was repeated with 500µL buffer AW2 and centrifuged at >10,000 x g for 3 minutes. The filtrate was discarded, and the Mini spin column centrifuged for a further minute to remove any remaining traces of ethanol. The Mini spin column was placed in a new labelled 1.5mL microcentrifuge tube and the DNA was eluted into 100µL pre-heated (42°C) buffer AE and stored at -20°C prior to quantification.

Quantification of extracted DNA by droplet digital PCR (ddPCR)

Quantification of extracted plasma DNA was performed using Bio-Rad QX-200™ ddPCR System. For DNA extracted from plasma, a multiplex assay with *HOGA1* (4-hydroxy-2-oxoglutarate aldolase), *IRAK4* (interleukin-1 receptor-associated kinase 4) and *OR4C12* (Olfactory receptor 4C12) reference genes was used. *HOGA1* was VIC labelled while *IRAK4* and *OR4C12* were 6-FAM labelled. The full list of reagents for the triplex cocktail can be found in the following **table 2**.

		Supplier	Cat No.
Triplex in House (HOGA1, IRAK4 and OR4C12)			
1 μ l	HOGA1 <i>Primer Fw:</i> AGGTGGACATTGCGGGTATC <i>Primer Rv:</i> CCTCTGCAGTGGCAGTGAAG <i>Probe in VIC:</i> CCCCCCTGTGACCAC		In-house
1.5 μ l	IRAK4, Human PrimePCR™ ddPCR™ Copy Number Assay	Bio-Rad	dHsaCP25 06307
2 μ l	OR4C12 <i>Primer Fw:</i> CCAATGTTAAATCCCGTGGTCTA <i>Primer Rv:</i> TCCAAAGCTTCCTTATTGCACTT <i>Probe in FAM:</i> ACACTCAGAAATGCTG		In-house
2X Droplet digital PCR Supermix for Probes		Bio-Rad	1863010
Nuclease Free water		Life Technologies	4387936

Table 2. Triplex in-house design for quantification of plasma DNA.

PCR reactions consisted of 10 μ L ddPCR Supermix for probes (Bio-Rad), 4.5 μ L of Triplex primer probe mix, 1 μ L of DNA eluate and nuclease free water made up to reach a total volume of 20 μ L (**table 3**). The reaction was then emulsified in 70 μ L of droplet generator oil into approximately >20,000 droplets per sample using the Automated Droplet Generator (BioRad QX200™ droplet generator, Auto-DG). Emulsified PCR reactions were transferred on to a 96 well plate and heat-sealed with foil. All experiments were run with at least one non-template control (NTC). PCR reactions were run on a G-Storm Quad thermocycler incubating the plates at 95°C for 10 min followed by 40 cycles at 95°C for 15 sec and 60°C for 60 secs, followed by 10 min incubation at 98°C.

Reagent	Volume per reaction (µl)	Volume per n reaction (µl)
Nuclease free H ₂ O	5.5	5.5*n
2 X Droplet digital PCR Supermix for Probes	10	10*n
Triplex primer probe mix	4.5	4.5*n
Total volume	20	
DNA template to be added	1	

Table 3. PCR reaction reagents for quantification using in-house triplex.

Quantification of extracted buffy coat DNA was done using RNaseP as the reference gene. PCR reactions consisted of 10µL ddPCR Supermix for probes (Bio-Rad), 1µL of TaqMan Copy Number Reference Assay, human, RNase P (RPPH1, Thermo Fisher Scientific 4403326) 1µL of DNA eluate and nuclease free water made up to reach a total volume of 20µL. Droplets were in this case generated mainly using Bio-Rad's manual droplet generation protocol, although some of the buffies were also processed using the Automated Droplet Generator. All plates generated were thermocycled with the same protocol as per plasma DNA quantification.

The readings were all performed on the QX200™ Droplet Digital™ reader system, with FAM and VIC signals. Output files were stored as .qlp files and analysed with Bio-Rad's QuantaSoft software v1.7.4. Droplets generated positive or negative clusters compared a population of 'empty' droplets. An estimation of the DNA concentration was obtained from copies/well obtained after ddPCR process and multiplying by the c-value (3.3pg), an estimation of the mass of a single haploid human genome.

2.11 Whole-genome sequencing of baseline tissue

Ultra-low passage whole-genome sequencing (ulWGS) of the DNA extracted from the archival tissue samples was conducted. Library preparation was performed using Illumina's KAPA HyperPlus Kit with Library Amplification (Catalogue No: 07962428001) as per manufacturer's instructions. Libraries were made up from 5-50ng input DNA and quantified using Illumina's Library Quantification Kit ABI Prism™ qPCR Master Mix (Catalogue No. 07960204001) as per manufacturer's instructions. Quality of libraries was checked using Bio-Rad's Agilent 2100 Bioanalyzer. Libraries were then sent to the Centre for Molecular Pathology at The Royal Marsden Hospital and The Institute of Cancer Research for next generation sequencing (NGS). Sequencing was performed using an SP 300 cycles flow cell aiming to 0.8X depth on the NovaSeq 6000 Sequencing System. Data were analysed for copy number variations (CNV) by alignment with reference hg19 genome using BWA. Duplicate removal used Picard tool (<http://broadinstitute.github.io/picard/>), purity assessment and copy number calling used ichorCNA [90] with settings for high tumour fraction to get a thresholded adjusted copy number call defined as amplification, gain, neutral, heterozygous deletion, or homozygous deletion. Adjusted values for a set of genes of interest were then plotted in a diagram for each sample. As these analysis can be limited in low tumour purity samples we adopted the same approach for our tissue samples as in prior work performed in ctDNA from our lab [68] by restricting copy number analysis to those tumours with at least 20% tumour purity, as scored in the initial pathologist review.

2.12 Targeted sequencing of paired plasma samples

Sequencing of paired C1D1 and EOT plasma samples was performed with the in-house targeted error-corrected capture panel RMH200, which includes 200 frequently altered genes in cancer including both mutations and copy number variations (panel can be found in Appendix 1). cfDNA extracted from plasma ranging from 10-25ng were aliquoted into 100µL elutions for

available paired samples and sent to the Centre for Molecular Pathology at The Royal Marsden Hospital and The Institute of Cancer Research for sequencing. Unique molecular identifiers (UMIs) from xGen IDT composed of 8 nucleotides unique dual barcode and 9 nucleotides long UMI sequence were used during library preparation for improving detection limits by removing errors introduced by PCR duplicates resulting in an improved accuracy of allele frequency. RMH 200 panel size was 1.2 Mb and 20000x depth was aimed resulting in ~24Gb required output per sample. Sequencing of plasma ctDNA was performed using S1 and S2 flow cells on the Illumina's NovaSeq 6000 Sequencing System. Samples were aligned using Burrows-Wheeler Aligner (BWA) [91], then annotated and combined into UMI consensus families using fgbio (<http://fulcrumgenomics.github.io/fgbio/>). Additionally, 16 plasma samples from healthy donors were sequenced in an SP flow cell also on the NovaSeq 6000 (Illumina) to generate an error model using a modified pileup pipeline [92]. The 16 healthy plasma samples were used as a training set to establish a background error rate for each sequenced position in the targeted panel after excluding germline SNPs. This was done using the IDES pipeline to generate a database of nonreference counts for each position in the panel. A Weibull distribution was fitted to the nonzero values or for positions with low counts of nonreference reads, a Gaussian distribution was used. For each ctDNA sample, after generating base counts at each position, these were then adjusted based on the rate of nonreference reads in the training set. These revised counts were then used to identify possible mutations. Variant calls were generated using VarDict [93] and pileup [93]. 4 alternative families of size 3 or more reads were required to call a mutation (5 alternative families for an indel) removing mutations with significant strand bias. All calls were manually curated with Integrative Genomics Viewer (IGV) [94], reported as allele frequency and annotated using annovar [95]. All plasma DNA sequencing was performed on the NovaSeq 6000 (Illumina). Functional predictions of *FAT1* mutations found as a result of the sequencing for exploratory work were assessed using Sift [96], MutationAssessor [97] and PROVEAN [98].

2.13 *PIK3CA* mutations validation and ctDNA ratio

A circulating DNA ratio between *PIK3CA* mutations in C1D1 and C2D1 (CDR₂₈) was performed with ddPCR for those *PIK3CA* mutant patients on the basis of screening or sequencing data. Singleplex *PIK3CA* assays were used for common mutations E542K (c.1624 G > A), E545K (c.1633 G > A), H1047R (c.3140 A > G), and H1047L (c.3140 A > T) located in exons 9 and 20 when known. Custom assays and multiplexes were initially intended to be designed for mutations outside these common ones but as they were only found to be a minority, for patients with multiple *PIK3CA* mutations, the mutation in exons 9 or 20 were used for CDR analysis. For patients with plasma sequencing data ddPCR was performed both for CDR₂₈ and validation of sequencing findings on C1D1. Analysis was performed as per prior work in our lab [56], using 0.25 ml plasma equivalent or 1.3 ng of DNA input, whichever larger, to allow sufficient calling for wild-type alleles to be confident with mutation calling. If less than 1.3ng available, analysis was performed with maximum input available and only considered for analysis if meeting further QC criteria. All plates were thermocycled with 54 degrees and 40 cycle program and readings were all performed on the QX200™ Droplet Digital™ PCR System with FAM and HEX signals. Only samples with at least 300 wild-types alleles detected were considered as undetectable. If this was not met, then the sample was repeated or considered failed if not enough material available. If repeated, a summatory of different experiments for the same sample was allowed in order to increase sensitivity by enriching both mutant and wild-type counts. To be able to perform estimates at very low concentration of template only *PIK3CA* mutations with ≥4 FAM droplets at C1D1 were further longitudinally analysed. Bio-Rad Quantasoft® software version 1.7.4 was used to calculate concentration of FAM and HEX-binding template. As varying plasma equivalents were used, weighted averages were calculated for analysis. Mutation assays were all run with two non-template controls (NTCs) per run.

2.14 Statistics

Patients enrolled in part B1 followed a two-stage minimax Simon's design [99], with an unacceptable response rate of 0.1 and an acceptable response rate of 0.3 (with a one-sided $\alpha=0.05$ and $\beta=0.2$). 15 patients were to be treated in stage one and if two or more responses observed 25 patients in total were recruited, with 6 responses in total required to infer efficacy. As part B2 was exploratory in nature we decided to use descriptive statistics and protocol allowed to allocate up to 38 patients in total (a minimum of 12 patients with *PIK3CA* mutant, ER-ve, HER2+ve advanced breast cancer, a minimum of 12 patients with *PIK3CA* mutant, triple negative advanced breast cancer and a minimum of 12 patients with advanced solid tumours with mutations leading to a hyperactivated PI3K-AKT pathway). To test a preliminary evaluation of the safety of palbociclib, taselisib and letrozole triplet, 6 patients were required to be enrolled in part B3 with this number being reflective of the patients that are enrolled into an expanded dose level of a standard phase I 3+3 design.

Statistical analysis was performed using software from GraphPad PRISM® version 8.2.1 and Strata version 15. Safety and efficacy analyses were performed in all patients who received at least one dose of study drugs (palbociclib, taselisib or fulvestrant). For ORR, CBR and PFS analysis, 95% CIs were estimated. Kaplan-Meier curves using log-rank test was used to test associations with PFS, with HRs calculated using the Mantel-Haenszel method. For CDR₂₈, nonparametric Wilcoxon matched-pairs signed-rank test was used to detect differences between C2D1 and C1D1 concentration, and Log-rank tests for testing potential PFS differences stratifying patients above or under a defined CDR₂₈. A p value <0.05 was considered for statistical significance in all analysis.

Chapter 3. Clinical findings

3.1 Introduction

The current standard for the treatment of metastatic ER+ve and HER2-ve breast cancer patients both relapsing on and off adjuvant endocrine therapy (ET) is a combination of a CDK 4/6 inhibitor with ET. There is broad clinical evidence that the three CDK4/6 inhibitors currently approved by the regulatory drug agencies (namely palbociclib, ribociclib and abemaciclib) provide a relatively similar efficacy resulting in a clinically meaningful improvement in progression-free survival, both as a first-line or second-line systemic treatment. Palbociclib was tested in combination with letrozole versus placebo plus letrozole in postmenopausal patients with advanced ER+ve HER2-ve breast cancer who had not received prior treatment for advanced disease in the PALOMA-2 study, and the combination of palbociclib was found to provide a significant survival advantage with a median PFS 24.8 months in the palbociclib plus letrozole group, as compared with 14.5 months in the placebo plus letrozole group (HR 0.58; 95% CI 0.46 to 0.72; $p < 0.001$) [14]. In patients who had received previous ET, the PALOMA-3 study also found a statistically significant improvement in PFS for the combination of palbociclib plus fulvestrant versus placebo plus fulvestrant, with a median PFS 9.5 months versus 4.6 months, respectively (HR 0.46, 95% CI 0.36–0.59, $p < 0.0001$) [100]. In addition, patients enrolled in the PALOMA-3 study who had sensitivity to previous ET, defined as either a documented clinical benefit (complete response, partial response, or stable disease for ≥ 24 weeks) from at least one previous endocrine therapy regimen in the context of metastatic disease or the receipt of at least 24 months of adjuvant endocrine therapy before recurrence, had longer overall survival (OS), with median 39.7 months in the palbociclib plus fulvestrant group and 29.7 months in the placebo plus fulvestrant group (HR 0.72; 95% CI 0.55 to 0.94; absolute difference of 10.0 months) [101]. A similar magnitude of benefit has also been reported for the respective studies carried on with ribociclib in the MONALEESA-2 and 3 [102, 103] and abemaciclib in the MONARCH-3 and 2 [104, 105]. The three currently

approved CDK4/6 inhibitors are generally well tolerated, with myelosuppression in the form of neutropenia (up to 80% of patients) being the most common adverse event, a reflection of the bone marrow cytostatic effect of these compounds.

A parallel strategy in drug development for the treatment of advanced ER+ve HER2-ve breast cancer patients has been the development of PI3K inhibitors, with a particular interest to target the patients harbouring a *PIK3CA* mutation which accounts for around 40% of metastatic breast cancer patients and results in greater sensitivity to this family of drugs. This has ultimately resulted in the FDA/EMA approval (but not MHRA at the present moment) approval of the α -selective PI3K inhibitor alpelisib in combination with fulvestrant, with the results of the SOLAR-1 study demonstrating an improvement in PFS in the *PIK3CA*-mutant population, with a median PFS 11.0 months in the alpelisib plus fulvestrant group, as compared with 5.7 months in the placebo plus fulvestrant group (HR 0.65; 95% CI 0.50 to 0.85; $p < 0.001$) [34]. The most frequent any-grade adverse events in the alpelisib group were hyperglycaemia (63.7%), diarrhoea (57.7%) and nausea (44.7%). The β -sparing PI3K inhibitor taselisib also showed a statistically significant improvement in PFS in a similar population, with 7.4 months in the taselisib plus fulvestrant group versus 5.4 months for the placebo plus fulvestrant group (HR 0.70; 95% CI 0.56-0.89; $p = 0.0037$) [31]. In the taselisib-treated group the most frequent any-grade adverse events were diarrhoea (60.1%), hyperglycaemia (40.4%) and nausea (34.1%). The most frequent grade 3/4 AEs in the taselisib-treated group were diarrhoea (11.5%), hyperglycaemia (10.8%) and rash (3.8%). In view of the safety profile the small clinical benefit was considered not enough to provide a clinical utility.

Although the introduction of the CDK4/6 and PI3K inhibitors have been important milestones in the treatment of ER+ve HER2-ve breast cancer patients, there are still patients intrinsically resistant to them and the rest will inevitably develop resistance over the course of their treatment. A potential strategy to prevent or delay resistance and improve survival in these patients

could be the combination of both CDK4/6 and PI3K inhibitors, and pre-clinical work showed synergistic efficacy in breast cancer models [38]. The PIPA study was designed to provide clinical evidence of whether such a combination using palbociclib and taselisib can be safely administered in humans, describe the toxicity profile, and provide preliminary efficacy data. In addition, the study was pre-planned to include PD analyses to help elucidate if the drug doses tested cause target modulation and included detailed biomarker work to potentially help selecting patients more likely benefiting from such a treatment strategy.

3.2 Patient demographics and characteristics

A total of 78 patients were enrolled overall in the trial from March 2015 to November 2018. Part A (escalation phase) included the following levels: palbociclib plus taselisib PO 100/2mg with both drugs on a 3 week on/1 week off schedule (level 1), 100/4mg with both drugs given 3 week on/1 week off (level 2), 125/2mg on a 3week on/1 week off schedule (level 3) and 125/2mg on a continuous taselisib schedule (level 4). Patients allocated in part A of the study followed a 3+3 dose escalation design for identifying the RP2D, as follows in **table 4**.

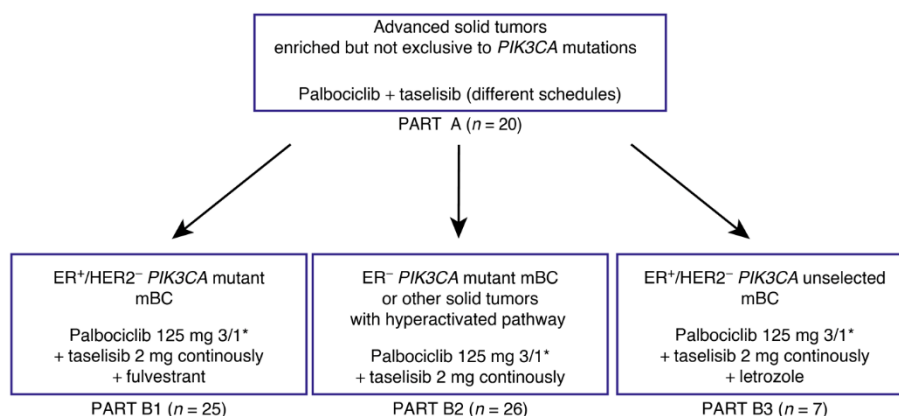
Dose Level	Palbociclib	Taselisib	Estimated No of patients
-1	75mg once daily 21-days-on and 7-days-off treatment	2mg once daily 21-days-on and 7-days-off treatment	3 + 3
1	100mg once daily 21-days-on and 7-days-off treatment	2mg once daily 21-days-on and 7-days-off treatment	3 + 3
2	100mg once daily 21-days-on and 7-days-off treatment	4 mg once daily 21-days-on and 7-days-off treatment	3 + 3
3	125mg once daily 21-days-on and 7-days-off treatment	2mg once daily 21-days-on and 7-days-off treatment	3 + 3
4	125mg once daily 21-days-on and 7-days-off treatment	2mg once daily Continuously	3 + 3

Table 4. Part A (escalation phase) dose levels with combination doses schedules and estimated number of patients to be treated per level.

Escalation phase recruitment was completed with 20 patients enrolled including 6 colorectal, 2 ER+ve HER2-ve breast, 1 ER+ve HER2+ve breast, 1 TNBC, 2 melanoma, 1 cervical, 1 mesothelioma, 1 oesophagus, 1 cholangiocarcinoma, 1 leiomyosarcoma, 1 Leydig cell tumour, 1 non-small cell lung cancer (NSCLC) and 1 head and neck squamous cell carcinoma (HNSCC) patient. After completion of the escalation phase, the safety review committee established the dose selected to subsequently administer in expansion cohorts (part B), which will be later detailed in section 3.5.

Part B1 was completed with 25 *PIK3CA*-mt ER+ve HER2-ve breast cancer patients enrolled, achieving the recruitment goal to have enough power to test the primary efficacy endpoint of the palbociclib, tselisib and fulvestrant triplet. Part B2 was closed with a total of 26 patients before planned completion due to low accrual with 12 *PIK3CA*-mt ER-ve advanced breast cancer (9 TNBC and 3 HER2+ve), 4 *PIK3CA*-mt colorectal adenocarcinoma,

3 *PIK3CA*-mt ER+ve HER2-ve (included as solid tumours subcohort), 1 *PIK3CA*-mt high grade serous ovarian cancer, 1 *PIK3CA*-mt clear cell ovarian carcinoma, 2 *PIK3CA*-mt NSCLC, 1 *PIK3CA*-mt endometrium, 1 *PIK3CA*-mt cervix (adenosquamous carcinoma) and 1 *PIK3CA*-mt anaplastic oligodendroglioma patient. Part B3 was completed with a final recruitment of 7 *PIK3CA*-unknown ER+ve HER2-ve breast patients, reflecting of the number of patients enrolled into an expanded phase I 3+3 design, and with a view to explore differences in toxicity with a triplet involving letrozole as opposed to fulvestrant. A summarized consort diagram enclosing final cohort recruitment is illustrated in the next **figure 5**.



*Following a safety review committee recommendation, in dose expansion (part B) palbociclib was administered at 100 mg once daily 3/1 for cycle 1, escalating to 125 mg once daily 3/1 in the absence of myelosuppression.

Figure 5. Consort diagram for clinical trial with final number of recruited patients Part A= escalation phase, part B= expansion phase.

Main characteristics for all enrolled patients are shown in the following **table 5**. Of note, median age for the overall population was 59.9, 82% were female and patients have had a median of 3 prior lines of systemic treatment and 2 prior lines of chemotherapy for advanced disease, reflecting a heavily pre-treated population.

		A (N=20)	B1 (N=25)	B2 ER-ve (N=12)	B2 Solid tumours (N=14)	B3 (N=7)	Total (N=78)	
Median age, years (IQR)		66.2 (53.7-70.5)	57.8 (51.2-65.3)	59.5 (52.2-65.6)	63.4 (52.8-68.4)	56.2 (52.6-61.1)	59.9 (52.4-68.4)	
Performance status, n (%)	PS 0	5 (25)	14 (56)	9 (75)	2 (14)	4 (57)	34 (44)	
	PS1	15 (75)	11 (44)	3 (25)	12 (86)	3 (43)	44 (56)	
Gender, n (%)	Male	10 (50)	0 (0)	0 (0)	4 (29)	0 (0)	14 (18)	
	Female	10 (50)	25 (100)	12 (100)	10 (71)	7 (100)	64 (82)	
Median prior lines of systemic therapy for advanced disease (range)		3 (1-10)	3 (1-9)	2 (1-10)	3 (2-8)	2 (1-4)	3 (1-10)	
Median prior lines of cytotoxic chemotherapy for advanced disease (range)		2 (0-5)	1 (0-7)	2 (1-6)	3 (0-7)	0 (0-2)	2 (0-7)	
Prior cytotoxic chemotherapy, n (%)	Yes	19 (95)	25/25 (100)	12/12 (100)	13 (93)	7/7 (100)	76 (97)	
	No	1 (5)	0/25 (0)	0/12 (0)	1 (7)	0/7 (0)	2 (3)	
Prior ET, n (%)	Yes	NA	25/25 (100)	5/12 (42)	NA	7/7 (100)	37 (84) *	
	No	NA	0/25 (0)	7/12 (58)	NA	0/7 (0)	7 (16) *	
Prior Tamoxifen, n (%)	Yes	NA	20/25 (80)	3/12 (25)	NA	7/7 (100)	30 (68) *	
	No	NA	5/25 (20)	9/12 (75)	NA	0/7 (0)	14 (32) *	
Prior AI, n (%)	Yes	NA	25/25 (100)	5/12 (42)	NA	7/7 (100)	37 (84) *	
	No	NA	0/25 (0)	7/12 (58)	NA	0/7 (0)	7 (26) *	
Prior fulvestrant, n (%)	Yes	NA	6/25 (24)	0/12 (0)	NA	1/7 (14)	7 (16) *	
	No	NA	19/25 (76)	12/12 (100)	NA	6/7 (86)	37 (84) *	
Prior everolimus, n (%)	Yes	NA	10/25 (40)	0/12 (0)	NA	3/7 (43)	13 (30) *	
	No	NA	15/25 (60)	12/12 (100)	NA	4/7 (57)	31 (70) *	
Mutations as per enrolment, n (%)	PIK3CA Single	H1047R	0 (0)	10 (40)	3 (25)	2 (14)	0 (0)	15 (19)
		H1047L	0 (0)	2 (8)	0 (0)	0 (0)	0 (0)	2 (3)
		E542K	0 (0)	5 (20)	2 (17)	3 (22)	0 (0)	10 (13)
		E545K	0 (0)	6 (24)	2 (17)	1 (7)	0 (0)	9 (12)
		Others	1 (5)	0 (0)	2 (17)	6 (43)	0 (0)	9 (12)
		Unknown	5 (25)	0 (0)	1 (8)	1 (7)	1 (14)	8 (10)
	PIK3CA Multiple	H1047R + D350G	0 (0)	1 (4)	0 (0)	0 (0)	0 (0)	1 (1)
		E542K + N347K	0 (0)	1 (4)	0 (0)	0 (0)	0 (0)	1 (1)
		E545K + p.*1069Wext*4 (Nonstop extension)	0 (0)	0 (0)	1 (8)	0 (0)	0 (0)	1 (1)
		H1047R + I1058L + I1058F	0 (0)	0 (0)	1 (8)	0 (0)	0 (0)	1 (1)
	Others non-PIK3CA		10 (50)	0 (0)	0 (0)	1 (7)	0 (0)	11 (14)
	No mutation known		4 (20)	0 (0)	0 (0)	0 (0)	6 (86)	10 (13)

NA= Not applicable, not breast-exclusive cohorts. ET= Endocrine therapy. AI= Aromatase inhibitor.

* Calculated from breast cancer patients exclusive.

Table 5. Demographic characteristics of enrolled patients and mutation distribution as per enrolment screening.

3.3 Pharmacokinetics

In the dose escalation arm, taselisib had similar PK properties in the 2/100mg and 2/125mg cohorts with mean plasma C_{max} levels at 29.6 and

31.0 ng/mL respectively. Exposure of the compound was also comparable at mean 504.5 and 554.8 h*ng/mL. Patient variability was evident in the 4/100mg cohort (n=2) with a mean C_{max} of 109.3 ng/mL and an AUC of 1708.6 h*ng/mL. At dose levels 2/100mg and 2/125mg, the mean was not significantly different to previously observed historic data from PMT4979g study given the patient variability. For palbociclib, mean C_{max} values were 78.5, 86.8 and 120 ng/mL in the three cohorts (2/100, 4/100 and 2/125mg). Mean exposure of palbociclib in the dose escalation arm gave values of 1324, 1398 and 2066 h*ng/mL respectively. The 2/100mg dose level is very comparable to the historic data from the A5481001 single agent study (mean C_{max} 95 ng/mL and mean exposure AUC 1633ng*hr/mL) and differences observed in the 2/125mg dose level were considered not significant given the patient variability. There was only data from two patients dosed on the 4/100mg cohort. This data when normalized to the 125mg dose was within 15% of the single agent study data. Mean taselisib and fulvestrant PK parameters for both taselisib and palbociclib in the escalation phase are shown in **table 6** and PK curves are shown in the following **figure 6**.

Cohort	Subject	Tmax (h)	Cmax (ng/mL)	AUC (h*ng/mL)
Taselisib				
2/100	Mean	3.0	29.58	504.53
	Median	2.0	26.35	512.25
	Range	4.0	16.80	130.40
	CV%	66.7	26.50	12.40
4/100	Mean	3.0	109.30	1708.55
	Median	3.0	109.30	1708.55
	Range	2.0	115.40	1719.70
	CV%	47.1	74.70	71.20
2/125	Mean	4.6	30.99	554.83
	Median	4.0	30.30	541.65
	Range	6.0	22.30	498.14
	CV%	41.2	24.90	26.00
Palbociclib				
2/100	Geometric Mean	5.8	78.46	1324.24
	Median	6.0	82.15	1377.35
	Range	4.0	48.40	647.20
	CV%	29.1	27.1	21.62
4/100	Geometric Mean	3.5	86.77	1398.20
	Median	4.0	88.35	1421.60
	Range	4.0	33.30	513.80
	CV%	91.0	27.47	26.28
2/125	Geometric Mean	5.0	119.94	2066.46
	Median	6.0	109.50	2012.50
	Range	6.0	116.10	1511.80
	CV%	56.9	26.04	19.68

Table 6. PK parameters for taselisib and palbociclib in the escalation phase (part A).

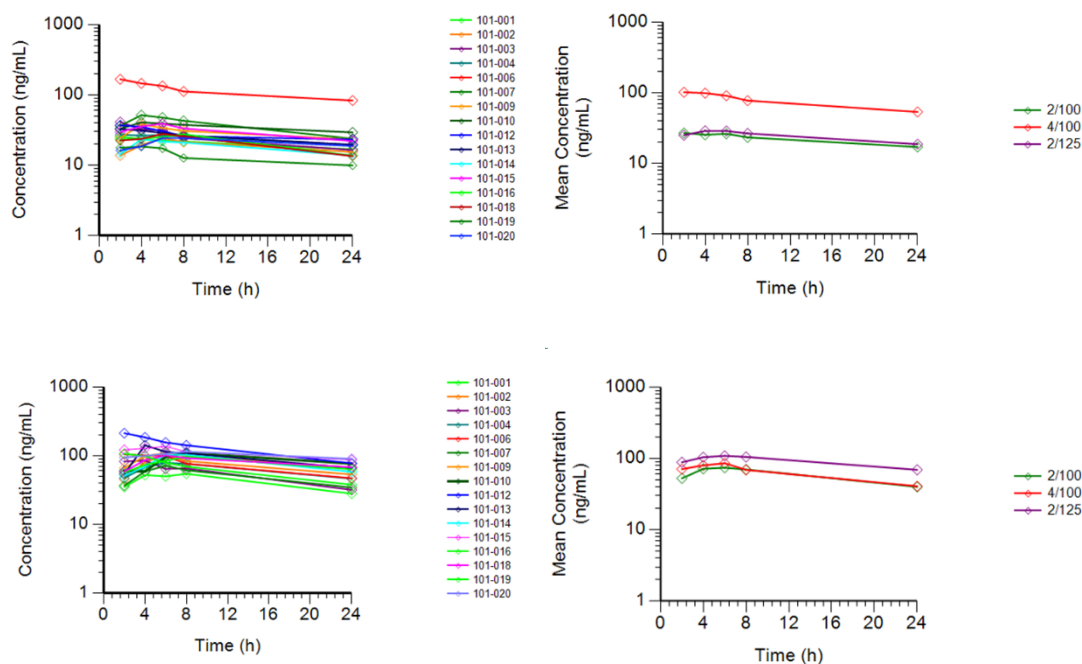


Figure 6. Pharmacokinetic analysis in the escalation phase (part A) presented as all patients analysed and per dose level for taselisib (top) and palbociclib (bottom). Three patients excluded from the analysis following dose interruption/reduction due to serious adverse event (SAE).

Although dose expansion arm was limited in PK sampling there is no suggestion of any drug-drug interaction in the double combination study (part B2) at steady state (C1D15). Based on limited data, fulvestrant does not appear to have any effect on either the palbociclib or taselisib plasma concentrations at steady state (C1D15) in the triplet combination study (part B1). Data reflecting previous statement can be found in the following **table 7**.

Dose Escalation Study	Taselisib concentration (ng/mL)							
	C1D1			C1D15			C2D15	
	Pre	2h	4h	Pre	2h	4h	Pre	2h
Mean	BLOQ	10.8	8.6	15.8	26.9	25.5	22	32.9
Geometric Mean	BLOQ	10.4	8.5	15.7	25.1	25	21.1	32.4
Median	BLOQ	9.9	8.9	16.1	26.4	25.1	26	33.3
n	4	4	4	4	4	4	4	4
Conc > to Pre-dose		10.8	8.6		11.2	9.7	10.9	

Dose Expansion B1	Taselisib Concentration (ng/mL)				Fulvestrant Concentration (ng/mL)			
	C1D15		C2D15		C1D15		C2D15	
	Pre	4h	Pre	4h	Pre	4 hr	Pre	4 hr
Mean	17.6	27.4	19.8	27.7	11.8	11.9	17.6	16.6
Geometric Mean	16.6	26.1	17.5	25.6	10.8	10.9	16.3	15.4
Median	17.7	26.4	15.8	23.2	9.8	10.1	16.5	15.6
n	26	22	24	23	19	17	19	18
Conc > to Pre-dose	9.9		8		0.1		-1.0	

Dose Expansion B2	Taselisib Concentration (ng/mL)			
	C1D15		C2D15	
	Pre	4h	Pre	4h
Mean	21.2	30.6	24.5	31.4
Geometric Mean	16.8	26.4	18.9	26.6
Median	16.9	29.9	18.7	25.3
n	24	23	19	15
Conc > to Pre-dose	9.3		6.9	

Dose Escalation Study	Palbociclib Concentration (ng/mL)							
	C1D1			C1D15			C2D15	
	Pre	2h	4h	Pre	2h	4h	Pre	2h
Mean	BLOQ	16.4	24	36.7	52.7	71.6	49.3	65.1
Geometric Mean	BLOQ	15.5	22.2	34.8	50	70.4	45.5	64.5
Median	BLOQ	15.7	20.9	35.6	46.5	74.5	58.9	67.5
n	4	4	3	4	4	4	3	3
Conc > to Pre-dose		16.4	24		16	34.9	15.8	

Dose Expansion B1	Palbociclib Concentration (ng/mL)				Fulvestrant Concentration (ng/mL)			
	C1D15		C2D15		C1D15		C2D15	
	Pre	4hr	Pre	4hr	Pre	4 hr	Pre	4 hr
Mean	53.8	79.8	55.7	86.2	11.8	11.9	17.6	16.6
Geometric Mean	49.8	70.4	52.2	78.4	10.8	10.9	16.3	15.4
Median	55.2	79.3	50.9	87.6	9.8	10.1	16.5	15.6
n	20	16	19	19	19	17	19	18
Conc > to Pre-dose	26		30.5		0.1		-1.0	

Dose Expansion B2	Palbociclib Concentration (ng/mL)			
	C1D15		C2D15	
	Pre-dose	4hr	Pre-dose	4hr
Mean	55.6	78	62.6	71
Geometric Mean	50.3	72.5	57.8	64.5
Median	45.4	70.3	56	70.8
n	21	21	18	15
Conc > to Pre-dose	22.5		8.4	

Table 7. Pharmacokinetic (PK) analysis of taselisib and palbociclib concentrations in both triplet (with fulvestrant added) and doublet combination in the expansion phase (part B1 and B2). PK data from escalation phase also provided for comparison.

3.4 Pharmacodynamics

In the dose escalation part, platelet rich plasma (PRP) was analysed from 20/20 patients at baseline and on-treatment for AKT and GSK3 β phosphorylation. At the 2mg taselisib dose (in dose levels 3 and 4) there was 39% decreased AKT phosphorylation at C1D1 4h ($p < 0.05$), 21% decrease at C1D15 6h ($p < 0.05$) and 30% decrease at C1D15 8h ($p < 0.01$) and 19% decrease in GSK3 β phosphorylation at C1D1 4h ($p < 0.01$), 23% decrease at C1D15 6h ($p < 0.01$) and 27% decrease at C1D15 8h ($p < 0.001$) (**figure 7**). There was a 24% increase in phosphorylation of AKT at C1D8 pre-dose ($p < 0.05$) and also a 21% increase in GSK3 β phosphorylation at C1D8 pre-dose ($p < 0.01$) which may indicate compensatory upregulation often seen in PI3K/AKT inhibition, potentially suggesting incomplete PI3K pathway inhibition.

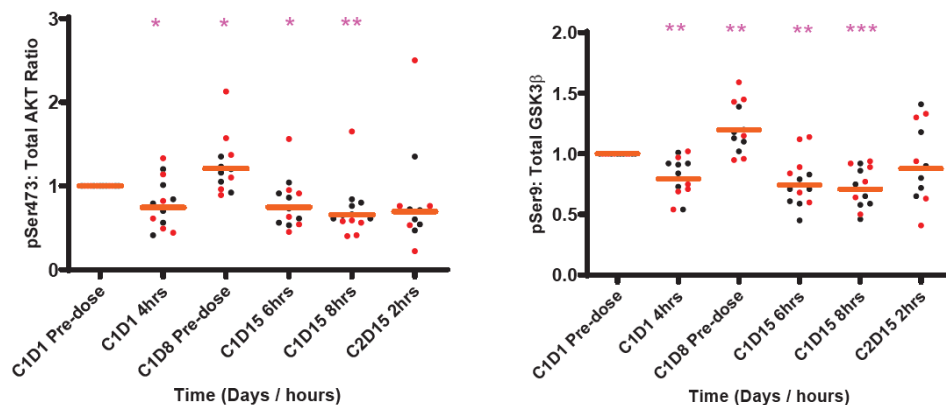


Figure 7. Pharmacodynamic (PD) analysis in platelet-rich plasma (PRP) for pSer473: total AKT ratio (left) and pSer9: total GSK3 β ratio (right) at dose levels 3 & 4 (taselisib 2mg). * $p < 0.05$, ** $p < 0.01$, *** $p < 0.001$, paired t-test.

Five patients treated at different schedules in part A were analysed for biomarkers of interest on their tumour tissue sample at C1D1 pre-dose (Baseline), C1D15 pre-dose and disease progression timepoints. Grouping all these five patients, there was a significant 25% decrease in the ratio of phosphoSer780-Rb to total Rb at C1D15 pre-dose when compared to C1D1 pre-dose ($p < 0.05$) in the five patient tumour samples indicating CDK4/6 signalling modulation as predicted for palbociclib treatment (**figure 8**).

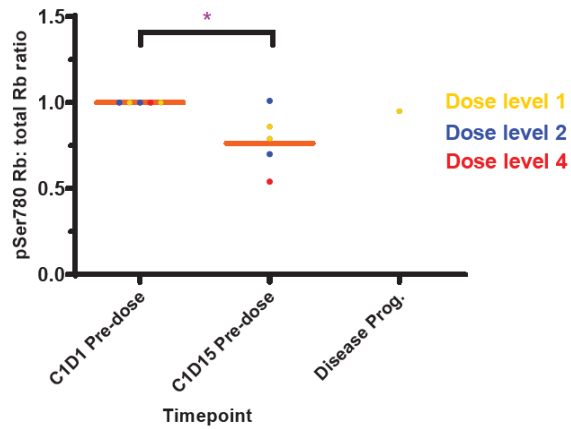


Figure 8. Pharmacodynamic (PD) analysis of pSer780 Rb: total Rb ratio in tumour samples for all dose levels grouped showing significant decrease at C1D15 indicating target modulation. *Paired t-test: $p < 0.05$.

No significant modulation to the biomarker ratios pSer473-AKT: total AKT, pSer9-GSK3 β : total GSK3 β and pThr421/Ser424-P70S6K: total P70S6K was found (**figure 9**). It was not possible to compare the molecular effects of taselesib at different dose levels due to small number of patients assessed.

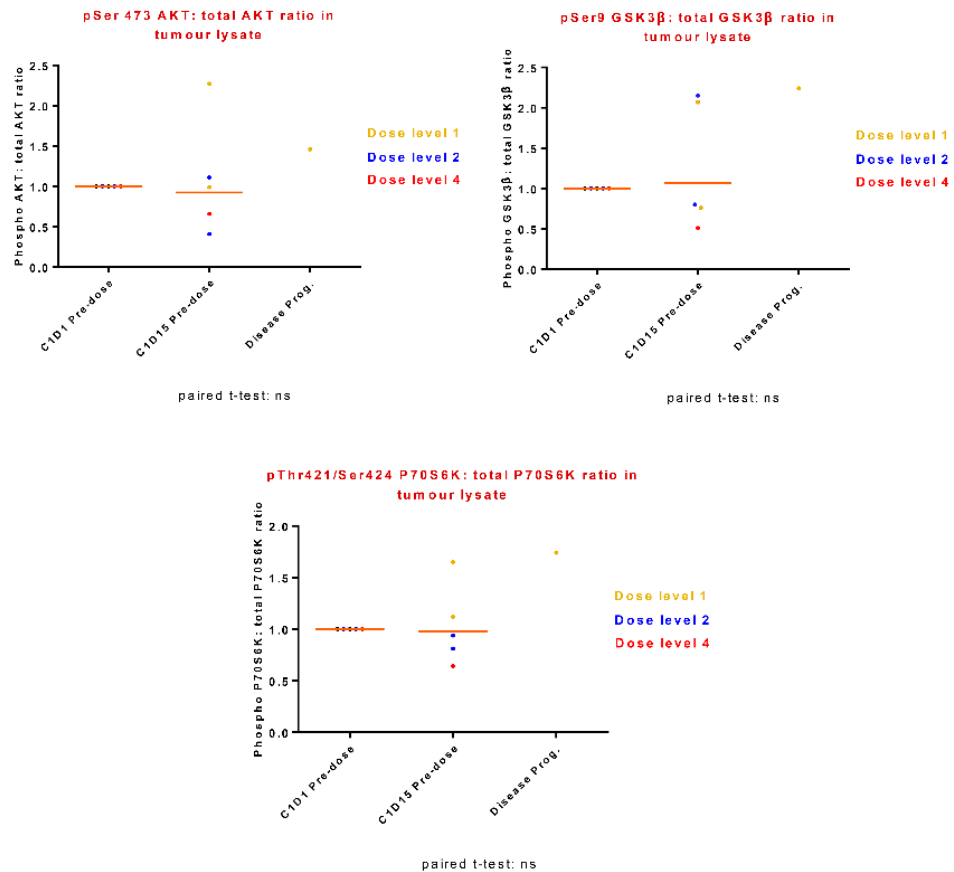


Figure 9. Pharmacodynamic (PD) analysis of pSer473-AKT: total AKT, pSer9-GSK3β: total GSK3β and pThr421/Ser424-P70S6K: total P70S6K in tumour samples for all dose levels grouped. Paired t-test: $p > 0.05$.

3.5 Safety and RDP2

In part A (dose escalation), patients were enrolled in dose levels 1, 2, 3 and 4 as shown in **figure 10**. Three dose limiting toxicities (DLTs) appeared in 2 patients when taseleisib was administered at the 4mg dose in dose level 2, in the form of grade 3 mucositis, grade 3 hyperglycaemia and grade 3 fatigue. The final recommended dose for phase 2 (RDP2) was established as 125mg palbociclib on a 3-week on/1-week off schedule plus 2mg taseleisib continuously administered. A safety review committee was held before the enrolment in part B started, and it was decided to administer palbociclib at the 100mg dose for the first cycle and then escalate to 125mg in the absence of grade 3/4 myelosuppression.

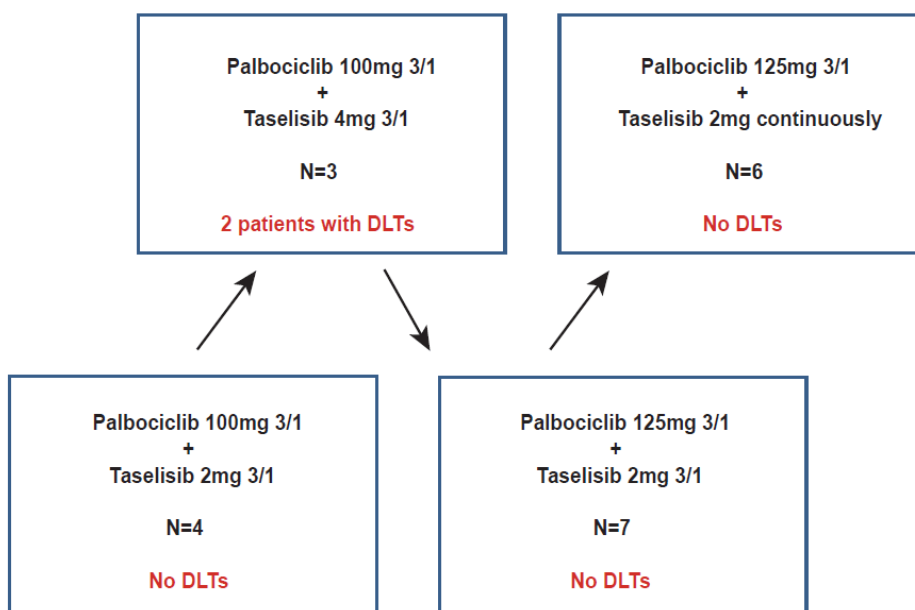


Figure 10. Part A (escalation phase) final patient recruitment and dose-limiting toxicities observed in each dose level. 3/1= three weeks on/one week off.

A data snapshot for final analysis was performed in August 2019. Safety was acquired and organized in conjunction with ICR Clinical Statistics Unit with subsequent review and grouping of equivalent terminologies for the same adverse event. A complete record of all adverse events reported in >10% of the patients is shown in the following **table 8**.

All adverse events reported >10%	Escalation		Expansion								Total (n=78)	Total %	G3-4 %
	A (n=20)		B1 (n=25)		B2 ER-ve (n=12)		B2 solid tumours (n=14)		B3 (n=7)				
	G.1-G.2	G.3-G.4	G.1-G.2	G.3-G.4	G.1-G.2	G.3-G.4	G.1-G.2	G.3-G.4	G.1-G.2	G.3-G.4			
Neutropenia	12	6	8	15	4	7	6	4	2	5	69	88.5	47.4
Thrombocytopenia	10	4	10	1	7	0	8	0	7	0	47	60.3	6.4
Anaemia	11	3	11	1	4	0	7	1	4	0	42	53.8	6.4
Fatigue	10	1	11	0	4	0	5	0	6	0	37	47.4	1.3
Mucositis oral	4	1	10	1	6	0	3	1	3	1	30	38.5	5.1
Diarrhoea	9	1	8	1	3	1	2	0	5	0	30	38.5	3.8
Nausea	9	0	10	0	2	0	5	0	0	0	26	33.3	0.0
Leukopenia	2	1	3	7	5	1	0	1	1	3	24	30.8	16.7
Rash	6	2	6	2	3	1	0	1	2	0	23	29.5	7.7
Abdominal pain	5	0	8	1	1	0	6	0	1	1	23	29.5	2.6
ALT Elevation	5	1	6	2	1	0	1	2	3	0	21	26.9	6.4
Mucosal inflammation	10	0	3	0	2	1	2	0	0	0	18	23.1	1.3
Cough	2	0	10	0	3	0	1	0	2	0	18	23.1	0.0
Constipation	4	0	5	0	2	0	4	0	2	0	17	21.8	0.0
AST Elevation	6	0	4	2	0	0	3	0	0	1	16	20.5	3.8
Headache	2	1	5	0	3	0	3	0	2	0	16	20.5	1.3
Vomiting	4	0	3	2	1	0	3	1	1	0	15	19.2	3.8
Hypokalaemia	2	1	2	1	0	0	6	1	1	0	14	17.9	3.8
Decreased appetite	8	0	6	0	0	0	0	0	0	0	14	17.9	0.0
Dyspnoea	2	0	4	4	1	0	0	0	1	0	12	15.4	5.1
Musculoskeletal pain	3	0	2	1	2	0	1	0	2	0	11	14.1	1.3
Oropharyngeal pain	1	0	4	0	1	0	0	0	5	0	11	14.1	0.0
Alkaline phosphatase increased	3	0	2	0	1	0	1	1	1	0	9	11.5	1.3
Dyspepsia	1	0	7	0	1	0	0	0	0	0	9	11.5	0.0
Pain in extremity	2	0	4	0	0	0	0	0	3	0	9	11.5	0.0
Rhinitis	0	0	4	0	2	0	0	0	3	0	9	11.5	0.0
Upper respiratory tract infection	4	0	1	0	1	0	0	0	3	0	9	11.5	0.0
Gamma-glutamyltransferase increased	0	2	2	2	0	1	0	1	0	0	8	10.3	7.7
Hyponatraemia	1	3	0	1	0	1	1	1	0	0	8	10.3	7.7
Abdominal distension	2	0	2	1	0	0	2	0	1	0	8	10.3	1.3
Pyrexia	4	0	3	0	0	0	0	0	1	0	8	10.3	0.0
Urinary tract infection	1	0	2	0	0	0	2	0	3	0	8	10.3	0.0

Table 8. All adverse events reported for >10% patients with grading.

Focusing in the 58 patients enrolled in the expansion cohorts that ended up receiving the RDP2, the most frequently reported all-grade adverse events (AEs) across them were neutropenia (88%), thrombocytopenia (57%),

anaemia (48%), fatigue (45%), mucositis (41%), leukopenia (36%) and diarrhoea (34%). Other all-grade clinically relevant toxicities included rash (26%) and ALT elevation (26%). The most common grade 3/4 AEs in the 58 expansion phase patients were neutropenia (53%) and leukopenia (21%), while the most common grade 3/4 treatment-related AEs were again neutropenia (53%) and leukopenia (19%).

Overall, 24/78 patients (30.8%) had 35 serious adverse events (SAEs) of which 9/35 of these (25.7%) were considered as definitely, probably or possibly related to treatment. There were no treatment-related deaths. A detailed count of SAEs, serious adverse reactions (SARs) and suspected unexpected serious adverse reactions (SUSARs) is reported in the following **table 9**:

	Palbo-100mg, Tase-2mg and 21-day cycle N=4		Palbo-100mg, Tase-4mg and 21-day cycle N=3		Palbo-125mg, Tase-2mg and 21-day cycle N=7		Palbo-125mg, Tase-2mg and 28-day cycle N=6		Total Part A N=20		Total Part B1 N=25		Breast N=12		Solid tumour N=14		Total Part B2 N=26		Total Part B3 N=7	
	n	%	n	%	n	%	n	%	n	%	n	%	n	%	n	%	n	%	n	%
SAE	0	0	4	12	5	15	0	0	9	27	6	18	4	12	5	15	9	27	0	0
SAR	0	0	2	6	0	0	0	0	2	6	6	18	0	0	0	0	0	0	1	3
SUSAR	0	0	0	0	0	0	0	0	0	0	0	0	0	0	0	0	0	0	0	0

Table 9. Serious adverse events (SAEs), serious adverse reactions (SARs) and suspected unexpected serious adverse reactions (SUSARs) in the different cohorts of the study.

Dose interruptions, defined as any missed dose during the cycle due to AEs, patient error or any other event leading to it, were required for taselesib in 45 of 78 patients (58%) and for palbociclib in 39 of 78 (50%) patients. In part B1, 1 of 25 patients (4%) required interruption for fulvestrant, and in part B3 4/7 (57.1%) for letrozole. Dose reductions for taselesib were required in 13 of 78

(17%) patients enrolled, 15 of 78 (19%) for palbociclib. There were delays, defined as any delay starting a cycle of treatment, in 28 of 78 patients (36%) for taselisib and in 41 of 78 (53%) for palbociclib. Treatment was discontinued in 54 of 77 patients (70%) following radiographical progression, 13 of 77 (17%) following clinical progression, 3 of 77 (4%) due to adverse events and 7 of 77 (9%) due to other factors. A detailed summary of treatment interruption, reduction, delay and discontinuation per part and cohort can be found in **table 10** as follows:

Part A (N=20):

Treatment	Interruption		Reduction		Delay		Discontinuation	
	n	%	n	%	n	%	n	%
Taselisib (n=20)	10	50	4	20	5	25	6	20
Palbociclib (n=20)	9	45	2	10	11	55	5	25

Part B1 (N=25):

Treatment	Interruption		Reduction		Delay		Increase		Extra doses		Discontinuation	
	n	%	n	%	n	%	n	%	n	%	n	%
Taselisib (n=25)	19	76	5	20	13	52	0	0	0	0	8	32
Palbociclib (n=25)	16	64	7	28	16	64	2	8	2	8	8	32
Fulvestrant (n=25)	1	4	0	0	0	0	0	0	0	0	4	16

Part B2 breast and solid tumours (N=26):

	Treatment	Interruption		Reduction		Increased		Delayed		Discontinuation	
		n	%	n	%	n	%	n	%	n	%
Breast (n=12)	Taselisib	6	50	2	16.7	0	0	4	33.3	5	41.7

	Palbociclib	4	33.3	1	8.3	2	16.7	6	50	5	41.7
Solid tumour (n=14)	Taselisib	5	35.7	1	7.1	0	0	1	7.1	11	78.6
	Palbociclib	4	28.6	3	21.4	1	7.1	3	21.4	10	71.4
All B2 patients (n=26)	Taselisib	11	42.3	3	11.5	0	0	5	19.2	16	61.5
	Palbociclib	8	30.7	4	15.4	3	11.5	9	34.6	15	57.7

Part B3 (N=7):

Treatment	Interruption		Reduction		Delay		Discontinuation	
	n	%	n	%	n	%	n	%
Taselisib	5	71.4	1	14.3	5	71.4	0	0
Palbociclib	6	85.7	2	28.6	5	71.4	0	0
Letrozole	4	57.1	0	0	0	0	0	0

Table 10. Treatment administration in the different cohorts of the study.

3.6 Response analysis

In part A (escalation phase), there were 19/20 (95%) evaluable patients. Response rate (partial or complete response) was 5.3% (1/19, 95% CI 0.1 – 26.0) and clinical benefit rate (partial or complete response or SD \geq 24 weeks) in the evaluable population was 5.3% (1/19, 95% CI 0.1 – 26.0).

For part B1, 25 patients with PIK3CA-mt ER+ve HER2-ve advanced breast cancer were treated with the triplet of taselisib plus palbociclib plus fulvestrant, one patient was not assessable for the primary endpoint per protocol as they had not completed first cycle of treatment. The confirmed objective response rate (ORR) was 37.5% (9/24, 95% CI 18.8-59.4). A waterfall plot with best percentage of tumour change and overall response is

depicted in **figure 11**. Clinical benefit rate (CBR) was 58.3% (14/24, 95% CI 36.6-77.9). There were objective responses even amongst patients with several prior lines of chemotherapy for advanced disease and in patients having received prior fulvestrant, everolimus or both.

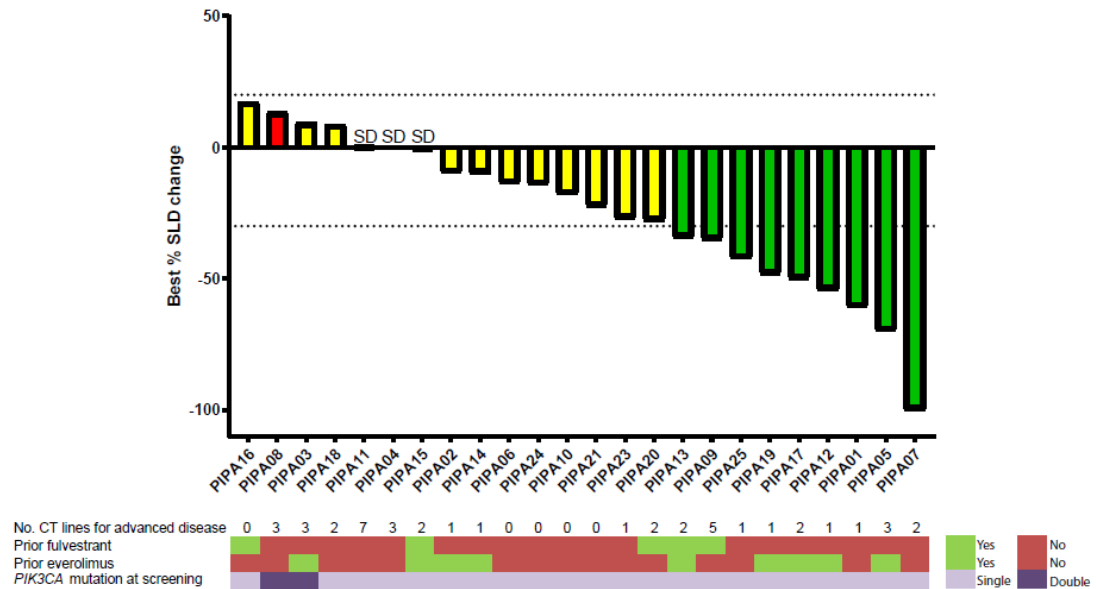


Figure 11. Waterfall plot with best percentage of tumour change from baseline sum of the longest diameter in target lesions and best confirmed overall response for evaluable patients in part B1 (N=24) [89]. SLD= Sum of the longest diameter. Best overall response colour code: green= partial response (PR), yellow= stable disease (SD), red= progressive disease (PD). Below a schematic view of prior relevant treatment.

Part B2 recruited a total of 26 patients. Twelve patients with *PIK3CA*-mt ER-ve advanced breast cancer (9 TNBC and 3 HER2+ve) were treated with palbociclib plus taselisib, and 10 of them were evaluable for efficacy (8TNBC and 2 HER2+ve). The ORR was 10% (1/10, 95% CI 0.2-26.5) and CBR 30% (3/10, 95% CI 6.7-65.2). The only objective response identified was in a TNBC patient. A waterfall plot illustrating this is shown in **figure 12**.

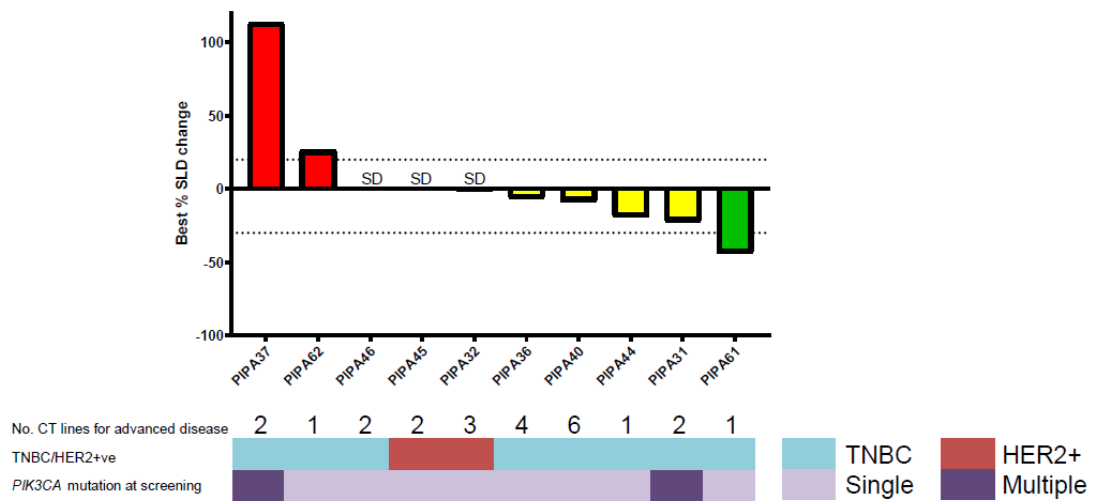


Figure 12. Waterfall plot with percentage of tumour change and best overall response for evaluable ER-ve breast patients in part B2 (N=10) [89]. Below a schematic view of phenotypic classification (TNBC vs ER-ve/HER2+ve) and single vs multiple PIK3CA mutation as per enrolment.

There were 14 patients with solid tumours of various subtypes treated in part B2; 4 *PIK3CA*-mt colorectal adenocarcinoma, 3 *PIK3CA*-mt ER+ve/HER2-ve breast cancer (included as part of the solid tumours subcohort), 1 *PIK3CA*-mt high grade serous ovarian cancer, 1 *PIK3CA*-mt clear cell ovarian carcinoma, 2 *PIK3CA*-mt non-small cell lung cancer (NSCLC), 1 *PIK3CA*-mt endometrial cancer, 1 *PIK3CA*-mt cervical cancer (adenosquamous carcinoma) and 1 *PIK3CG*-mt anaplastic oligodendroglioma. For the 12 evaluable solid tumours in part B2, ORR was 0% (0/12, 95% CI 0-26.5) and CBR 16.7% (2/12, 95% CI 2.1-48.4). **Figure 13** shows waterfall plot with responses.

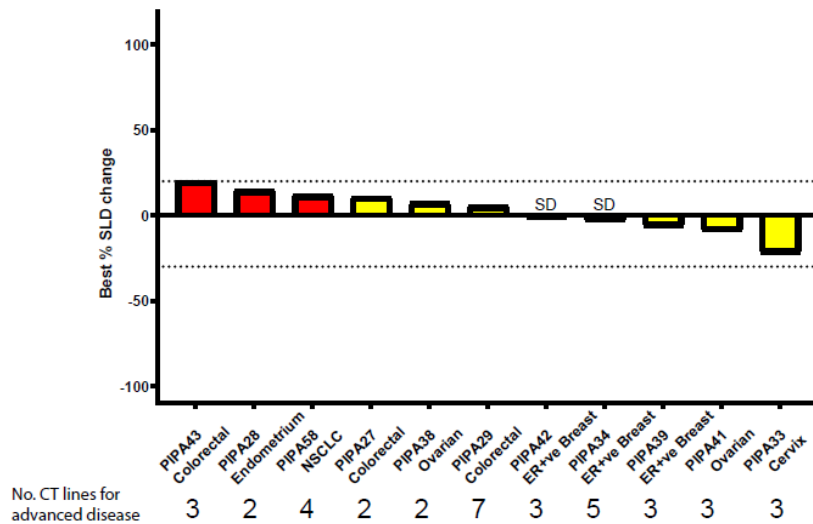


Figure 13. Waterfall plot with percentage of tumour change and best overall response for evaluable solid tumours patients in part B2 with follow-up to assess confirmed response (N=11). Below a schematic view of tumour type classification

Part B3 recruited 7 patients, 6 of whom were evaluable. Measurable disease was not a requirement for B3 entry and only 2 patients had measurable disease with target lesions to follow. ORR was 0% (0/6, 95% CI 0-45.9) and CBR 50% (3/6, 95% CI 11.8-88.1).

3.7 Exploratory survival

An exploratory PFS analysis for the different cohorts of patients enrolled in the expansion phase was conducted, although the fact that this was a non-randomized trial, and the population had a wide range of prior lines of treatment limits any robust conclusions in this regard.

For the 24 response evaluable patients enrolled in part B1, median PFS was 7.2 months (95% CI 3.9-9.9) as shown in **figure 14**.

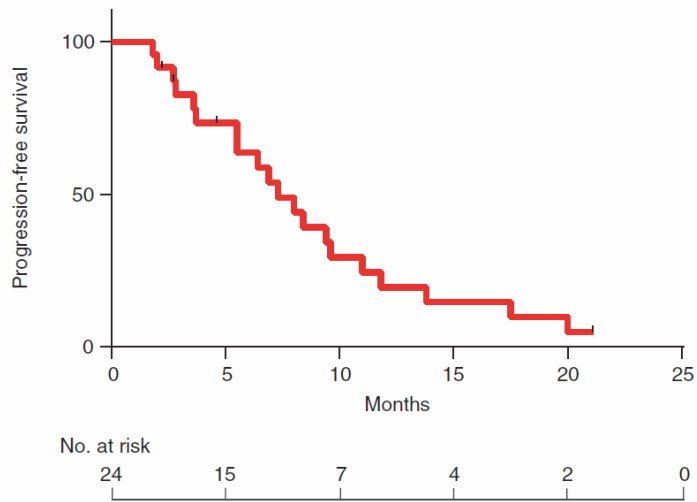


Figure 14. PFS for patients in part B1 (treated with the triplet palbociclib, taselesib and fulvestrant).

As the population recruited into part B2 was very heterogeneous, efficacy analyses were conducted separately for the *PIK3CA*-mt ER-ve breast cancer patients and the rest of the patients enrolled as solid tumour sub-cohort. For the 10 response evaluable ER-ve breast cancer patients enrolled in part B2, median PFS was 3.6 months (95% CI 1.7-5.6), shown in **figure 15**.

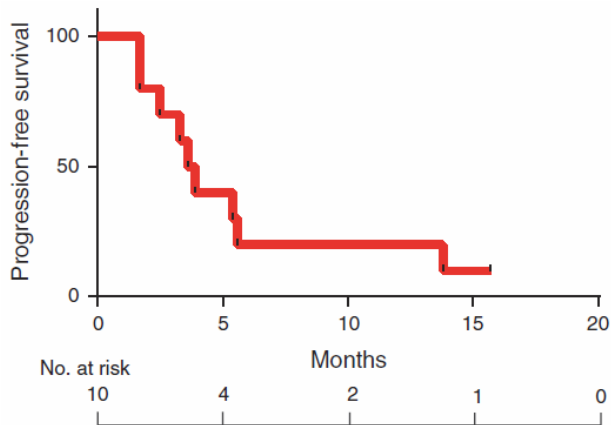


Figure 15. PFS for ER-ve breast patients enrolled in part B2 (treated with the doublet palbociclib and taselesib).

For the 12 response evaluable solid tumours patients enrolled in part B2 there was median PFS of 3.8 months (95% CI 1.2-5.0), illustrated in **figure 16**.

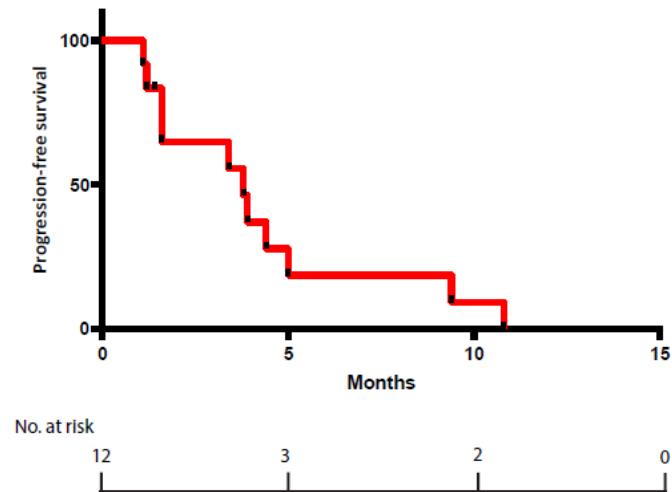


Figure 16. PFS for solid tumour patients enrolled in part B2 (treated with the doublet palbociclib and taselisib).

Finally, for the 7 response evaluable *PIK3CA*-agnostic ER+ve HER2-ve breast cancer patients treated with the triplet of palbociclib, taselisib and letrozole enrolled in part B3, median PFS was 8.7 months (95% CI, 1.6-24.2). This small cohort was less pre-treated than B1, with median 2 lines of prior systemic treatment and median 0 lines of prior chemotherapy for advanced disease.

3.8 Discussion

The clinical part of this study provided sufficient evidence for the safe administration of the combination of palbociclib and taselisib in a range of different solid tumours, with the final RDP2 established in the usual dose for palbociclib (125mg) in combination with a reduced dose of taselisib (2mg). This observation was supported by PK analysis not showing any suggestion of drug-drug interaction and by the adverse event profile described here, which overall shows the expected pattern of toxicity. As anticipated, there is a high rate of myelosuppression in the form of neutropenia, in line with

multiple prior reports in other studies involving palbociclib. This adverse event is a constant for CDK4/6 inhibitors and is a result of the bone marrow cytostatic effect induced by these drugs. This neutropenia did not lead to febrile neutropenia events, also matching prior reports. PI3K class-related toxicities like oral mucositis, diarrhoea and rash also appeared at relatively predicted rates, but the low rate of treatment discontinuation following AEs likely reflects the favourable safety profile of the combination and strongly suggests that this is a manageable strategy to further explore clinically. It is possible that treatment delays may have reduced the efficacy of the triplet combination, and future triple combination trials should be designed to limit the incidence of such delays.

Taselisib was finally administered at a reduced dose in the expansion phase (2mg), however there was pharmacodynamic evidence of target modulation even at this dose, as reflected in the fact that samples taken at C1D15 6h and 8h showed significant suppression. Overall, this indicates that tselisib is inhibiting the target. However, there was a rebound found on the C1D8 sample, suggesting that the PI3K inhibition may have not been sustained across all cycle. In addition, the absence of inhibition in biomarker ratios pSer473-AKT:total AKT and pSer9-GSK3 β :total GSK3 β in tumour lysate samples suggests the possibility that the amount of tselisib used was not high enough to modulate these biomarkers in the tumours via PI3K inhibition, although it must be noted that an alternative possibility for this negative finding could be the fact that there were insufficient tumours analysed and additionally some degree of variability when grouping different dose levels is inevitable. Further development of triplet combinations with alternative PI3K or AKT inhibitors may maximise the potential of such triplet therapy by optimising PI3K-AKT pathway suppression.

In terms of efficacy, this trial shows encouraging response rates and although exploratory suggests good survival outcome for patients receiving the triplet combination, despite being a heavily pre-treated population. The main limitation of these clinical findings is the fact that is not possible from a single arm study like this to determine exactly how much efficacy can be

attributed to each of the drugs included in the triplet. In fact, the excellent efficacy previously shown for palbociclib in combination with fulvestrant in the PALOMA-3 trial, and the significant efficacy advantage of alpelisib in combination with fulvestrant shown in the SOLAR-1 trial, can potentially preclude any efficacy synergy shown in this study. However, there is evidence in this work that suggests the triplet combination can represent an improvement. The biggest and most reliable source of data for palbociclib and fulvestrant treatment in a pretreated population to date is the randomized phase 3 PALOMA-3. Here, there was an ORR of 24.6% for patients with measurable disease treated with the combination (N=138) and specifically 23% for those patients with measurable disease and a *PIK3CA* mutation (N=57) [100]. Results shown in the PIPA trial should be directly compared to PALOMA-3 and represent an improvement in terms of ORR. Moreover, the population enrolled in PIPA is much more pretreated. PALOMA-3 allowed for 1 line of chemotherapy in the advanced disease but only 33% of patients treated with the combination had received it in this context. In PIPA, median chemotherapy lines for advanced disease in patients treated with the palbociclib, taselesib and fulvestrant triplet was 1, but there were 12/24 evaluable patients (50%) receiving 2 or more advanced chemo lines. Also, PALOMA-3 excluded for prior fulvestrant and/or everolimus while this study allowed for it and 11/24 evaluable patients (46%) had prior fulvestrant, everolimus or both. There is broad evidence that prior lines of chemotherapy treatment can heavily decrease response rates in subsequent lines of therapy for metastatic breast cancer patients, with responses rates falling approximately by half in every subsequent line [106-108].

Taken together, there is sufficient higher activity shown in this study to support the hypothesis of combination efficacy between palbociclib and taselesib.

Chapter 4. Baseline prognostic and predictive biomarkers

4.1 Introduction

The translational research conducted for the PIPA study has involved a number of pre-planned analyses to search for potential prognostic and predictive biomarkers. Tissue samples were used for biomarker studies with a view to perform ultra-low whole-genome sequencing (ulWGS) in order to explore a range of potential baseline prognostic copy-number events and histopathology techniques (both IHC and FISH) to test for potential predictive biomarkers based in prior literature.

The ulWGS analysis was carried in order to have an estimation of baseline CNV for genes of interest that are known to play an important role in cell-cycle regulation (*CCND1*, *CCNE1*, *CDK2*, *CDK4*, *CDK6* and *RB1* among others), in the PI3K pathway (*AKT1*, *AKT2*, *AKT3*, *PIK3CA* and *PTEN*) or known to have a prominent biological function in other pathways relevant to breast cancer or in cancer cell signalling in general (*EGFR*, *ERBB2*, *FGFR1*, *KRAS*, *NRAS*, *MYC* and *TP53* among others) and compare this baseline CNV profile with survival of patients enrolled in the trial.

Cyclin D1 was additionally explored in this study using both IHC to test protein expression and FISH assays to determine potential amplification of *CCND1*, the gene encoding cyclin D1, the latter having been also explored with ulWGS. Cyclin D1 is a well described protein which is involved in the cell-cycle progression from G1 to S phase among other cyclin-CDK complexes. Cyclin D1 couples with CDK4 and 6, which in turn leads to phosphorylation of the Rb protein thereby relieving the suppression of E2F family of transcription factors and allowing S-phase entry via promotion of E-type cyclin and CDK2 expression and resulting in cell-cycle progression [109]. High expression of cyclin D1 is a common feature of ER+ve breast cancer [16, 110] and has been linked to worse prognosis in this subtype [62, 111]. However, there have been conflicting reports in the past showing good prognosis associated with cyclin D1 expression [61, 112]. This analysis

aimed to test amplification of *CCND1* and overexpression of cyclin D1 in patients enrolled in the PIPA trial, with a view to specifically test in the *PIK3CA*-mt ER+ve HER2-ve metastatic breast cancer group treated with the triplet combination whether it has a value as a prognostic biomarker.

Cyclin E1 was also explored using IHC in this study, to test if different levels of protein expression can be used as a biomarker for treatment efficacy also on the triplet combination. In the cell-cycle, cyclin E1 couples with CDK2 to promote S-phase entry, and bypass activation of CDK2 has been previously suggested as a mechanism of resistance to CDK4/6 inhibitors [113] with pre-clinical work correlating high cyclin E expression with palbociclib resistance [38]. There is also clinical evidence from the randomized PALOMA-3 trial that showed high levels of cyclin E1 mRNA expression conferring relative resistance to patients treated with palbociclib plus fulvestrant [63]. This study aimed to test if high levels of cyclin E1 measured at the protein level can also predict for efficacy in a triplet combination that included palbociclib.

Androgen receptor (AR) expression is the defining feature of a distinctive TNBC subtype called luminal androgen receptor (LAR), defined by Lehmann et al, which also displays high frequency of *PIK3CA* mutations that makes it more resembling to common ER+ve luminal subtypes, despite having absence of ER and PR expression [40]. Theoretically, targeting the androgen receptor could be used as a non-chemotherapy targeted approach, and such strategy has led to the conduction of clinical trials showing modest activity of drugs antagonizing AR in the metastatic setting [41, 42]. There is also pre-clinical evidence that CDK4/6 inhibitors have an enhanced activity for this subtype and that there is a predicted synergy when combined with PI3K inhibitors [39]. Although only a small number of TNBC patients went into the PIPA trial, all of them were defined as having a *PIK3CA* mutation, and therefore it was theorized that a high proportion of them would show some degree of AR expression and that this could be used as a predictive biomarker for the doublet combination of palbociclib and taselesib.

4.2 Samples analysed for baseline biomarker work

All patients enrolled in the study were requested to provide a mandatory archival sample of their tumour and an optional progression sample where suitable for re-biopsy. No samples from the escalation phase other than those coming from breast cancer patients were used for translational analyses as an intent to have an homogeneous population treated with the recommended combination doses while allowing for enrichment of breast cancer patients to further conduct biomarker analyses. As a result, a total of 59 archival FFPE blocks were finally retrieved for translational analysis. After external pathology review, these consisted in 4 blocks coming from the breast patients enrolled in part A (2 ER+ve/HER2-ve, 1 ER+ve/HER2+ve, 1 TNBC), 25 from patients in part B1 (all ER+ve/HER2-ve breast cancer patients), 26 from patients coming from part B2 (9 TNBC, 3 ER-ve/HER2+ve breast patients, 3 ER+ve/HER2-ve breast included as solid tumours, 4 colorectal adenocarcinoma, 2 non-small cell lung cancer, 1 high-grade serous ovarian cancer, 1 clear cell ovarian carcinoma, 1 endometrial cancer, 1 adenosquamous cervical carcinoma and 1 anaplastic oligodendroglioma) and 4 from patients in part B3 (all ER+ve/HER2-ve breast cancer patients). Biopsies had been taken a median of 4.67 years before the first dosing of trial medication, 54% coming from metastatic and 46% coming from primary specimens.

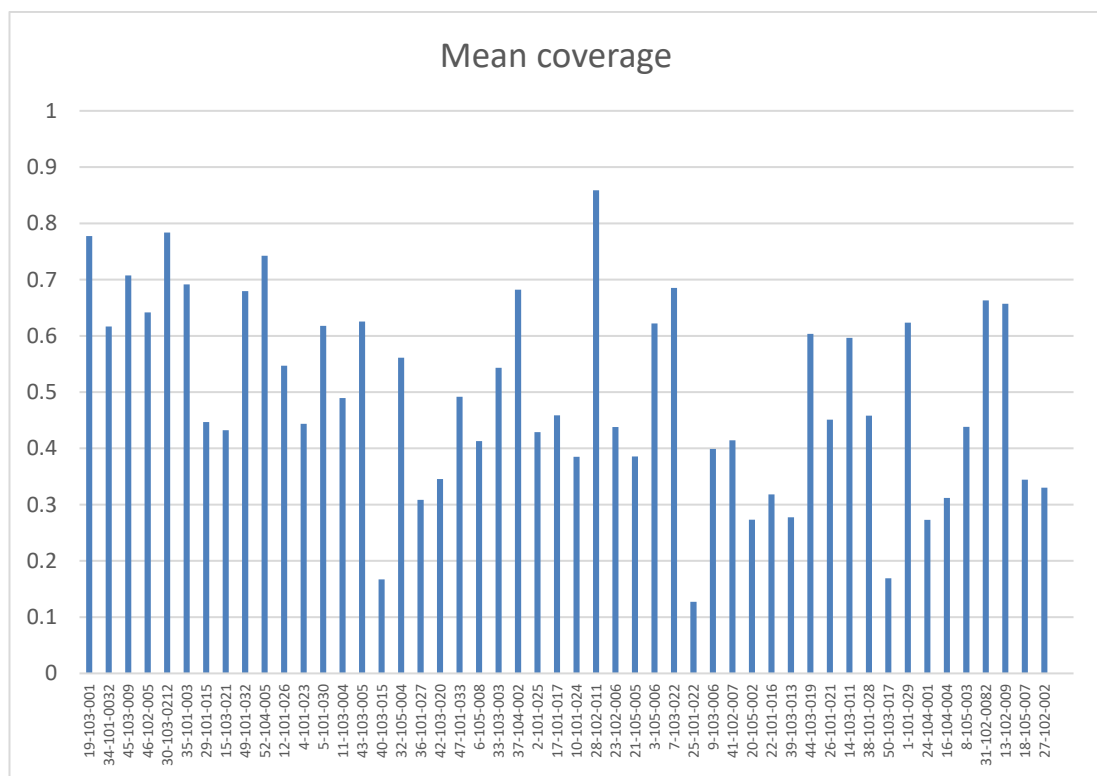
4.3 Baseline tissue whole-genome sequencing for CNV analysis

After a first external review, which identified some blocks without viable tumour, a total of 54 FFPE blocks were used for DNA extraction. DNA quantification using an RNaseP ddPCR assay found median DNA concentration of 4.42 ng/ μ L (range 0.06-60.32) for first elution and median 0.71 ng/ μ L (range 0.01-4.10) for second elution from these samples.

Libraries for WGS were then prepared (as detailed in 2.11) and quantified by qPCR and stock size adjusted in order to even input for sequencing. A quality assessment sampling was then performed with Bio-Rad's Bioanalyzer

for 30 of the total 54 samples ranging from original high to low DNA concentration, and 4 samples in the low DNA input side were flagged as not adequate for further sequencing on the basis of low % of libraries between 200 and 1000bp (<60%) and therefore expected to not contain sufficient ctDNA to get good quality sequencing data, leaving the total samples used for whole-genome sequencing to 50, 47 coming from baseline archival blocks and 3 on-progression samples.

Quality control tests were run for the whole-genome sequencing experiment as illustrated in **figure 17**. The mean coverage was 0.49X for the whole run, with mean 0.43 purity and mean 1.91 ploidy. Only three samples were identified as having <20% purity and therefore removed from further analysis as per prior literature and work in our laboratory [68].



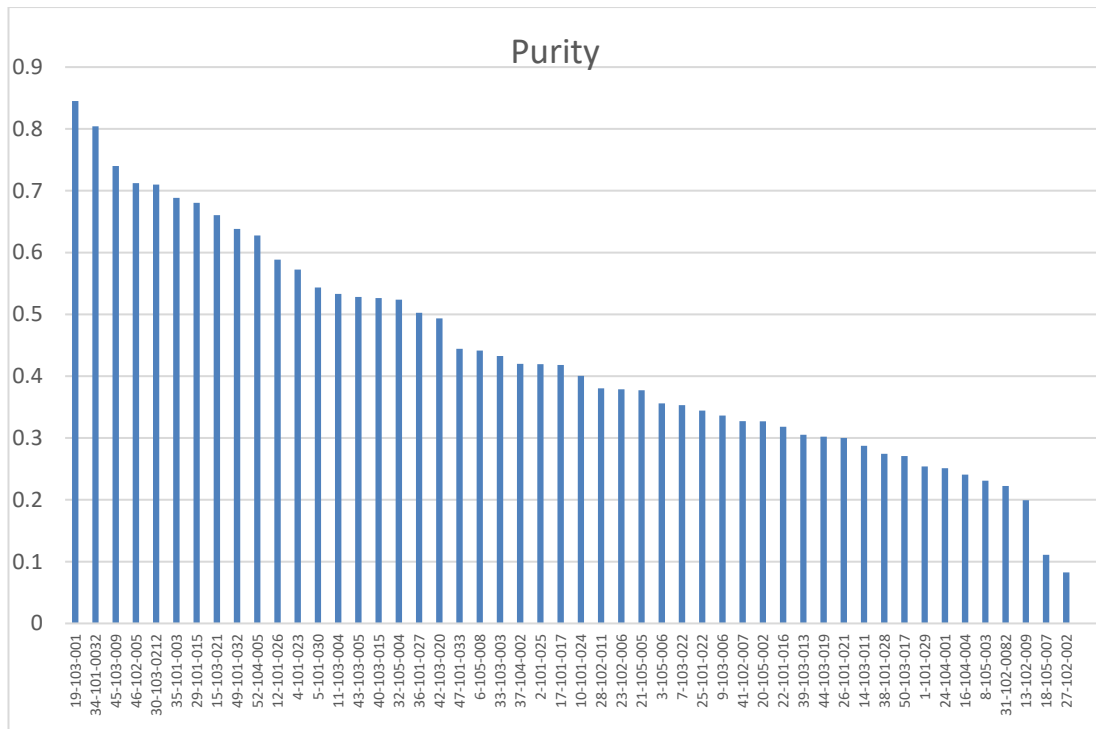


Figure 17. Quality control for the ultra-low whole-genome sequencing experiment showing mean coverage and purity per sample sequenced.

As a way of improving accuracy of potential prognostic capabilities for CNV in PFS, tumour ultra-low whole-genome analysis for copy number assessment was finally restricted to 43 evaluable patients, two of them with paired on-progression samples. This baseline CNV profile was then explored as a potential prognostic biomarker and data generated from uIWGS was also compared with data from IHC and FISH analysis.

Baseline uIWGS for CNV analysis in evaluable patients with *PIK3CA*-mt ER+ve/HER2-ve breast cancer treated with the triplet combination in part B1 showed 6/17 patients (35%) had a *CCND1* amplification, 9/17 (53%) had a *FGFR1* amplification, and 2/17 (12%) cases had *CCNE1* amplification (**figure 18**). There was no association found between baseline copy number aberrations and efficacy in terms of PFS for main genes of interest using log-rank test as exemplified by *AKT1* (median 7.5 vs 8.3 months for amplified vs non-amplified, $p=0.45$), *CCNE1* (median 5.6 vs 8.5 months for amplified vs non-amplified, $p=0.26$), *CCNE2* (median 7.5 vs 7.0 months for amplified vs non-amplified, $p=0.98$), *ESR1* (median 4.5 vs 8.5 months for amplified vs

non-amplified, $p=0.09$), *PIK3CA* (median 8.0 vs 5.4 months for amplified vs non-amplified, $p=0.69$) or *PTEN* (median 3.9 vs 8.0 months for patients with any deletion vs non-deletion, $p=0.29$). There was a significant difference for *AKT3* amplification vs gains (9.7 vs 3.6 months respectively, $p<0.01$), but it must be noted that all patients in part B1 had a thresholded call of either a gain or an amplification for this gene (with no neutral or deletion status found) and therefore this finding was considered not biologically relevant.

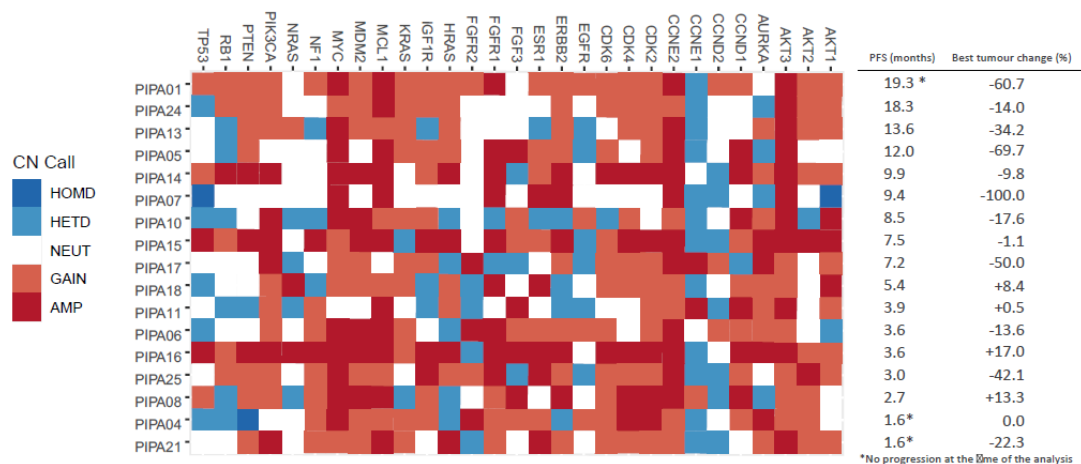


Figure 18. Ultra-low whole genome sequencing (ulWGS) for baseline CNV in the sequenced *PIK3CA*-mt ER+ve/HER2-ve breast patients treated with the triplet in part B1 (N=17), reported as thresholded adjusted copy number call (amplification/gain/neutral/heterozygous deletion/homozygous deletion). On the right, best tumour change and progression-free survival (PFS) per patient.

For the 7 evaluable sequenced patients with *PIK3CA*-mt ER-ve breast cancer (5 triple negatives and 2 ER-ve/HER2+ve) treated with the doublet combination in part B2, there were 2/7 patients (29%) *CCND1* amplifications, 2/7 (29%) *FGFR1* amplification and no patient was identified to harbour a *CCNE1* amplification (**figure 19**). The small numbers within this subgroup limited further efficacy analysis.

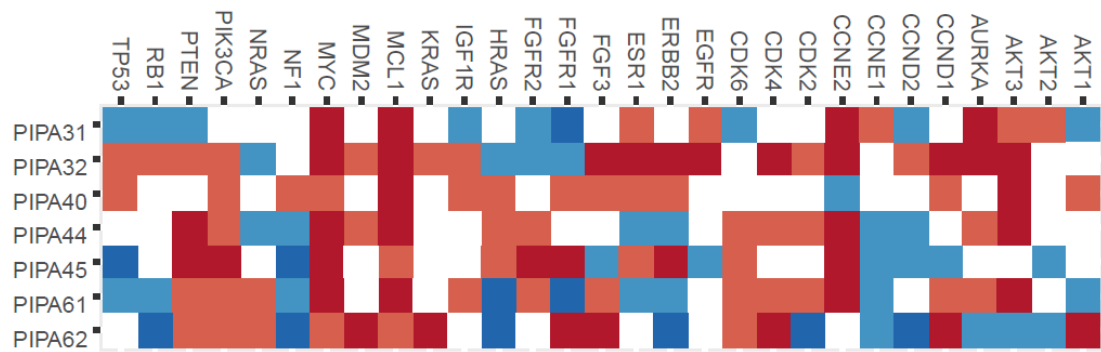


Figure 19. Ultra-low whole genome sequencing (ulWGS) for baseline CNV in the sequenced PIK3CA-mt ER-ve breast patients treated with the doublet in part B2 (N=7), reported as thresholded adjusted copy number call (amplification/gain/neutral/heterozygous deletion/homozygous deletion).

There were 8 evaluable sequenced patients with PI3K hyperactivated solid tumours. These were composed of 7 *PIK3CA* and 1 *PIK3CG* mutant (CNS-anaplastic oligodendroglioma) patients treated with the doublet combination in part B2. Whole-genome sequencing revealed 0/8 patients (0%) with *CCND1* amplifications, 3/8 (38%) *FGFR1* amplifications and 3/8 (38%) *CCNE1* amplifications (**figure 20**). Once more, the small numbers within this subgroup and the heterogeneity of the different tumour types limited any further efficacy associations.

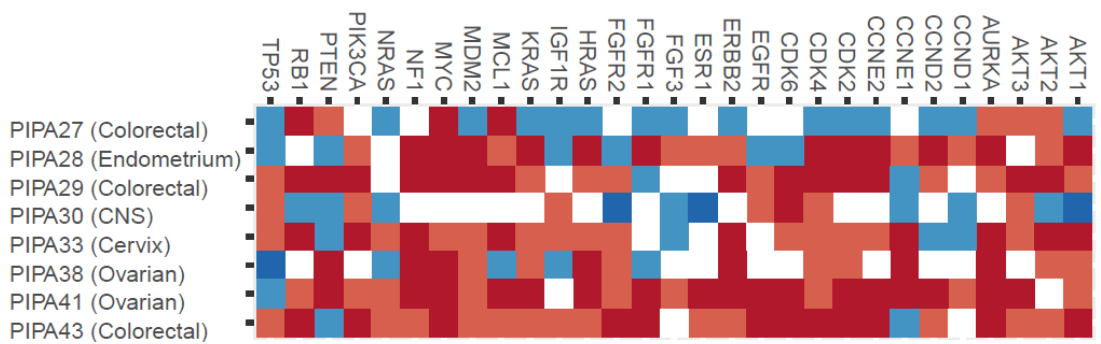


Figure 20. Ultra-low whole genome sequencing (ulWGS) for baseline CNV in the sequenced PI3K hyperactivated solid tumour patients treated with the doublet in part B2 (N=8), reported as thresholded adjusted copy number call (amplification/gain/neutral/heterozygous deletion/homozygous deletion).

There were two patients with paired baseline/progression tissue samples undergoing ulWGS. This was composed of a *PIK3CA*-mt ER-ve/HER2+ve breast cancer patient (PIPA45) treated with the doublet in cohort B2 and a

non-*PIK3CA*-mt triple-negative breast cancer patient (PIPA54) treated with the doublet in part A (escalation phase, dose level 1). CNV analysis for the two available patients showed mostly chromosomal stability, with evidence of homozygous deletion of *RB1* in one patient not seen in baseline, suggesting that this might have been an acquired mechanism of resistance developed through treatment (**figure 21**).

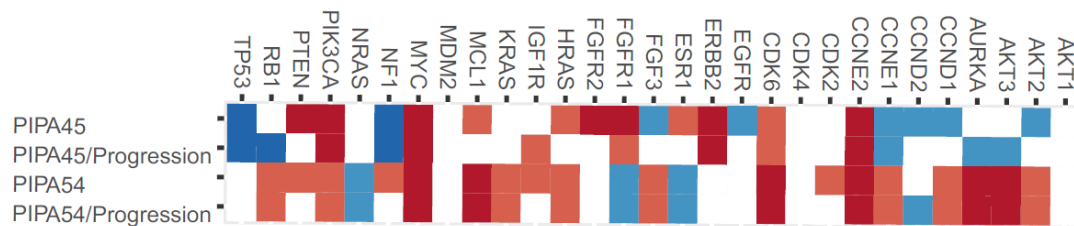


Figure 21. Ultra-low whole genome sequencing (ulWGS) for paired baseline/progression CNV in available patients treated with the doublet (N=2), reported as thresholded adjusted copy number call (amplification/gain/neutral/heterozygous deletion/homozygous deletion).

4.4 Baseline tissue IHC and FISH analysis

Baseline tissue samples were also analysed for IHC and FISH (see methods) as a way of testing potential biomarkers cyclin D1, cyclin E1 and androgen receptor (AR) and explore its value as predictors of efficacy on palbociclib combinations. To allow for enough samples within homogeneous subgroups to enable fair comparisons, all available breast samples retrieved for translational analysis were used to obtain a better estimate of median IHC and FISH scoring, but survival analyses were restricted to part B1 and ER-ve breast patients enrolled in part B2.

Cyclin D1 expression assessment by immunohistochemistry

A total of 42 archival FFPE tissue samples from breast cancer patients enrolled in the study had successful analysis of cyclin D1 immunostaining. H-score was calculated by multiplying the percentage of tumour cells stained (0-100) by the intensity grading score (0-3), resulting in a value ranging from

0 to 300. An example for different levels of intensity can be found in **figure 22**.

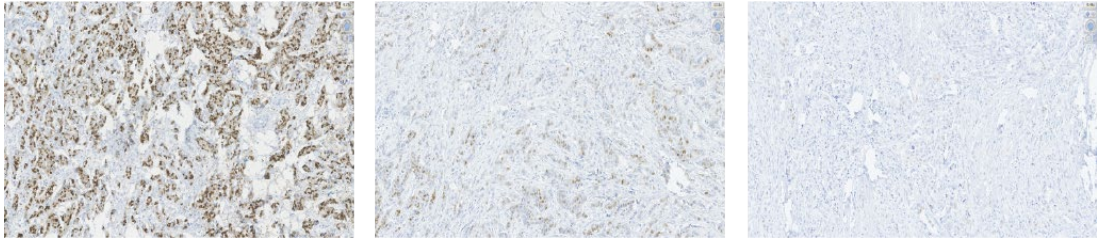


Figure 22. Examples of cyclin D1 IHC staining (left to right: high, moderate and low staining).

Median and mean H-score was 140 (range 0-240) and 135 (95% CI, 118-152) respectively. A distribution of frequencies for cyclin D1 H-score across all tested samples is depicted in the following **figure 23**:

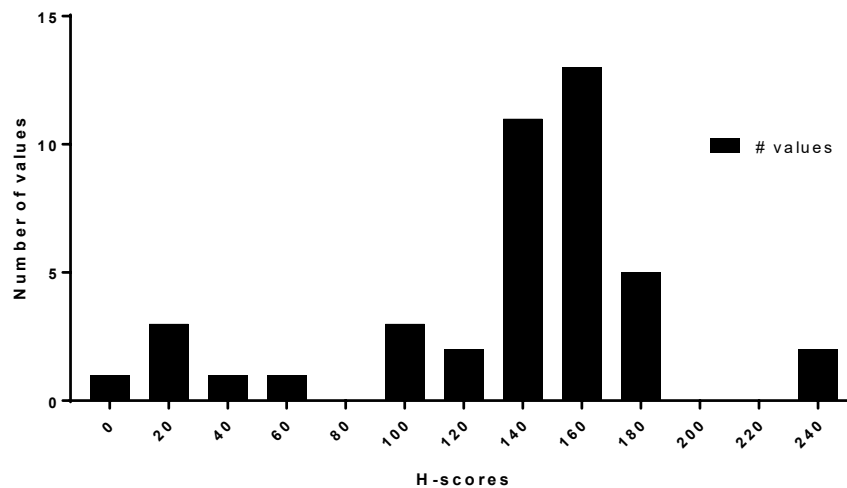


Figure 23. Histogram of cyclin D1 IHC H-score frequency distribution in 42 breast cancer patients with successful staining (N=42).

To assess whether cyclin D1 expression measured via immunohistochemistry could be used as a prognostic factor for therapy efficacy, median H-score was used to test potential differences in progression-free survival.

PIK3CA-mt ER+ve/HER2-ve breast patients with valid scoring treated with the triplet in part B1 (N=21) were found to have exactly the same PFS irrespectively of being classified above or below median H-score. PFS was 7.2 months vs 7.2 months respectively ($p=0.35$, log-rank test), as illustrated in **figure 24**.

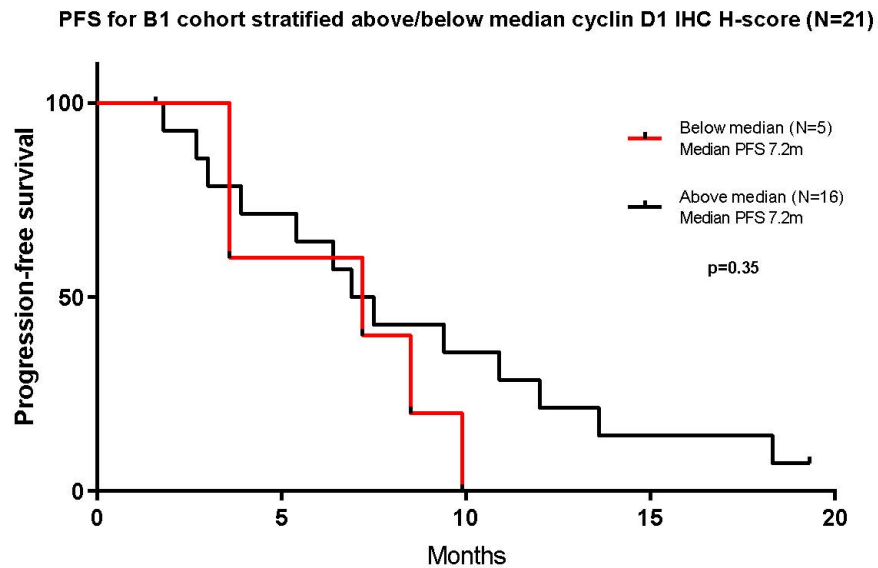


Figure 24. PFS for B1 cohort stratified above/below median cyclin D1 H-score (N=21). Median PFS 7.2m vs 7.2m, respectively. $p=0.35$, log-rank test.

For the available *PIK3CA*-mt ER-ve breast patients (N=8) treated with the doublet in part B2, again no statistically significant differences in survival were noted when stratifying patients above and below median H-score, with PFS 4.7 months vs 8.7 months respectively ($p=0.37$, log-rank test) as shown in **figure 25**.

PFS for B2 ER-ve breast cohort stratified above/below median cyclin D1 IHC H-score (N=8)

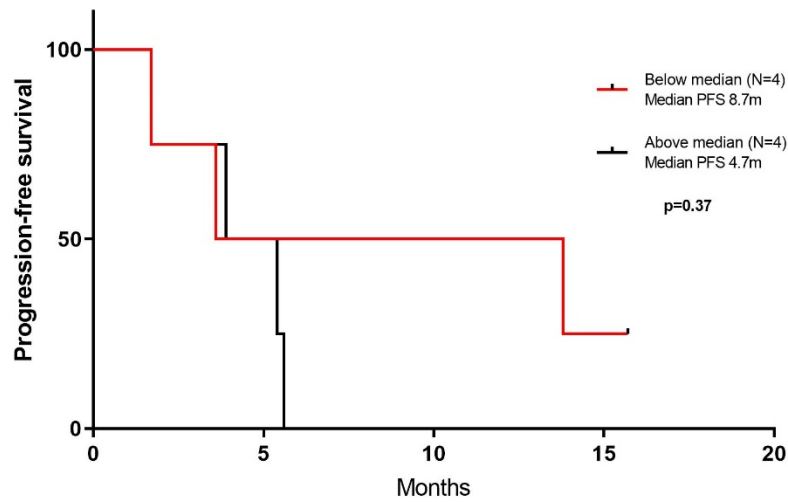


Figure 25. PFS for available ER-ve breast patients in part B2 stratified above/below median cyclin D1 H-score (N=8). Median PFS 4.7m vs 8.7m, respectively. $p=0.37$, log-rank test.

Therefore, no significant differences were found for PFS when stratifying breast cancer patients by median cyclin D1, irrespectively of them being ER+ve or ER-ve.

Cyclin D1 amplification assessment by immunofluorescence

A total of 41 samples had successful cyclin D1 FISH assessment. Only 2 amplifications (defined as CCND1/CEP11 ratio ≥ 2) were found, both in part B1 (**figure 26**).

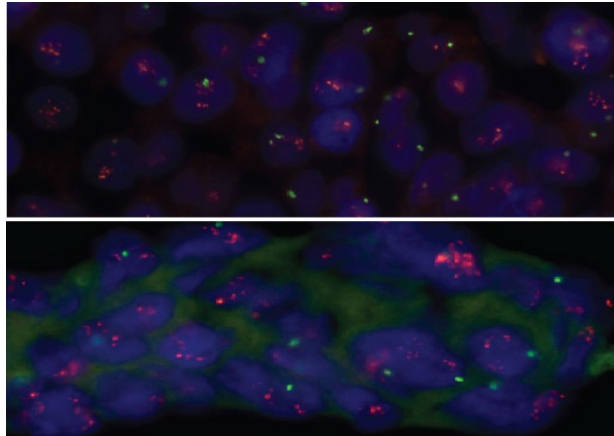


Figure 26. Examples of FISH amplification for cyclin D1 for the two patients considered amplified. Red probe is for *CCND1* and green probe for *CEP11*.

There was good correlation in part B1 between available amplified cases by FISH and WGS with 2/2 (100%) concordance. However, only 2/6 (33%) of amplified cases by WGS in part B1 were also amplified by FISH (**figure 27**).

		Copy number amplification		Total	PPV = 1 NPV = 0.75
		Yes	No		
FISH amplification	Yes	2	0	2	
	No	4	12	16	
	Total	6	12	18	

Sensitivity = 33% Specificity = 100%

Figure 27. Contingency table representing predictive positive and negative values for copy number gain vs FISH amplification for *CCND1*.

For available amplified versus non-amplified patients in part B1 (N=20), no significant survival differences could be found, with PFS 7.8 months vs 7.35 months respectively (p=0.97, log-rank test).

Cyclin E1 expression assessment by immunohistochemistry

A total of 42 blocks from breast cancer patients had successful analysis of cyclin E1 immunostaining (**figure 28**). H-score could not be calculated as the

intensity grading for E1 was not obtained (as described in methods). Analysis was performed using percentage of tumour cells stained (0-100%) data.

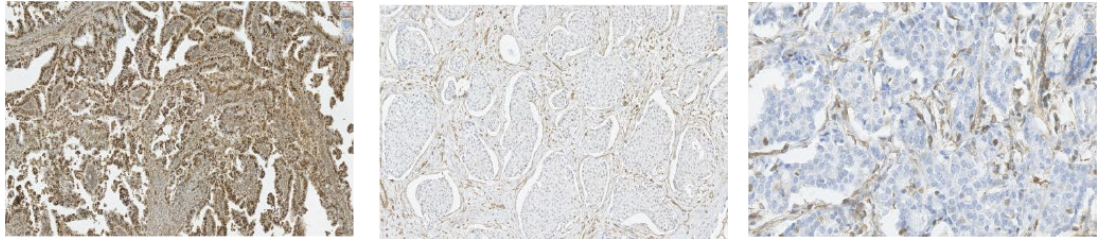


Figure 28. Examples of cyclin E1 IHC staining (left to right: 90%, 40% and 10% invasive nuclei stained).

Median and mean percentage of staining was 30% (0-90%) and 36.45% (95% CI, 27.56-45.33) respectively. A distribution of frequencies for cyclin E1 % staining is shown in **figure 29**:

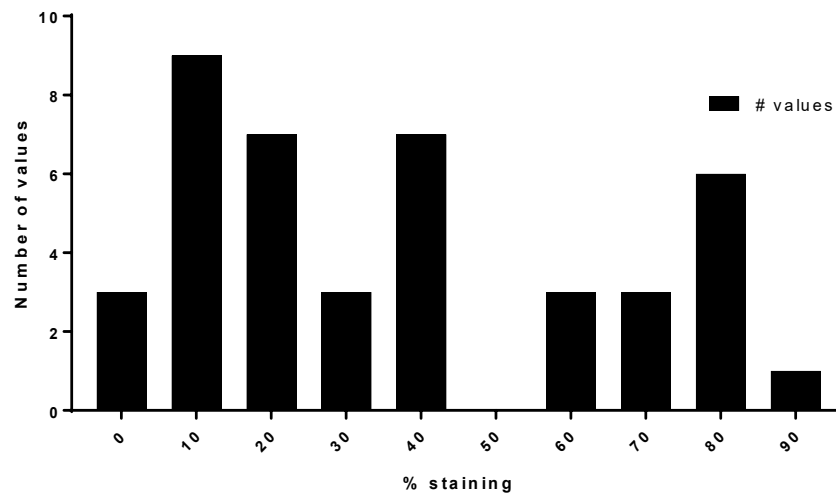


Figure 29. Histogram of cyclin E1 IHC % staining frequency distribution in 42 breast cancer patients with successful staining.

When stratifying by median, significant survival differences for patients with valid scoring were found when stratifying above and below median in cohort B1 (N=21). PFS was 6.4 months vs 10.4 months respectively (HR 4.16, 95%CI 1.32-13.11, p=0.02, log-rank test), shown in **figure 30**.

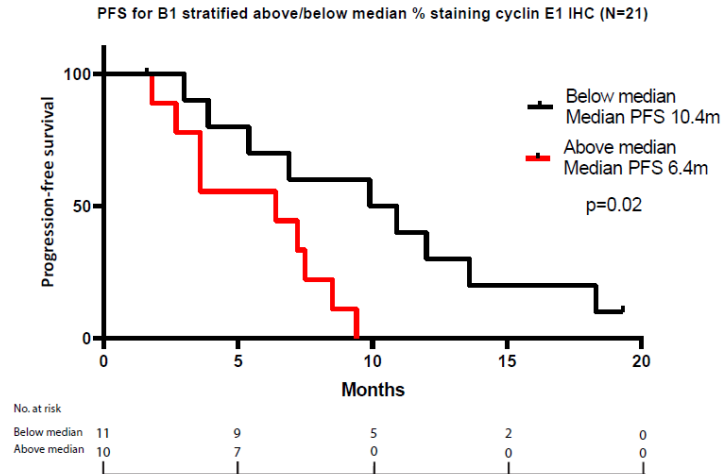


Figure 30. PFS for part B1 stratified by above/below median cyclin E percentage of invasive nuclei stained. HR 4.16 (95% CI 1.32-13.11), $p=0.02$, log-rank test. Patients at risk per timepoint in each subgroup can be found below the graph.

For available ER-ve breast cancer patients in cohort B2 (N=8), PFS was 4.5 months vs 8.85 months respectively (HR 1.25, 95% CI 0.24-6.37, $p=0.79$, log-rank test), shown in **figure 31**.

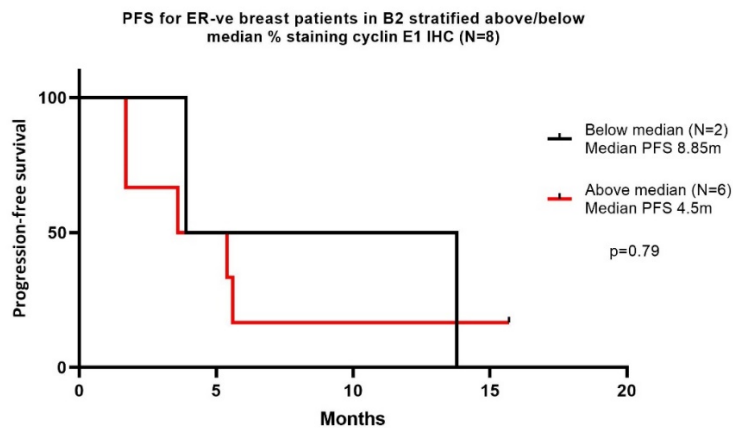


Figure 31. PFS for ER-ve breast in part B2 stratified by above/below median cyclin E percentage of invasive nuclei stained. HR 1.25 (95% CI 0.24-6.37), $p=0.79$, log-rank test.

Androgen receptor expression assessment in TNBC by immunohistochemistry

To explore the potential value of androgen receptor (AR) expression as a predictive biomarker for the doublet combination therapy in TNBC patients,

IHC staining was conducted. A total of 8 blocks from TNBC patients had successful analysis of AR immunostaining (**figure 32**).

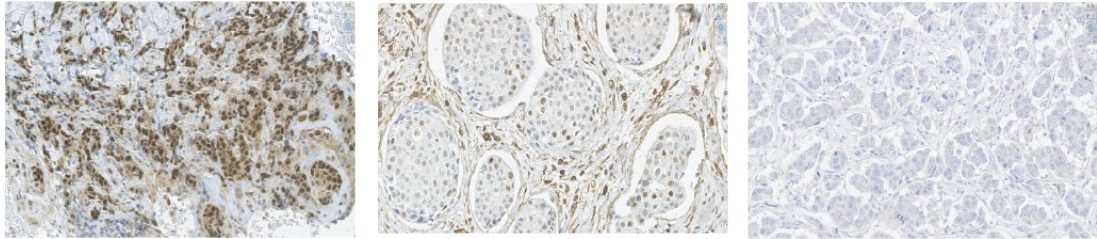


Figure 32. Examples of AR IHC staining (left to right: high, moderate and low staining).

As with cyclin D1, both percentage of stained invasive cells and H-score was calculated to establish a cut-off that could select for efficacy differences. Median and mean H-score was 140 (0-270) and 152.5 (95% CI, 59.21-245.78) respectively. Median and mean percentage of stained cells was 70% (0-90%) and 59.37% (95% CI, 28.21-90.53) respectively. Frequencies distributions for both % staining and H-score can be found in **figure 33** below:

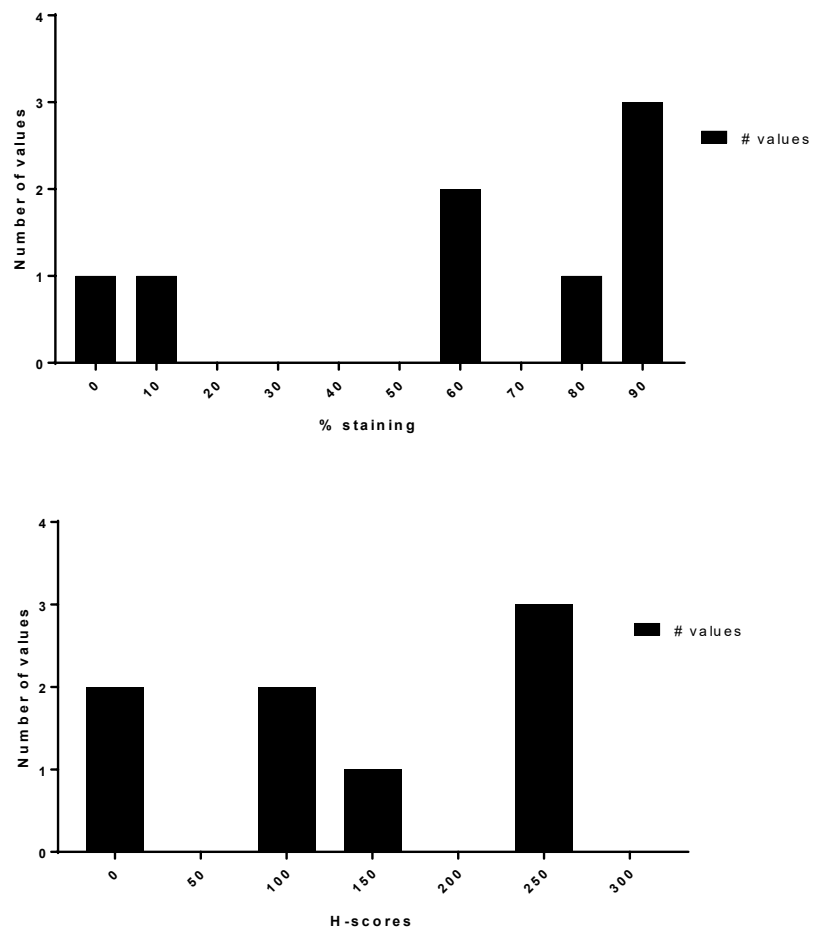


Figure 33. Histogram of % staining (above) and AR IHC H-score (below) showing frequency distribution in 8 TNBC patients.

Overall, 7 out of 8 stained *PIK3CA*-mutant TNBC patients (87.5%) had positivity for AR, a proportion maintained when focusing on the efficacy-evaluable population with 6 out of 7 (86%) patients staining for AR. A non-statistically significant numerical difference was found for evaluable patients classified above and below baseline median H-score, with PFS 8.15 months vs 3.6 months (HR 0.44, 95% CI 0.07-2.83, $p=0.39$, log-rank test), depicted in **figure 34**.

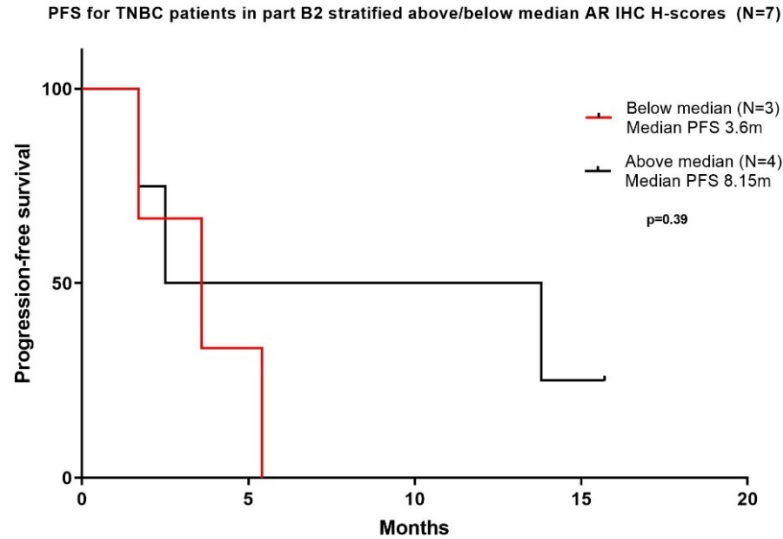


Figure 34. PFS for TNBC in part B2 stratified by above/below median AR H-score (N=7). HR 0.44 (95% CI 0.07-2.83), p=0.39, log-rank test.

Interestingly, the two patients with long-term clinical benefit and additionally a third patient being the only one achieving a RECIST 1.1 confirmed partial response had high AR expression in their tumour, with median 270 vs 90 H-score for patients achieving CBR vs non-CBR, respectively (p=0.20, Mann-Whitney test), as shown in **figure 35**.

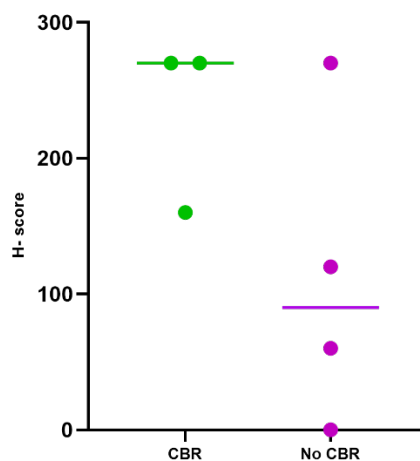


Figure 35. H-score for androgen receptor (AR) expression distribution in available baseline tumours of TNBC patients available (N=7). Median 270 H-score for patients achieving CBR (N=3) vs 90 H-score for patients without CBR (N=4), p=0.20, Mann-Whitney test.

Of note, only one evaluable patient was found to have <10% AR staining, and therefore further analyses using a 10% cutoff as per prior literature was not possible.

4.5 Discussion

Baseline molecular profiling using tissue biopsies has been widely explored in cancer research to identify potential prognostic and/or predictive biomarkers. In this study, ultra-low whole genome sequencing profiling and additional IHC and FISH studies were performed in tissue samples as an attempt to explore baseline status of clinically relevant genes and their prognostic value. Cyclin D1 is known to play an important role in cell-cycle regulation through coupling with CDK4/6, with gene amplification linked to higher proliferation and worse prognosis in luminal A and B breast cancer subtypes. In this study, cyclin D1 amplification (*CCND1* amplification) was found to be a common event in *PIK3CA* mutant ER+ve HER2-ve breast cancer (6/17, 35%), as expected from prior knowledge, but it did not provide any additional prognostic value for patients treated with the triplet combination of palbociclib, taselisib and fulvestrant in our dataset. These results were mirrored in both cyclin D1 IHC and FISH analyses, with no significant prognostic value conferred by stratification of patients above and below median. This absence of prognostic value for either *CCND1* amplification or cyclin D1 overexpression mirrors previous observation in the PALOMA-1 clinical trial, where *CCND1* amplifications were not predictive of palbociclib efficacy [114]. Of note, amplification was defined by *CCND1*-to-CEP11 ratio >1.5 in PALOMA-1 (as opposed to >2.0 in this study). The optimal ratio to call an amplification varies between genes and there is no standard for *CCND1*, therefore any ratio used for predictions needs to be considered exploratory. Perhaps higher ratios representing high levels of amplification can be more informative although the two patients amplified in this trial did show fairly high ratios (4 and 10) with no signal towards different prognosis. Overall, there is controversial literature in this respect and more functional work will be required to provide definitive certainty that a

hypothetical aberrant overexpression resulting from gene amplification confers worse prognosis. On the contrary, cyclin E1 was only found amplified in a minority of *PIK3CA* mutant ER+ve HER2-ve breast cancer (2/17, 12%) patients, and although this limited any further analysis, it was not found to have any evident impact in PFS. However, expression analyses via IHC provided significant differences in survival for patients treated with the triplet when classified as high or low cyclin E expression, an observation that has been recently demonstrated for patients treated with the combination of palbociclib and fulvestrant [63]. We also explored other genes known to confer worse outcome when amplified. *FGFR1* is a clinically targetable gene amplified in ~10% of breast cancer patients. We did not find prognostic value in this dataset although it is worth mentioning that the percentage of *FGFR1* amplified patients amongst *PIK3CA* mutant ER+ve HER2-ve breast cancer patients treated with the triplet was higher than expected (57%). Other potentially relevant copy number alterations in genes involved in the PI3K pathway, like *AKT* amplifications and *PTEN* deletions, or in the cell-cycle regulation like *RB1* deletions, were also rather infrequent and failed to provide any obvious prognostic value, although the small number of samples analysed might have elicited any robust observation. Interestingly, 6 of 7 evaluable patients with *PIK3CA* mutant TNBC in our study had some degree of IHC expression for AR, a finding that adds evidence to TNBC LAR subtypes being enriched for *PIK3CA* mutations. Previous studies have demonstrated the potential of non-chemotherapy approaches for selected TNBC subtypes [41, 42], with the potential for antiandrogen therapy in TNBC with AR expression. This study suggests that combinations of CDK4/6 and PI3K inhibitors might be especially active in TNBC LAR subtype with a demonstrated hyperactivation of the PI3K pathway.

Chapter 5. Longitudinal predictive biomarkers

5.1 Introduction

All patients enrolled in the PIPA study were required to provide a blood sample for research purposes on every first day of their cycles of treatment and on progression or an alternative end-of-study timepoint. Plasma-derived ctDNA was used in this project as the only resource of genetic material to conduct longitudinal biomarker analysis. These consisted in the analysis of early changes in ctDNA abundance (between the first and second cycles of treatment) to explore whether a drop in these levels or a potential cutoff could select patients deriving better efficacy from the combination treatment and the analysis of long-term ctDNA changes in the mutation profile (between first cycle of treatment and the end-of-study sample) to study genomic evolution under therapy.

Early *PIK3CA* dynamics in ctDNA have been shown to predict patient outcomes in both the PALOMA-3 study of palbociclib plus fulvestrant versus placebo plus fulvestrant [56], and the BEECH study of capivasertib plus paclitaxel versus placebo plus paclitaxel [57], both in ER+ve/HER2-ve metastatic breast cancer patients. In both studies, a ctDNA drop was predictive of better outcomes. More specifically, a decline in mutant copies/ml (median relative change 0.076, $p < 0.0001$) was demonstrated in matched day 15 samples compared to day 1 for patients treated with the combination of palbociclib and fulvestrant in PALOMA-3 [56] and additionally patients above an optimally defined ctDNA ratio (CDR) using Harrel's c-index had worse median PFS in comparison to patients below such CDR (HR 4.92, $p = 0.0002$). Comparable results were also shown for patients enrolled in the BEECH study, with patients identified to have suppressed ctDNA at 4 weeks deriving better PFS than patients with high ctDNA (HR 0.20, $p < 0.0001$) [57].

Analysis of the ctDNA in patients enrolled in the PALOMA-3 trial has been used successfully to detect baseline biomarkers with prognostic implications, with both *TP53* mutations and *FGFR1* amplifications associated with worse PFS [115] irrespective of the treatment arm. Additionally, paired baseline and

end-of-treatment plasma samples were sequenced in 195 patients in PALOMA-3, providing comprehensive evidence of genomic evolution under fulvestrant with or without the addition of palbociclib [116]. *RB1* mutations had been anticipated to occur as a result of acquired resistance to palbociclib combinations but only a minority of 4.7% patients in the palbociclib plus fulvestrant arm had the mutation identified in the progression sample. There was evidence of new *PIK3CA* and *ESR1* (particularly Y537S) mutations emerging in both treatment arms, and this occurred more frequently in patients exposed for longer to treatment.

Interrogation of ctDNA was also performed in this project to test for potential genomic determinants of sensitivity and resistance to the PI3K inhibitor used in the combination. Prior work had identified that patients harbouring double *PIK3CA* mutations accounts for 12-15% in breast cancer, and that when those mutations are located on the same allele (i.e. in *cis*) the tumours have increased oncogenicity but also improved sensitivity to α -selective PI3K inhibitors [117]. *PTEN* is a tumour suppressor gene that acts dephosphorylating PIP3, therefore acting as a negative regulator of the pathway. Its loss of function has also been linked specifically to α -selective PI3K inhibitor resistance via hyperactivation of PI3K β [18]. The targeted panel used for testing ctDNA in patients enrolled in the PIPA trial included these and other relevant genes involved in cancer and often with prior evidence of resistance or sensitivity to some of the compounds used in the combination treatment tested in this trial, and therefore a survival analysis based on some of these proposed biomarkers was possible.

5.2 Early changes in *PIK3CA* mutations in ctDNA for predicting treatment benefit

Mostly all patients enrolled in the PIPA trial had a *PIK3CA* mutation and a PI3K inhibitor was part of the combination treatment. This, in addition to the fact that the Molecular Oncology laboratory had wide experience using ddPCR assays for the detection of different *PIK3CA* mutations, prompted the selection of *PIK3CA* mutations as the optimal biomarker to track to measure

ctDNA abundance changes. A total of 40 C1D1-C2D1 plasma sample pairs were analysed with an ultra-sensitive methodology (ddPCR) for early *PIK3CA* ctDNA dynamics, to explore whether an early drop in ctDNA abundance (taking *PIK3CA* mutation as a proxy for this) could select patients achieving better outcomes from therapy. From the initial set, there were 10 pairs excluded for failing pre-defined quality control (as described in methods), leaving the total number of pairs to 30. Following methodology from prior work exploring the applicability of a ctDNA ratio (CDR) as a tool to stratify for responders versus non-responders, we conducted all analysis both for allele frequency (AF) and mutant copies per ml equivalent.

Comparing the *PIK3CA* mutation AF between C2D1 and C1D1 in all samples, the median CDR₂₈ (AF in C2D1 relative to AF in C1D1) was 0.74 (range 0-3.46). When analysing all evaluable patients passing quality control (N=30) there was a significant decrease from baseline (p<0.01, Wilcoxon signed-rank test), likely reflecting overall ctDNA suppression after one cycle of treatment (**figure 36**).

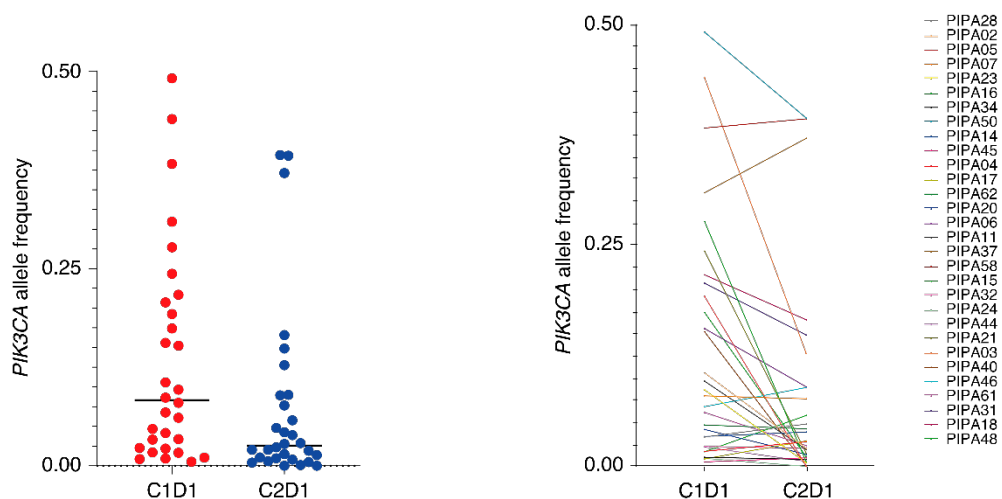


Figure 36. Left: early *PIK3CA* mutation dynamics comparing C1D1 to C2D1 allele frequency for the whole population analysed passing predefined quality control for longitudinal analysis (N=30). p<0.01, Wilcoxon signed-rank test (paired). Right: same analysis represented as change per patient.

In order to keep patient homogeneity for accurately exploring the predictive value of this ctDNA suppression, a further analysis was restricted to the 16 evaluable patients with *PIK3CA*-mt ER+ve/HER2-ve breast cancer in part B1 receiving triplet therapy. The significant drop previously identified was maintained ($p < 0.01$, Wilcoxon signed-rank test) with median CDR_{28} as measured by AF change being 0.31 (0-3.46), **figure 37**.

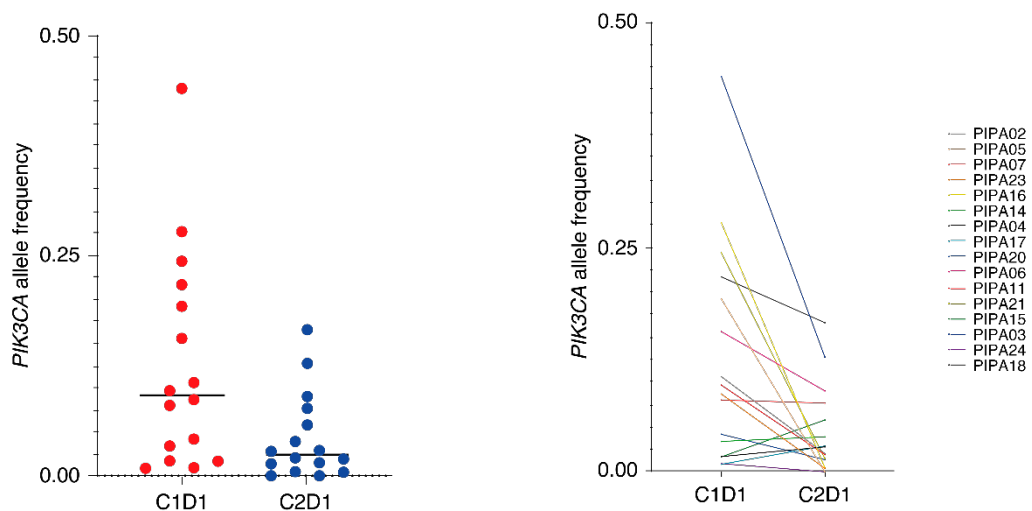


Figure 37. Left: early *PIK3CA* mutation dynamics comparing C1D1 to C2D1 allele frequency for evaluable *PIK3CA*-mt ER+/HER2-ve breast cancer patients enrolled in part B1 (N=16). $p < 0.01$, Wilcoxon signed-rank test (paired). Right: same analysis represented as change per patient.

To explore the potential impact that a CDR_{28} could have in patient survival, patients in part B1 were first stratified above and below median CDR_{28} and a non-significant trend was found (7.9 vs 11.8m respectively, HR 2.1, 95% CI 0.49-8.75, $p = 0.33$, Log-rank test).

Next, a CDR_{28} cutoff of 0.1 was applied to stratify patients as ctDNA suppressed (< 0.1) or non-suppressed (> 0.1), and account for potential survival differences as per prior work carried on in patients treated with palbociclib and fulvestrant which defined a relatively similar cutoff as an optimal one [56]. Patients without suppressed CDR_{28} (> 0.1) had worse PFS than patients with suppressed (< 0.1) CDR_{28} (6.9 vs 15.2m respectively, HR 5.23, 95% CI 1.41-19.4, $p = 0.04$, Log-rank test). Moreover, only two patients were found to

derive complete ctDNA suppression (C1D1 positive and C2D1 under the limit of detection), both in part B1. Patients with complete versus incomplete ctDNA suppression had improved PFS (6.9 vs 15.2m respectively, HR 5.14, 95% CI 1.28-20.59, $p=0.02$, log-rank test), as shown in **figure 38**.

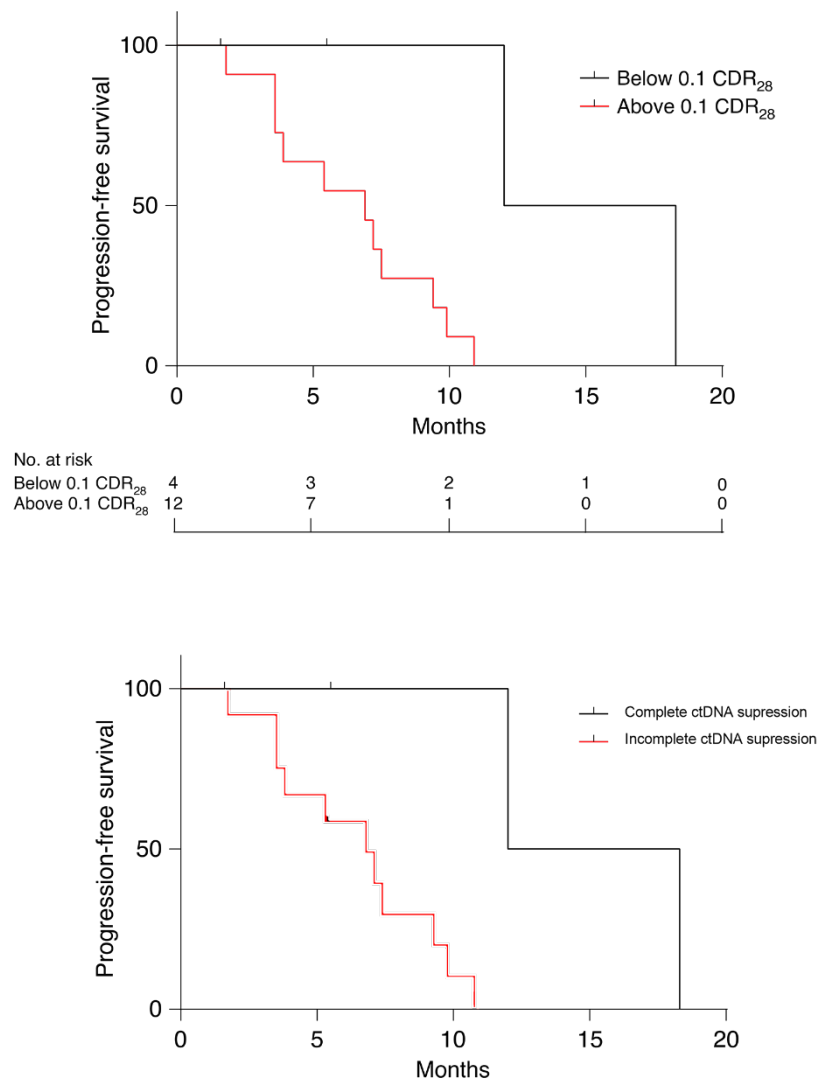


Figure 38. Above: Kaplan-Meier curve representing progression-free survival (PFS) for patients in part B1 stratified above/below 0.1 CDR₂₈ derived from allele frequency. Median PFS 6.9m vs 15.15m, respectively. HR 5.23 (95% CI 1.41-19.42), $p=0.04$, log-rank test. Below: same analysis for patients in part B1 stratified for incomplete/complete ctDNA suppression. Median PFS 6.9m vs 15.15m, respectively. HR 5.14 (95% CI 1.28-20.59), $p=0.02$, log-rank test.

The previous analyses were also repeated accounting for the volume of plasma (in ml/equivalent) used for the ddPCR reaction (0.25 ml/equivalent or the ml/equivalent corresponding to 1.3ng, whichever larger, as described in methods) to try and estimate the ctDNA dynamics using absolute changes in mutant copies/ml.

For all 30 evaluable patients, there was a clear trend towards a drop in mutant copies/ml between C1D1 and C2D1 ($p=0.05$, Wilcoxon signed-rank test), mirroring findings for AF calculations (**figure 39**).

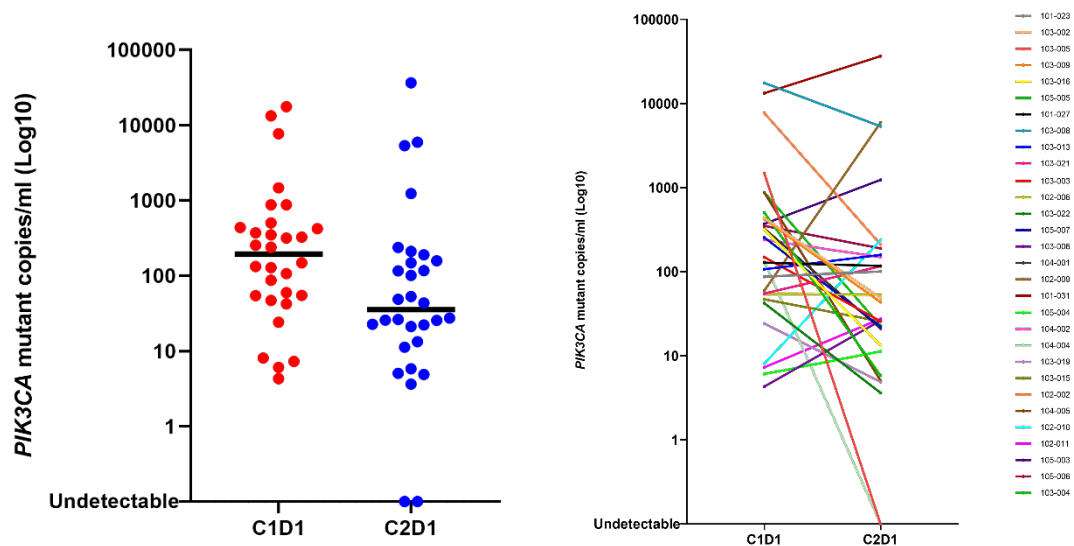


Figure 39. Left: early *PIK3CA* mutation dynamics comparing C1D1 to C2D1 mutant copies/ml for the whole population analysed passing predefined quality control for longitudinal analysis (N=30). $p=0.05$, Wilcoxon signed-rank test (paired). Right: same analysis represented as change per patient.

Moreover, when restricting the analysis to *PIK3CA*-mt ER+ve/HER2-ve patients enrolled in part B1 (N=16), again a significant drop was detected ($p<0.01$, Wilcoxon signed-rank test, **figure 40**), confirming that both AF and mutant copies/ml can robustly identify ctDNA suppression when an homogeneous population treated with similar therapy are explored.

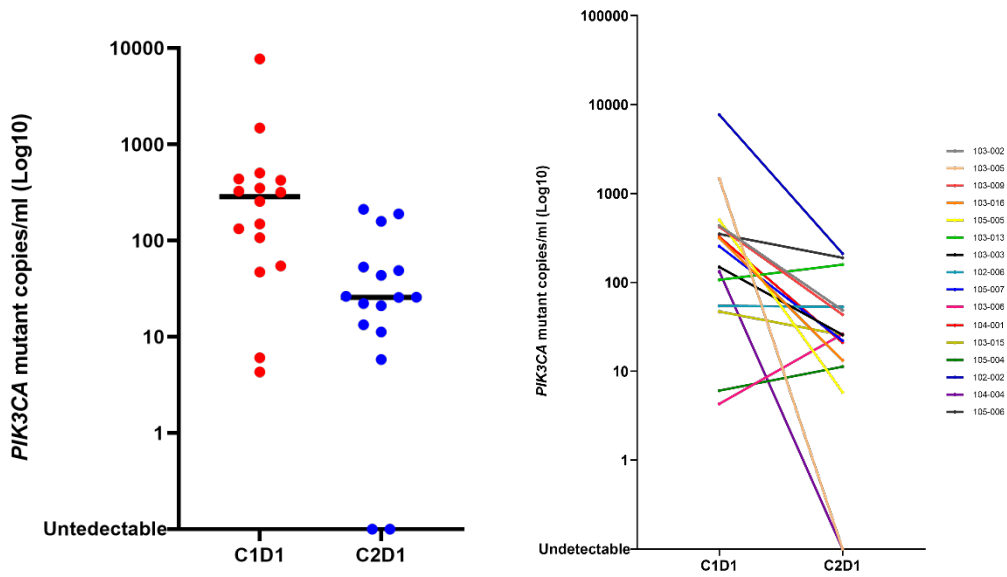


Figure 40. Left: early *PIK3CA* mutation dynamics comparing C1D1 to C2D1 mutant copies/ml for evaluable *PIK3CA*-mt ER+/HER2-ve breast cancer patients enrolled in part B1 (N=16). $p < 0.01$, Wilcoxon signed-rank test (paired). Right: same analysis represented as change per patient.

Conversely, applying a 0.1 CDR₂₈ cutoff using mutant copies/ml was not able to predict differences in survival. Patients with and without suppressed CDR₂₈ had no significantly different PFS (6.9 vs 7.5 months respectively, HR 1.39, 95% CI 0.41-4.71, $p = 0.60$, Log-rank test, **figure 41**).

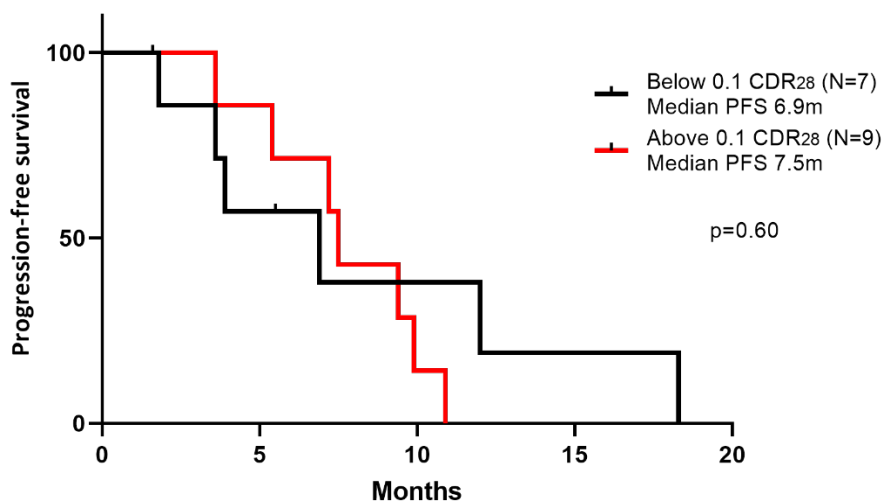


Figure 41. Kaplan-Meier curve representing progression-free survival (PFS) for patients in part B1 stratified above/below 0.1 CDR₂₈ using mutant copies/ml. Median PFS 7.5m vs 6.9m, respectively. HR 1.39 (95% CI 0.41-4.71), $p = 0.60$, log-rank test.

5.3 Paired baseline and end-of-treatment plasma ctDNA analysis to study genomic evolution through treatment.

To investigate genomic evolution through therapy, paired error corrected ctDNA sequencing with a 200 cancer driver gene panel (**appendix 1** for genes and regions included) was performed in C1D1-EOT pairs for a selection of 23 patients.

These included 16 patients from part B1, 4 patients from B2 (1 *PIK3CA*-mt endometrium, 2 *PIK3CA*-mt ER+ve/HER2-ve breast and 1 *PIK3CA*-mt ER-ve/HER2+ breast), and 3 from B3 (2 *PIK3CA*-mt and 1 *PIK3CA* non-mutant ER+ve/HER2-ve breast). From these, 20/23 (87%) had confirmed progression on their EOT sample. Summed together, there were 20 *PIK3CA*-mt ER+ve/HER2-ve breast patients with sequencing data, 16 within part B1.

Median family coverage for all sequenced samples was 696X (11-1880).

Metrics for all patients sequenced can be found in **table 11**.

Names	percent.ontarget	mean.coverage	median.coverage
1902326-101-023_C1D1	88%	1,407.2	1477
1902327-101-023_EOT	87%	1,705.5	1759
1902328-102-005_C1D1	81%	1,011.7	1089
1902329-102-005_EOT	78%	1,397.8	1494
1902330-103-002_C1D1	78%	911.0	965
1902331-103-002_EOT	83%	991.3	1053
1902332-103-005_C1D1	83%	1,265.4	1269
1902333-103-005_EOT	85%	2,027.9	1880
1902334-103-009_C1D1	80%	855.0	930
1902335-103-009_EOT	85%	1,393.6	1455
1902336-103-016_C1D1	86%	1,606.0	1659
1902337-103-016_EOT	78%	840.8	894
1902338-103-021_C1D1	85%	1,535.6	1551
1902339-103-021_EOT	80%	1,099.5	1168
1902340-105-005_C1D1	84%	1,324.4	1154
1902341-105-005_EOT	84%	1,133.9	1073
1905504-101-027_C1D1	68%	477.7	478
1905505-101-027_EOT	68%	439.7	458
1905506-102-002_C1D1	41%	154.5	133
1905507-102-002_EOT	28%	92.2	11
1905508-102-006_C1D1	49%	331.0	341
1905509-102-006_EOT	53%	357.3	363
1905510-103-008_C1D1	45%	167.7	165
1905511-103-008_EOT	61%	363.6	347
1905512-103-011_C1D1	70%	616.2	637
1905513-103-011_EOT	57%	372.1	389
1905514-103-013_C1D1	50%	261.7	267
1905515-103-013_EOT	31%	129.1	129
1905516-103-017_C1D1	54%	335.5	347
1905517-103-017_EOT	67%	416.9	426
1905520-105-007_C1D1	55%	270.4	270
1905521-105-007_EOT	40%	225.8	222
1905528-104-001_C1D1	50%	462.9	456
1905529-104-001_EOT	53%	627.2	614
1905542-105-006_C1D1	63%	512.9	504
1905543-105-006_EOT	49%	626.0	604
1905546-103-014_C1D1	69%	701.5	699
1905547-103-014_EOT	74%	818.0	828
1905550-102-001_C1D1	21%	156.1	160
1905551-102-001_EOT	63%	445.6	485
1905558-102-003_C1D1	47%	143.7	143
1905559-102-003_EOT	63%	324.6	329
1905560-103-006_C1D1	63%	238.1	242
1905561-103-006_EOT	45%	231.6	215
1905562-105-002_C1D1	57%	437.1	446
1905563-105-002_EOT	54%	399.1	420

Table 11. Percentage on target, mean and median coverage for 23 patients undergoing paired cycle 1-day 1 (C1D1) - end of treatment (EOT) plasma sequencing.

The genomic landscape revealed 23 baseline *PIK3CA* mutations in 19 different patients (**figure 42**). There was 20/23 (87%) concordance in baseline *PIK3CA* status between ctDNA sequencing using the RMH200 targeted panel and the mutational assessment as per enrolment (which could have used either tissue or ctDNA testing generally via a targeted identification approach performed by an accredited laboratory). Discordant patients were PIPA10 (H1047L mutation that was not found in ctDNA sequencing at C1D1 but was found in EOT sample), PIPA17 (E545K mutation not found in ctDNA sequencing at C1D1 but confirmed to be present in a ddPCR assay) and PIPA39 (H1047R mutation not passing the threshold for variant calling as per methodology but found in one read).

Baseline genetic landscape for *PIK3CA* mutations showed that most common mutations were found in known hotspots E542K, E545K and H1047R located in exons 9 and 20, as expected.

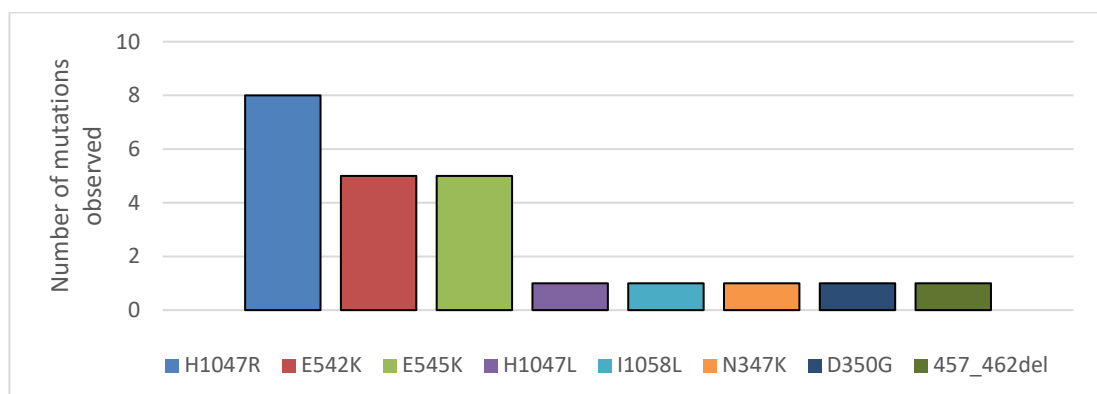


Figure 42. *PIK3CA* mutations identified at baseline (N=23) with the RMH200 panel.

There were 23 different *PIK3CA* mutations at the EOT timepoint identified in 20 patients. Overall, 5 of 23 (22%) patients were found to have multiple *PIK3CA* mutations in any of the timepoints sequenced. Dynamics for *PIK3CA* mutations in the 4 patients with at least 1 read in each timepoint clearly suggested subclonal second *PIK3CA* mutations in 2 patients (**figure 43**).

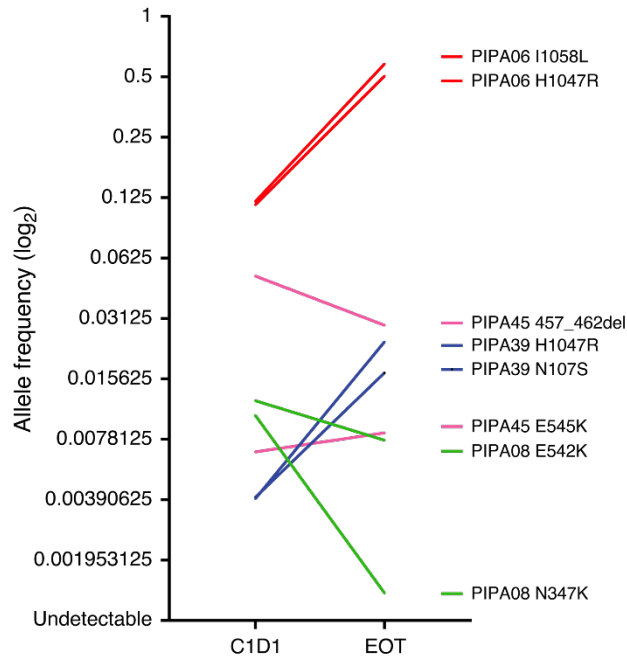


Figure 43. Double *PIK3CA* mutation allele frequencies dynamics for patients with at least 1 read in any both timepoints (N=4) represented in a log₂ scale. C1D1= Cycle 1 Day 1, EOT= End of treatment.

In part B1 (*PIK3CA*-mt ER+ve/HER2-ve breast cancer), 3 of 16 (19%) evaluable sequenced patients had double *PIK3CA* mutations. PFS was shorter for double vs single *PIK3CA* mutants (median PFS 2.7 vs 8.5m respectively HR 663.5, 95% CI 28.8-15286, p<0.0001, Log-rank test) (**figure 44**).

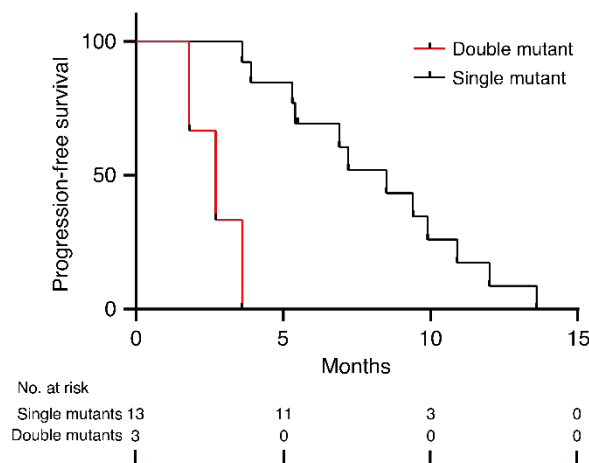


Figure 44. Kaplan-Meier curves for patients in part B1 stratified as double vs single *PIK3CA*-mutant (N=16). Median PFS 2.7 vs 8.5m, respectively. p<0.0001, log-rank test.

Most breast cancer patients enrolled in the trial had received prior AI (84%), and *ESR1* mutations appearing as a result of such exposure has been associated with poor outcomes. In total, 13 out of 23 (57%) patients had an *ESR1* mutation at any sequenced timepoint, with 3/13 (23%) patients harboring polyclonal mutations. Baseline landscape showed predominance of mutations arising in the ligand-binding domain (LBD), as predicted (**figure 45**).

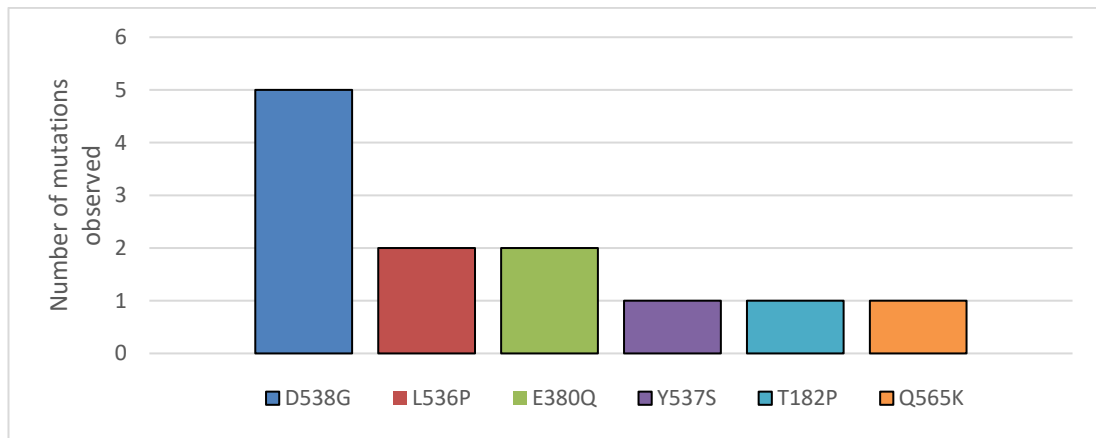


Figure 45. *ESR1* status at baseline (N=23) using RMH200 panel.

Interestingly, acquired Y537S (c.1610A>C) and Y537C (c.1610A>G) mutations were identified at EOT in two patients, matching prior knowledge that these particular mutations are frequently acquired as a result of fulvestrant exposure.

In addition, there was evidence of *ESR1* mutation deselection in both a single mutant and double mutant patient (**figure 46**).

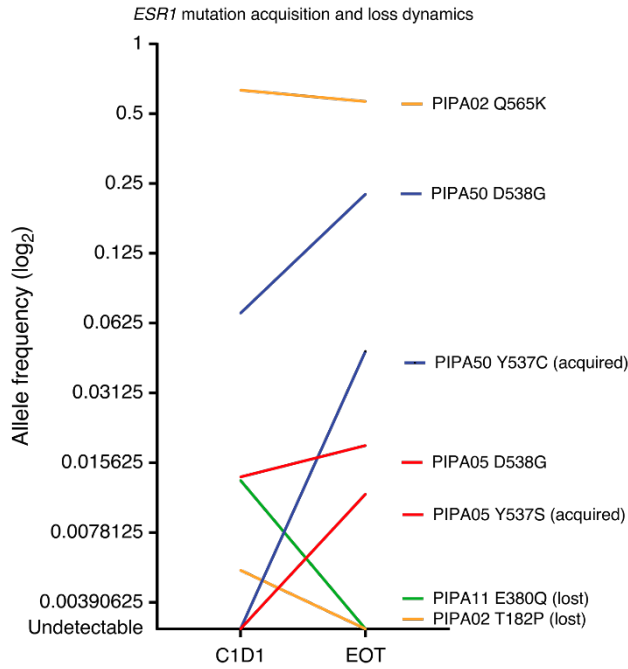


Figure 46. *ESR1* mutation allele frequencies dynamics with frequent acquisition and loss of *ESR1* mutations. Evidence of a second Y537S and Y537C acquisition, loss of T182P in a double mutant patient and loss of E380Q in a single mutant patient.

Among the evaluable *PIK3CA*-mt ER+ve/HER2-ve breast cancer patients sequenced in part B1, 11/16 (69%) had an *ESR1* mutation. PFS was not significantly different for patients with *ESR1* mutant tumours compared to wild-type (HR 0.35, 95% CI 0.09-1.40, $p=0.13$, log-rank test), but the analysis was underpowered (**figure 47**).

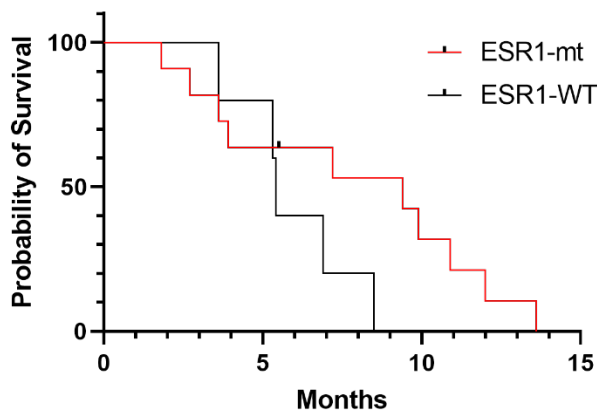


Figure 47. Kaplan-Meier curve representing progression-free survival (PFS) for patients in part B1 stratified as *ESR1* mutant/wild-type. Median PFS 9.4m vs 5.4m, respectively. HR 0.35, 95% CI 0.09-1.40, $p=0.13$, log-rank test.

Overall, 5 of 23 (22%) patients were found to have *FAT1* mutations predicted to be truncating (2 with stop-gains, 3 with nonsynonymous) in any timepoint (**figure 48**), with evidence of one patient acquiring a *FAT1* A1058P missense mutation at EOT (predicted to be truncating using common mutational effect classifier software) that was not present at C1D1 (**figure 49**). Of the two patients harbouring *FAT1* stop-gain mutations, one was an ER+/HER2-ve breast cancer patient treated with the triplet that was censored after 5.5m for compliance, and the second one was an endometrial cancer treated with the doublet that had early progression after only 1.1m of treatment, so unfortunately a survival effect analysis restricted to stop-gain mutations (which are more likely to have produced a truncated non-functional resulting protein) could not be performed.

There was only one *PTEN* and one *RB1* non-synonymous mutation across the 23 patients with paired sequencing and both mutations were shared between C1D1 and EOT timepoints, suggesting acquisitions and losses of these particular genes are probably infrequent. There was no strong evidence for other potential genetic mechanisms of resistance in the paired sequencing.

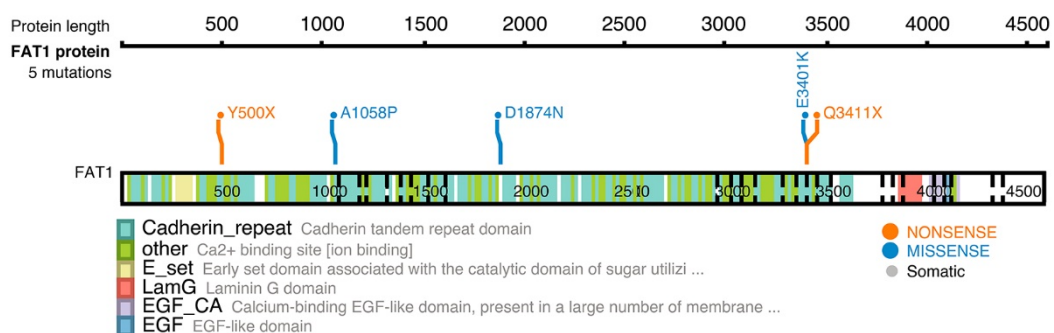


Figure 48. Lollipop diagram for predicted truncating *FAT1* mutations.

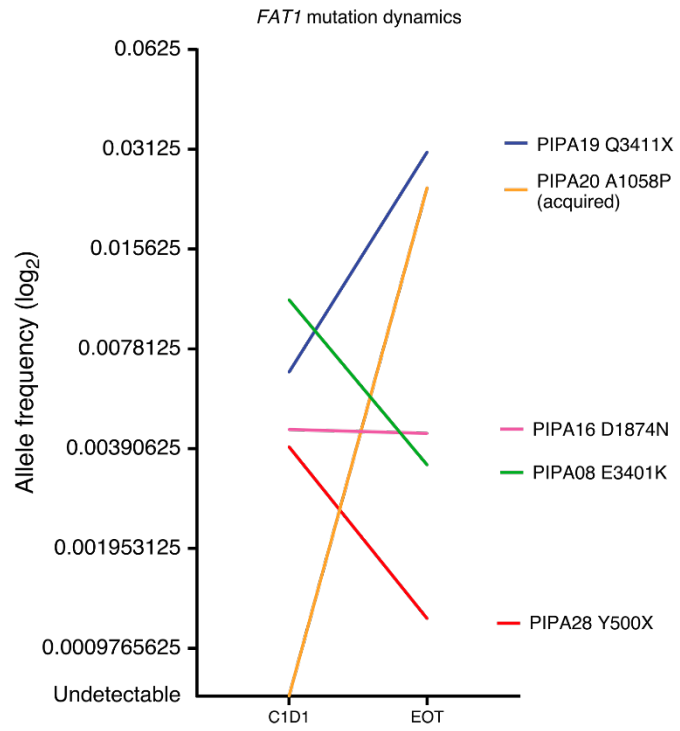


Figure 49. *FAT1* mutation allele frequencies dynamics represented in a log₂ scale. PIPA20 had an acquisition.

5.4 Discussion

A rich longitudinal predictive biomarker work was successfully conducted for this project, using plasma ctDNA as the source of nucleic acids, adding evidence that liquid biopsies can be used to assess early changes in ctDNA abundance and genomic evolution through therapy. The analysis conducted in the PIPA trial further validate the findings from PALOMA-3 and BEECH clinical trials and adds evidence that early ctDNA dynamics could replace other more traditional assessments, with the potential of being implemented as an early prospective biomarker in the context of clinical trials. Patients with *PIK3CA*-mt ER+ve/HER2-ve breast cancer treated with the triplet with poor ctDNA suppression had worse PFS. Overall ctDNA suppression was less pronounced than previous analyses, with only 2 patients having absent (under the technical limit of detection) ctDNA at C2D1. A plausible explanation for this could be time of sampling, with the C2D1 samples in this study taken after at least 1 week-off palbociclib, whereas in prior work on PALOMA-3 samples were taken at C1D15. It is likely that ctDNA rebound occurred during the week “off palbociclib”, and that some element of rebound in ctDNA levels was not fully suppressed by taselesib.

Baseline *PIK3CA* mutation landscape in this study was consistent with multiple prior reports of exon 9 and 20 mutations being the most frequent, and multiple *PIK3CA* mutation rate in our study mirrored prior work [117]. Baseline *ESR1* mutation profile was also consistent with prior reports as all patients within part B1 had been previously exposed to AI. In this study, patients with double *PIK3CA* mutations had shorter PFS on triplet. This contrasts prior data suggesting that patients with multiple *PIK3CA* mutations in *cis* had higher response rates on taselesib at a higher dose [117]. Potentially this may reflect the lower dose of taselesib in the triplet, resulting in incomplete PI3 kinase inhibition in tumours with hyperactive multiple mutations. Another possible explanation is that double *PIK3CA* mutations found in this study could well be in *trans* and therefore result in a different resulting functional consequence. Unfortunately, it is not possible in this study to assess whether the mutations were in *cis* or *trans*, as *PIK3CA*

analysis was conducted in ctDNA and the short DNA fragments of ctDNA preclude such assessment. The only way of confirming the presence of two mutations in the same allele would be by identifying the two mutations in the same read, which would only be possible if they were very close to each other. ctDNA sequencing demonstrated ongoing cancer evolution during triplet combination therapy, with acquisition of a *FAT1* mutation in one patient, selection and loss of a second double *PIK3CA* mutation, and ongoing evolution of *ESR1* mutations. *ESR1* mutations are known to be frequently polyclonal and found at subclonal levels, with this study also confirming this observation and providing additional evidence that *ESR1* mutations frequently evolve through therapy with both acquisitions and losses demonstrated. The findings of this work are also consistent with prior observations that loss of the *FAT1* tumour suppressor promotes CDK4/6 resistance through CDK6 overexpression via the Hippo pathway [69], although the fact that the only acquired *FAT1* mutation was a missense one may limit the interpretation, as it is acknowledged that it may not have a functional impact in the resulting protein despite the truncating effect prediction given by the different software used, because the accuracy of these classifiers is often limited. This study also confirms previous observations that *ESR1* Y537S and Y537C are acquired through fulvestrant therapy [68], likely being a reflection of clonal selection with a survival advantage under treatment. In this study, only 1 of 23 (4.3%) patients was found to have an *RB1* mutation, and this was already present at C1D1, matching previous observation in the PALOMA-3 trial that *RB1* acquisition on palbociclib is a rather uncommon mechanism of resistance [68]. PTEN loss has been found to confer resistance to both CDK4/6 and α -selective PI3K inhibitors [118]. In patients sequenced with the RMH200 panel within this study, there was no evidence of acquired inactivating *PTEN* mutations that would have suggested bypass PI3K β activation [18], which was hypothesized as a possible mechanism of resistance in this study, given the fact that patients had received a β -sparing PI3K inhibition. No further mechanisms of resistance were identified with plasma sequencing.

Chapter 6. Conclusions

This study represents a modern clinical trial design where both clinical and translational endpoints were pre-planned and prospective biological samples were taken for this purpose. PIPA is the first clinical trial reporting full data on safety and exploratory efficacy of the triplet combination of CDK4/6, PI3K and ER signalling inhibition in breast cancer patients, as well as the first to provide data on palbociclib plus taselesib in a range of different *PIK3CA*-mutant solid tumours. The safety profile shown in patients receiving palbociclib 125mg 3-week on/1-week off in combination with taselesib 2mg daily is consistent with prior studies investigating palbociclib or taselesib in combination with fulvestrant [31, 119]. Myelosuppression is common in patients receiving CDK4/6 inhibitors as a result of a cytostatic effect. In this study, neutropenia levels are comparable to what had been reported in PALOMA-3 (88% vs 78.8%), although a higher degree of thrombocytopenia was found (57% vs 19.4%). Mucositis/stomatitis, diarrhoea and hyperglycaemia are common PI3K on-target AEs having led to frequent dose reductions or discontinuation in prior trials investigating both pan- and selective PI3K inhibitors [30, 78, 120, 121]. In this clinical trial, all-grade mucositis/stomatitis and diarrhoea were found at a similar rate to that in the phase 2 trial for taselesib and fulvestrant (38.5% vs 41.7% for mucositis and 38.5% vs 42% for diarrhoea). However, hyperglycaemia does not seem to be appearing at previously reported frequencies when taselesib is given at the 2mg dose.

Pharmacokinetic work performed in samples from patients enrolled in the escalation phase (part A) of this study showed consistent maximum concentration levels of palbociclib and taselesib (when given at the 2mg dose proposed for the RDP2) when compared with historical controls of their respective single agent studies, although in particular for taselesib the number of patients enrolled in the comparable cohorts was rather small, and therefore this data should be handled with caution. The samples tested in the expansion phase (part B) were very limited, however no drug interactions for the combination were noticed. Nonetheless, the safety profile shown across

all patients enrolled in the study strongly suggests that toxicities expected to be associated with taselesib were definitely not higher in frequency when given in combination with palbociclib.

Regardless of the dose reduction required for taselesib, there was pharmacodynamical evidence of target inhibition at this dose, as demonstrated by AKT pathway modulation in PRP taken at 4 hours post-dose on C1D1 and at 6-8h post-dose on C1D15. The increased AKT phosphorylation in PRP at 24h post dose (C1D8 pre-dose) suggests a rebound of PI3K pathway activation and highlights the fact that further development of triplet combinations with alternative PI3K or AKT inhibitors may maximise the potential of such triplet therapy by optimising PI3K-AKT pathway suppression.

In terms of efficacy, an objective response rate of 37.5% was shown for *PIK3CA* mutant ER-positive HER2-negative breast cancer patients treated with the triplet combination of palbociclib, taselesib and fulvestrant (part B1). This result is encouraging, as it compares favourably to the pivotal study for palbociclib and fulvestrant PALOMA-3 (37.5% vs 23% for patients with measurable disease). The response rate is also higher than found in the phase III trial for the doublet combination of taselesib plus fulvestrant (37.5% vs 28%).

Taselesib may well not be the ideal PI3K inhibitor to test forward for future triplet combinations though, as it has only shown a minor clinical benefit compared to current standard treatment when tested in large randomized trials [34], and the incomplete PI3K-pathway inhibition throughout the whole cycle seen in pharmacodynamics analyses suggests the overall efficacy could be even further limited as a result of the dose reduction required for triplet combinations. Also, taselesib might not be specific enough. Other triplet combinations have been explored in early-phase clinical trials using the pan-PI3K inhibitor buparlisib or the α -selective PI3K inhibitor alpelisib in combination with the CDK4/6 inhibitor ribociclib and the ER-degrader fulvestrant, but unfortunately this combination had to be stopped prematurely

due to elevated rates of rash that were clinically incompatible with long-term dosing, also with frequent diarrhoea, vomiting, increased liver function tests and hyperglycaemia [122]. Triplet combinations involving the mTOR inhibitor everolimus have shown proof of manageable safety but preliminary efficacy suggests only modest efficacy potentially limiting further development of this strategy [123]. Moreover, initial data suggests favourable toxicity for triplet combinations including the dual mTOR/PI3K inhibitor gedatolisib [124], but full reports are not yet available. Perhaps a more refined triplet combination will need to be designed once more specific α -selective PI3K inhibitors are developed or alternatively interchanging the PI3K inhibitor compound for a less toxic AKT inhibitor, with initial reports showing favourable safety profile [125]. In line with this, the phase 1b/3 trial IPATunity150 is testing the combination of the AKT inhibitor ipatasertib plus palbociclib plus fulvestrant versus placebo plus palbociclib plus fulvestrant in metastatic ER+ve HER2-ve breast cancer patients who have previously progressed on ET (NCT04060862).

Current standard of care for *PIK3CA* mutant ER-positive HER2-negative breast cancer patients who do not relapse on AI, is sequential doublets of AI plus CDK4/6 followed by fulvestrant plus PI3 kinase inhibition with alpelisib at progression, with phase 2 reports now confirming that the efficacy of the PI3K inhibition is maintained even after CDK4/6 inhibitor progression [126]. In this setting, a triplet combination will need to be assessed against the sequential therapy approach, however a triplet therapy is likely more relevant in the context of relapse on AI, where fulvestrant plus CDK4/6 inhibition is standard, and there is no clear role for subsequent alpelisib.

The trial included a small number of other breast cancer subtypes and an additional heterogeneous small group of solid tumours with pathway aberrations. Whilst the primary endpoint of establishing MTD and safety for the combination was met, the small numbers preclude any robust efficacy analysis. However, out of the seven TNBC patients treated with the doublet there was one confirmed RECIST 1.1 response and two long-term stabilizations, suggesting that a non-chemotherapy strategy for these

patients is an approach that will need to be further explored. These patients were characterized by high AR expression, which correlates with *in vitro* studies showing higher sensitivity to palbociclib in LAR TNBC [39], and adds evidence of LAR subtypes being enriched for *PIK3CA* mutations [127]. Although no objective responses were identified in the solid tumour cohort, there were some disease stabilizations in this heavily pre-treated population, with a CBR of 16.7%.

The Molecular Oncology Lab in the Institute of Cancer Research had previously led the biomarker studies for the combination of palbociclib and fulvestrant. Following this body of work, a pre-planned rich biomarker set of experiments were conducted here. In summary, this study suggests that biomarkers of CDK4/6 inhibitor plus ET resistance may also predict relative resistance to triplet combinations.

Results of this work match the already existing controversy over the value of cyclin D1 overexpression or amplification as a prognostic factor in breast cancer, with studies both showing overall better and worse prognosis [61, 62]. Moreover, its value as predictor of benefit in palbociclib-based trials has remained elusive [114, 128, 129]. In this study, neither cyclin D1 protein expression nor *CCND1* amplification assessed via FISH were found to predict for efficacy on triplet combination. Interestingly there was an evident discordance between FISH amplifications and copy number gains assessed via ulWGS, with a possible explanation being the fact that low-level polysomy can be difficult to assess using FISH assays and it might have limited the findings. Larger datasets will have to be used for proper correlation analysis between fluorescence and sequencing-based approaches to measure gene amplification.

The differences in outcomes found here when selecting patients with high or low baseline cyclin E1 expression, add evidence to previous findings on high cyclin E expression levels conferring resistance to palbociclib in pre-clinical models [38], and high mRNA levels of cyclin E1 conferring relative resistance to palbociclib for patients enrolled in PALOMA-3 [63]. The PFS was also very similar between groups of both trials. However, further confirmation that

cyclin E1 IHC assays can be clinically implemented as a selection tool are needed, and this will likely need to be assessed in independent large, randomized trials.

ER and/or PR positivity are the only well-established biomarkers predicting sensitivity to ET, and combination strategies for ER-positive breast cancer patients normally include an oestrogen deprivation component. There are however known biomarkers known to confer resistance to oestrogen deprivation like *ESR1* mutations appearing as a result of previous AI exposure [72], or activation of the PI3K/AKT/PTEN-pathway through promotion of both dependent and independent ER transcription [130-132]. Patients sequenced in this study display a similar landscape of baseline *ESR1* mutations as expected, with evidence of Y537C and Y537S acquisition under treatment. These acquisitions had been previously identified in work carried in patients in the PALOMA-3 trial, likely as a result of fulvestrant exposure [68], and this study provides additional evidence. Other potential biomarkers like loss of *RB1* function have been previously proposed as resistance mechanism for palbociclib, but prior work had shown that this is a very uncommon biological event [68]. This study also failed to demonstrate any *RB1* loss of function mutations acquired through triplet therapy.

PI3K-inhibition sensitivity has been shown to be enhanced in patients with *PIK3CA* activating mutations and deletions [80], with increased activity observed in patients with multiple mutations in *cis* [117]. In PIPA, 22% of sequenced patients were identified as having double *PIK3CA* mutations. Conversely, patients harbouring double mutations did worse on triplet therapy, suggesting that location of such double mutations might have an impact in drug sensitivity, but it also suggests that the PI3K inhibitor dose of 2mg used in this trial might have been insufficient to fully suppress a hyper-activated PI3K signalling pathway in these double mutant patients. PI3K inhibitors resistance has been shown to arise following PTEN loss through a proposed hyperactivation of PI3K β [18], but no acquired *PTEN* loss of function mutation was identified amongst patients treated with the triplet, suggesting this mechanism is probably uncommon at the genomic level, but

the possibility of loss of function at the protein level identified via IHC remains unanswered.

Finally, this study provides new and adds evidence that supports the use of early ctDNA changes as a measure of treatment efficacy. Both allele frequency and mutant copies/ml had been explored and found to predict treatment efficacy in other settings [56, 57]. This study replicates such findings, and it is worth highlighting that *PIK3CA* mutations were specifically measured, providing a good rationale for the identified predictive value.

In conclusion, this work demonstrates safe and manageable toxicity in solid tumours for the combination of palbociclib and taselesib with or without the addition of endocrine therapy. Data also suggests promising efficacy for the fulvestrant triplet combination in previously treated patients with *PIK3CA* mutant ER-positive HER2-negative metastatic breast cancer patients, with pharmacodynamic evidence of target modulation at the recommended combination doses. The study further supports high expression of cyclin E1 as a poor prognostic marker on palbociclib combinations and reinforce the evidence of early ctDNA changes predicting treatment efficacy. These findings provide preliminary proof-of-concept that support future combination approaches involving more potent and selective PI3K and cyclin-dependent pathway inhibitors.

References

1. Hanahan D, Weinberg RA. The hallmarks of cancer. *Cell* 2000; 100: 57-70.
2. Malumbres M, Barbacid M. Cell cycle, CDKs and cancer: a changing paradigm. *Nature Reviews Cancer* 2009; 9: 153.
3. Musgrove EA, Caldon CE, Barraclough J et al. Cyclin D as a therapeutic target in cancer. *Nature Reviews Cancer* 2011; 11: 558.
4. Kastan MB, Bartek J. Cell-cycle checkpoints and cancer. *Nature* 2004; 432: 316-323.
5. Rathkopf D, Dickson MA, Feldman DR et al. Phase I Study of Flavopiridol with Oxaliplatin and Fluorouracil/Leucovorin in Advanced Solid Tumors. *Clinical Cancer Research* 2009; 15: 7405.
6. Schwartz GK, O'Reilly E, Ilson D et al. Phase I Study of the Cyclin-Dependent Kinase Inhibitor Flavopiridol in Combination With Paclitaxel in Patients With Advanced Solid Tumors. *Journal of Clinical Oncology* 2002; 20: 2157-2170.
7. Senderowicz AM, Headlee D, Stinson SF et al. Phase I trial of continuous infusion flavopiridol, a novel cyclin-dependent kinase inhibitor, in patients with refractory neoplasms. *Journal of Clinical Oncology* 1998; 16: 2986-2999.
8. Benson C, White J, Bono JD et al. A phase I trial of the selective oral cyclin-dependent kinase inhibitor seliciclib (CYC202; R-Roscovitine), administered twice daily for 7 days every 21 days. *British Journal of Cancer* 2007; 96: 29-37.
9. Asghar U, Witkiewicz AK, Turner NC, Knudsen ES. The history and future of targeting cyclin-dependent kinases in cancer therapy. *Nat Rev Drug Discov* 2015; 14: 130-146.
10. Thibault S, Hu W, Hirakawa B et al. Intestinal Toxicity in Rats Following Administration of CDK4/6 Inhibitors Is Independent of Primary Pharmacology. *Molecular Cancer Therapeutics* 2019; 18: 257.
11. Fry DW, Harvey PJ, Keller PR et al. Specific inhibition of cyclin-dependent kinase 4/6 by PD 0332991 and associated antitumor activity in human tumor xenografts. *Molecular Cancer Therapeutics* 2004; 3: 1427.
12. Dean JL, McClendon AK, Hickey TE et al. Therapeutic response to CDK4/6 inhibition in breast cancer defined by ex vivo analyses of human tumors. *Cell cycle (Georgetown, Tex.)* 2012; 11: 2756-2761.
13. Turner NC, Ro J, André F et al. Palbociclib in Hormone-Receptor-Positive Advanced Breast Cancer. *New England Journal of Medicine* 2015; 373: 209-219.
14. Finn RS, Martin M, Rugo HS et al. Palbociclib and Letrozole in Advanced Breast Cancer. *New England Journal of Medicine* 2016; 375: 1925-1936.
15. Fruman DA, Chiu H, Hopkins BD et al. The PI3K Pathway in Human Disease. *Cell* 2017; 170: 605-635.
16. Comprehensive molecular portraits of human breast tumours. *Nature* 2012; 490: 61-70.

17. Tate JG, Bamford S, Jubb HC et al. COSMIC: the Catalogue Of Somatic Mutations In Cancer. *Nucleic Acids Research* 2018; 47: D941-D947.
18. Juric D, Castel P, Griffith M et al. Convergent loss of PTEN leads to clinical resistance to a PI(3)Kalpha inhibitor. *Nature* 2015; 518: 240-244.
19. Kofuji S, Kimura H, Nakanishi H et al. INPP4B Is a PtdIns(3,4,5)P₃ Phosphatase That Can Act as a Tumor Suppressor. *Cancer Discovery* 2015; 5: 730-739.
20. Fedele CG, Ooms LM, Ho M et al. Inositol polyphosphate 4-phosphatase II regulates PI3K/Akt signaling and is lost in human basal-like breast cancers. *Proceedings of the National Academy of Sciences of the United States of America* 2010; 107: 22231-22236.
21. Ooms LM, Binge LC, Davies EM et al. The Inositol Polyphosphate 5-Phosphatase PIPP Regulates AKT1-Dependent Breast Cancer Growth and Metastasis. *Cancer Cell* 2015; 28: 155-169.
22. Asleh-Aburaya K, Sheffield BS, Kos Z et al. Basal biomarkers nestin and INPP4b identify intrinsic subtypes accurately in breast cancers that are weakly positive for oestrogen receptor. *Histopathology* 2017; 70: 185-194.
23. Liu H, Paddock MN, Wang H et al. The INPP4B Tumor Suppressor Modulates EGFR Trafficking and Promotes Triple Negative Breast Cancer. *Cancer Discovery* 2020; CD-19-1262.
24. Gasser JA, Inuzuka H, Lau AW et al. SGK3 mediates INPP4B-dependent PI3K signaling in breast cancer. *Mol Cell* 2014; 56: 595-607.
25. Malik N, Macartney T, Hornberger A et al. Mechanism of activation of SGK3 by growth factors via the Class 1 and Class 3 PI3Ks. *Biochem J* 2018; 475: 117-135.
26. Janku F, Yap TA, Meric-Bernstam F. Targeting the PI3K pathway in cancer: are we making headway? *Nature Reviews Clinical Oncology* 2018; 15: 273.
27. Baselga J, Campone M, Piccart M et al. Everolimus in Postmenopausal Hormone-Receptor-Positive Advanced Breast Cancer. *New England Journal of Medicine* 2012; 366: 520-529.
28. Baselga J, Im S-A, Iwata H et al. Buparlisib plus fulvestrant versus placebo plus fulvestrant in postmenopausal, hormone receptor-positive, HER2-negative, advanced breast cancer (BELLE-2): a randomised, double-blind, placebo-controlled, phase 3 trial. *The Lancet Oncology* 2017; 18: 904-916.
29. Juric D, Krop I, Ramanathan RK et al. Phase I Dose-Escalation Study of Taselisib, an Oral PI3K Inhibitor, in Patients with Advanced Solid Tumors. *Cancer Discov* 2017; 7: 704-715.
30. Dickler MN, Saura C, Richards DA et al. Phase II Study of Taselisib (GDC-0032) in Combination with Fulvestrant in Patients with HER2-Negative, Hormone Receptor-Positive Advanced Breast Cancer. *Clinical Cancer Research* 2018; 24: 4380.
31. Dent S, Cortés J, Im YH et al. Phase III randomized study of tasiselisib or placebo with fulvestrant in estrogen receptor-positive, PIK3CA-mutant, HER2-negative, advanced breast cancer: the SANDPIPER trial. *Annals of Oncology* 2021; 32: 197-207.
32. Baird RD, van Rossum AG, Oliveira M et al. POSEIDON phase 1b results: safety, efficacy and ctDNA response of tasiselisib combined with

tamoxifen in hormone receptor positive metastatic breast cancer patients. *Clinical Cancer Research* 2019; clincanres.0508.2019.

33. Saura C, Hlauschek D, Oliveira M et al. Neoadjuvant letrozole plus taselisib versus letrozole plus placebo in postmenopausal women with oestrogen receptor-positive, HER2-negative, early-stage breast cancer (LORELEI): a multicentre, randomised, double-blind, placebo-controlled, phase 2 trial. *The Lancet Oncology* 2019; 20: 1226-1238.

34. André F, Ciruelos E, Rubovszky G et al. Alpelisib for PIK3CA-Mutated, Hormone Receptor-Positive Advanced Breast Cancer. *New England Journal of Medicine* 2019; 380: 1929-1940.

35. Rugo HS, Lerebours F, Ciruelos E et al. Alpelisib (ALP) + fulvestrant (FUL) in patients (pts) with PIK3CA-mutated (mut) hormone receptor-positive (HR+), human epidermal growth factor receptor 2-negative (HER2-) advanced breast cancer (ABC) previously treated with cyclin-dependent kinase 4/6 inhibitor (CDKi) + aromatase inhibitor (AI): BYLieve study results. *Journal of Clinical Oncology* 2020; 38: 1006-1006.

36. Vora SR, Juric D, Kim N et al. CDK 4/6 inhibitors sensitize PIK3CA mutant breast cancer to PI3K inhibitors. *Cancer Cell* 2014; 26: 136-149.

37. Bosch A, Li Z, Bergamaschi A et al. PI3K inhibition results in enhanced estrogen receptor function and dependence in hormone receptor-positive breast cancer. *Science Translational Medicine* 2015; 7: 283ra251.

38. Herrera-Abreu MT, Palafox M, Asghar U et al. Early Adaptation and Acquired Resistance to CDK4/6 Inhibition in Estrogen Receptor-Positive Breast Cancer. *Cancer Res* 2016; 76: 2301-2313.

39. Asghar US, Barr AR, Cutts R et al. Single-Cell Dynamics Determines Response to CDK4/6 Inhibition in Triple-Negative Breast Cancer. *Clin Cancer Res* 2017; 23: 5561-5572.

40. Lehmann BD, Bauer JA, Chen X et al. Identification of human triple-negative breast cancer subtypes and preclinical models for selection of targeted therapies. *The Journal of Clinical Investigation* 2011; 121: 2750-2767.

41. Traina TA, Miller K, Yardley DA et al. Enzalutamide for the Treatment of Androgen Receptor-Expressing Triple-Negative Breast Cancer. *Journal of Clinical Oncology* 2018; 36: 884-890.

42. Bonnefoi H, Grellety T, Tredan O et al. A phase II trial of abiraterone acetate plus prednisone in patients with triple-negative androgen receptor positive locally advanced or metastatic breast cancer (UCBG 12-1). *Annals of Oncology* 2016; 27: 812-818.

43. Liu C-Y, Lau K-Y, Hsu C-C et al. Combination of palbociclib with enzalutamide shows in vitro activity in RB proficient and androgen receptor positive triple negative breast cancer cells. *PloS one* 2017; 12: e0189007-e0189007.

44. Bonelli MA, Digiacoimo G, Fumarola C et al. Combined Inhibition of CDK4/6 and PI3K/AKT/mTOR Pathways Induces a Synergistic Anti-Tumor Effect in Malignant Pleural Mesothelioma Cells. *Neoplasia* 2017; 19: 637-648.

45. Wang Y, Li X, Liu X et al. Simultaneous inhibition of PI3K α and CDK4/6 synergistically suppresses KRAS-mutated non-small cell lung cancer. *Cancer Biol Med* 2019; 16: 66-83.

46. Jahr S, Hentze H, Englisch S et al. DNA fragments in the blood plasma of cancer patients: quantitations and evidence for their origin from apoptotic and necrotic cells. *Cancer Res* 2001; 61: 1659-1665.
47. Moss J, Magenheim J, Neiman D et al. Comprehensive human cell-type methylation atlas reveals origins of circulating cell-free DNA in health and disease. *Nature Communications* 2018; 9: 5068.
48. Mouliere F, Chandrananda D, Piskorz AM et al. Enhanced detection of circulating tumor DNA by fragment size analysis. *Science translational medicine* 2018; 10: eaat4921.
49. Diehl F, Schmidt K, Choti MA et al. Circulating mutant DNA to assess tumor dynamics. *Nature Medicine* 2008; 14: 985-990.
50. Bettegowda C, Sausen M, Leary RJ et al. Detection of circulating tumor DNA in early- and late-stage human malignancies. *Science translational medicine* 2014; 6: 224ra224-224ra224.
51. Dawson S-J, Tsui DWY, Murtaza M et al. Analysis of Circulating Tumor DNA to Monitor Metastatic Breast Cancer. *New England Journal of Medicine* 2013; 368: 1199-1209.
52. Olsson E, Winter C, George A et al. Serial monitoring of circulating tumor DNA in patients with primary breast cancer for detection of occult metastatic disease. *EMBO Mol Med* 2015; 7: 1034-1047.
53. Garcia-Murillas I, Schiavon G, Weigelt B et al. Mutation tracking in circulating tumor DNA predicts relapse in early breast cancer. *Sci Transl Med* 2015; 7: 302ra133.
54. Turner NC, Kingston B, Kilburn LS et al. Circulating tumour DNA analysis to direct therapy in advanced breast cancer (plasmaMATCH): a multicentre, multicohort, phase 2a, platform trial. *The Lancet Oncology*.
55. Garcia-Murillas I, Chopra N, Comino-Méndez I et al. Assessment of Molecular Relapse Detection in Early-Stage Breast Cancer. *JAMA Oncology* 2019; 5: 1473-1478.
56. O'Leary B, Hrebien S, Morden JP et al. Early circulating tumor DNA dynamics and clonal selection with palbociclib and fulvestrant for breast cancer. *Nat Commun* 2018; 9: 896.
57. Hrebien S, Citi V, Garcia-Murillas I et al. Early ctDNA dynamics as a surrogate for progression-free survival in advanced breast cancer in the BEECH trial. *Annals of Oncology* 2019; 30: 945-952.
58. Coakley M, Garcia-Murillas I, Turner NC. Molecular residual disease and adjuvant trials design in solid tumors. *Clinical Cancer Research* 2019; clincanres.0152.2019.
59. Barra GB, Santa Rita TH, de Almeida Vasques J et al. EDTA-mediated inhibition of DNases protects circulating cell-free DNA from ex vivo degradation in blood samples. *Clin Biochem* 2015; 48: 976-981.
60. Abbosh C, Swanton C, Birkbak NJ. Clonal haematopoiesis: a source of biological noise in cell-free DNA analyses. *Annals of Oncology* 2019; 30: 358-359.
61. van Diest PJ, Michalides RJ, Jannink L et al. Cyclin D1 expression in invasive breast cancer. Correlations and prognostic value. *The American journal of pathology* 1997; 150: 705-711.
62. Ortiz AB, Garcia D, Vicente Y et al. Prognostic significance of cyclin D1 protein expression and gene amplification in invasive breast carcinoma. *PLoS One* 2017; 12: e0188068.

63. Turner NC, Liu Y, Zhu Z et al. Cyclin E1 Expression and Palbociclib Efficacy in Previously Treated Hormone Receptor–Positive Metastatic Breast Cancer. *Journal of Clinical Oncology* 2019; JCO.18.00925.
64. Weintraub SJ, Chow KNB, Luo RX et al. Mechanism of active transcriptional repression by the retinoblastoma protein. *Nature* 1995; 375: 812-816.
65. Weintraub SJ, Prater CA, Dean DC. Retinoblastoma protein switches the E2F site from positive to negative element. *Nature* 1992; 358: 259-261.
66. Sellers WR, Rodgers JW, Kaelin WG, Jr. A potent transrepression domain in the retinoblastoma protein induces a cell cycle arrest when bound to E2F sites. *Proceedings of the National Academy of Sciences of the United States of America* 1995; 92: 11544-11548.
67. Condorelli R, Spring L, O'Shaughnessy J et al. Polyclonal RB1 mutations and acquired resistance to CDK 4/6 inhibitors in patients with metastatic breast cancer. *Ann Oncol* 2018; 29: 640-645.
68. O'Leary B, Cutts RJ, Liu Y et al. The genetic landscape and clonal evolution of breast cancer resistance to palbociclib plus fulvestrant in the PALOMA-3 trial. *Cancer Discovery* 2018; CD-18-0264.
69. Li Z, Razavi P, Li Q et al. Loss of the FAT1 Tumor Suppressor Promotes Resistance to CDK4/6 Inhibitors via the Hippo Pathway. *Cancer Cell* 2018; 34: 893-905.e898.
70. Toy W, Shen Y, Won H et al. ESR1 ligand-binding domain mutations in hormone-resistant breast cancer. *Nat Genet* 2013; 45: 1439-1445.
71. Robinson DR, Wu YM, Vats P et al. Activating ESR1 mutations in hormone-resistant metastatic breast cancer. *Nat Genet* 2013; 45: 1446-1451.
72. Fribbens C, O'Leary B, Kilburn L et al. Plasma ESR1 Mutations and the Treatment of Estrogen Receptor-Positive Advanced Breast Cancer. *J Clin Oncol* 2016; 34: 2961-2968.
73. Isakoff SJ, Engelman JA, Irie HY et al. Breast cancer-associated PIK3CA mutations are oncogenic in mammary epithelial cells. *Cancer Res* 2005; 65: 10992-11000.
74. Zhao JJ, Gjoerup OV, Subramanian RR et al. Human mammary epithelial cell transformation through the activation of phosphatidylinositol 3-kinase. *Cancer Cell* 2003; 3: 483-495.
75. Koboldt DC, Fulton RS, McLellan MD et al. Comprehensive molecular portraits of human breast tumours. *Nature* 2012; 490: 61-70.
76. Razavi P, Chang MT, Xu G et al. The Genomic Landscape of Endocrine-Resistant Advanced Breast Cancers. *Cancer Cell* 2018; 34: 427-438.e426.
77. Shah SP, Roth A, Goya R et al. The clonal and mutational evolution spectrum of primary triple-negative breast cancers. *Nature* 2012; 486: 395.
78. Baselga J, Dent SF, Cortés J et al. Phase III study of taselelisib (GDC-0032) + fulvestrant (FULV) v FULV in patients (pts) with estrogen receptor (ER)-positive, PIK3CA-mutant (MUT), locally advanced or metastatic breast cancer (MBC): Primary analysis from SANDPIPER. *Journal of Clinical Oncology* 2018; 36: LBA1006-LBA1006.
79. Juric D, Janku F, Rodón J et al. Alpelisib Plus Fulvestrant in PIK3CA-Altered and PIK3CA-Wild-Type Estrogen Receptor–Positive Advanced Breast Cancer: A Phase 1b Clinical Trial Alpelisib Plus Fulvestrant in PIK3CA-Altered and PIK3CA-Wild-Type Estrogen Receptor–Positive Breast

Cancer Alpelisib Plus Fulvestrant in PIK3CA-Altered and PIK3CA-Wild-Type Estrogen Receptor-Positive Breast Cancer. *JAMA Oncology* 2019; 5: e184475-e184475.

80. Croessmann S, Sheehan JH, Lee KM et al. PIK3CA C2 Domain Deletions Hyperactivate Phosphoinositide 3-kinase (PI3K), Generate Oncogene Dependence, and Are Exquisitely Sensitive to PI3Kalpha Inhibitors. *Clin Cancer Res* 2018; 24: 1426-1435.

81. Stambolic V, Suzuki A, de la Pompa JL et al. Negative Regulation of PKB/Akt-Dependent Cell Survival by the Tumor Suppressor PTEN. *Cell* 1998; 95: 29-39.

82. Jia S, Liu Z, Zhang S et al. Essential roles of PI(3)K-p110 β in cell growth, metabolism and tumorigenesis. *Nature* 2008; 454: 776-779.

83. Irie HY, Pearline RV, Grueneberg D et al. Distinct roles of Akt1 and Akt2 in regulating cell migration and epithelial-mesenchymal transition. *The Journal of Cell Biology* 2005; 171: 1023-1034.

84. Carpten JD, Faber AL, Horn C et al. A transforming mutation in the pleckstrin homology domain of AKT1 in cancer. *Nature* 2007; 448: 439-444.

85. Ihle NT, Lemos R, Jr., Wipf P et al. Mutations in the phosphatidylinositol-3-kinase pathway predict for antitumor activity of the inhibitor PX-866 whereas oncogenic Ras is a dominant predictor for resistance. *Cancer Res* 2009; 69: 143-150.

86. Gowan SM, Hardcastle A, Hallsworth AE et al. Application of Meso Scale Technology for the Measurement of Phosphoproteins in Human Tumor Xenografts. *ASSAY and Drug Development Technologies* 2007; 5: 391-402.

87. Yap TA, Yan L, Patnaik A et al. Interrogating Two Schedules of the AKT Inhibitor MK-2206 in Patients with Advanced Solid Tumors Incorporating Novel Pharmacodynamic and Functional Imaging Biomarkers. *Clinical Cancer Research* 2014; 20: 5672-5685.

88. Eisenhauer EA, Therasse P, Bogaerts J et al. New response evaluation criteria in solid tumours: revised RECIST guideline (version 1.1). *Eur J Cancer* 2009; 45: 228-247.

89. Pascual J, Lim JSJ, Macpherson IR et al. Triplet Therapy with Palbociclib, Taselisib, and Fulvestrant in PIK3CA-Mutant Breast Cancer and Doublet Palbociclib and Taselisib in Pathway-Mutant Solid Cancers. *Cancer Discovery* 2021; 11: 92.

90. Adalsteinsson VA, Ha G, Freeman SS et al. Scalable whole-exome sequencing of cell-free DNA reveals high concordance with metastatic tumors. *Nature Communications* 2017; 8: 1324.

91. Hoffman KE, McCarthy EP, Recklitis CJ, Ng AK. Psychological distress in long-term survivors of adult-onset cancer: Results from a national survey. *Archives of Internal Medicine* 2009; 169: 1274-1281.

92. Newman AM, Lovejoy AF, Klass DM et al. Integrated digital error suppression for improved detection of circulating tumor DNA. *Nature Biotechnology* 2016; 34: 547-555.

93. Lai Z, Markovets A, Ahdesmaki M et al. VarDict: a novel and versatile variant caller for next-generation sequencing in cancer research. *Nucleic Acids Research* 2016; 44: e108-e108.

94. Robinson JT, Thorvaldsdóttir H, Winckler W et al. Integrative genomics viewer. *Nature Biotechnology* 2011; 29: 24-26.

95. Wang K, Li M, Hakonarson H. ANNOVAR: functional annotation of genetic variants from high-throughput sequencing data. *Nucleic Acids Research* 2010; 38: e164-e164.
96. Vaser R, Adusumalli S, Leng SN et al. SIFT missense predictions for genomes. *Nature Protocols* 2016; 11: 1-9.
97. Reva B, Antipin Y, Sander C. Predicting the functional impact of protein mutations: application to cancer genomics. *Nucleic Acids Research* 2011; 39: e118-e118.
98. Choi Y, Chan AP. PROVEAN web server: a tool to predict the functional effect of amino acid substitutions and indels. *Bioinformatics* 2015; 31: 2745-2747.
99. Simon R. Optimal two-stage designs for phase II clinical trials. *Control Clin Trials* 1989; 10: 1-10.
100. Cristofanilli M, Turner NC, Bondarenko I et al. Fulvestrant plus palbociclib versus fulvestrant plus placebo for treatment of hormone-receptor-positive, HER2-negative metastatic breast cancer that progressed on previous endocrine therapy (PALOMA-3): final analysis of the multicentre, double-blind, phase 3 randomised controlled trial. *Lancet Oncol* 2016; 17: 425-439.
101. Turner NC, Slamon DJ, Ro J et al. Overall Survival with Palbociclib and Fulvestrant in Advanced Breast Cancer. *New England Journal of Medicine* 2018; 379: 1926-1936.
102. Hortobagyi GN, Stemmer SM, Burris HA et al. Ribociclib as First-Line Therapy for HR-Positive, Advanced Breast Cancer. *New England Journal of Medicine* 2016; 375: 1738-1748.
103. Slamon DJ, Neven P, Chia S et al. Phase III Randomized Study of Ribociclib and Fulvestrant in Hormone Receptor-Positive, Human Epidermal Growth Factor Receptor 2-Negative Advanced Breast Cancer: MONALEESA-3. *J Clin Oncol* 2018; 36: 2465-2472.
104. Goetz MP, Toi M, Campone M et al. MONARCH 3: Abemaciclib As Initial Therapy for Advanced Breast Cancer. *Journal of Clinical Oncology* 2017; 35: 3638-3646.
105. George W, Sledge J, Toi M, Neven P et al. MONARCH 2: Abemaciclib in Combination With Fulvestrant in Women With HR+/HER2- Advanced Breast Cancer Who Had Progressed While Receiving Endocrine Therapy. *Journal of Clinical Oncology* 2017; 35: 2875-2884.
106. Jones SE. Metastatic Breast Cancer: The Treatment Challenge. *Clinical Breast Cancer* 2008; 8: 224-233.
107. Roché H, Vahdat LT. Treatment of metastatic breast cancer: second line and beyond. *Annals of Oncology* 2011; 22: 1000-1010.
108. Park IH, Lee KS, Ro J. Effects of second and subsequent lines of chemotherapy for metastatic breast cancer. *Clin Breast Cancer* 2015; 15: e55-62.
109. Burkhardt DL, Sage J. Cellular mechanisms of tumour suppression by the retinoblastoma gene. *Nat Rev Cancer* 2008; 8: 671-682.
110. Perou CM, Sørlie T, Eisen MB et al. Molecular portraits of human breast tumours. *Nature* 2000; 406: 747-752.
111. Kenny FS, Hui R, Musgrove EA et al. Overexpression of cyclin D1 messenger RNA predicts for poor prognosis in estrogen receptor-positive breast cancer. *Clin Cancer Res* 1999; 5: 2069-2076.

112. Gillett C, Smith P, Gregory W et al. Cyclin D1 and prognosis in human breast cancer. *International Journal of Cancer* 1996; 69: 92-99.
113. Dean JL, Thangavel C, McClendon AK et al. Therapeutic CDK4/6 inhibition in breast cancer: key mechanisms of response and failure. *Oncogene* 2010; 29: 4018-4032.
114. Finn RS, Crown JP, Lang I et al. The cyclin-dependent kinase 4/6 inhibitor palbociclib in combination with letrozole versus letrozole alone as first-line treatment of oestrogen receptor-positive, HER2-negative, advanced breast cancer (PALOMA-1/TRIO-18): a randomised phase 2 study. *The Lancet Oncology* 2015; 16: 25-35.
115. O'Leary B, Cutts RJ, Huang X et al. Circulating Tumor DNA Markers for Early Progression on Fulvestrant With or Without Palbociclib in ER+ Advanced Breast Cancer. *JNCI: Journal of the National Cancer Institute* 2020; 113: 309-317.
116. O'Leary B, Cutts RJ, Liu Y et al. The Genetic Landscape and Clonal Evolution of Breast Cancer Resistance to Palbociclib plus Fulvestrant in the PALOMA-3 Trial. *Cancer Discovery* 2018; 8: 1390-1403.
117. Vasan N, Razavi P, Johnson JL et al. Double *PIK3CA* mutations in cis increase oncogenicity and sensitivity to PI3K α inhibitors. *Science* 2019; 366: 714-723.
118. Costa C, Wang Y, Ly A et al. PTEN Loss Mediates Clinical Cross-Resistance to CDK4/6 and PI3K α Inhibitors in Breast Cancer. *Cancer Discovery* 2020; 10: 72-85.
119. Turner NC, Huang Bartlett C, Cristofanilli M. Palbociclib in Hormone-Receptor-Positive Advanced Breast Cancer. *N Engl J Med* 2015; 373: 1672-1673.
120. Baselga J, Im SA, Iwata H et al. Buparlisib plus fulvestrant versus placebo plus fulvestrant in postmenopausal, hormone receptor-positive, HER2-negative, advanced breast cancer (BELLE-2): a randomised, double-blind, placebo-controlled, phase 3 trial. *Lancet Oncol* 2017; 18: 904-916.
121. Di Leo A, Johnston S, Lee KS et al. Buparlisib plus fulvestrant in postmenopausal women with hormone-receptor-positive, HER2-negative, advanced breast cancer progressing on or after mTOR inhibition (BELLE-3): a randomised, double-blind, placebo-controlled, phase 3 trial. *Lancet Oncol* 2018; 19: 87-100.
122. Tolaney SM, Im Y-H, Calvo E et al. Phase Ib Study of Ribociclib plus Fulvestrant and Ribociclib plus Fulvestrant plus PI3K Inhibitor (Alpelisib or Buparlisib) for HR⁺ Advanced Breast Cancer. *Clinical Cancer Research* 2021; 27: 418-428.
123. Bardia A, Hurvitz SA, DeMichele A et al. Triplet therapy (continuous ribociclib, everolimus, exemestane) in HR+/HER2- advanced breast cancer postprogression on a CDK4/6 inhibitor (TRINITY-1): Efficacy, safety, and biomarker results. *Journal of Clinical Oncology* 2019; 37: 1016-1016.
124. Forero-Torres A, Han H, Dees EC et al. Phase Ib study of gedatolisib in combination with palbociclib and endocrine therapy (ET) in women with estrogen receptor (ER) positive (+) metastatic breast cancer (MBC) (B2151009). *Journal of Clinical Oncology* 2018; 36: 1040-1040.
125. Wander SA, Juric D, Supko JG et al. Phase Ib trial to evaluate safety and anti-tumor activity of the AKT inhibitor, ipatasertib, in combination with endocrine therapy and a CDK4/6 inhibitor for patients with hormone receptor

- positive (HR+)/HER2 negative metastatic breast cancer (MBC) (TAKTIC). *Journal of Clinical Oncology* 2020; 38: 1066-1066.
126. Rugo HS, Lerebours F, Ciruelos E et al. Alpelisib plus fulvestrant in PIK3CA-mutated, hormone receptor-positive advanced breast cancer after a CDK4/6 inhibitor (BYLieve): one cohort of a phase 2, multicentre, open-label, non-comparative study. *The Lancet Oncology* 2021; 22: 489-498.
127. Lehmann BD, Bauer JA, Schafer JM et al. PIK3CA mutations in androgen receptor-positive triple negative breast cancer confer sensitivity to the combination of PI3K and androgen receptor inhibitors. *Breast Cancer Res* 2014; 16: 406.
128. Finn R, Jiang Y, Rugo H et al. Biomarker analyses from the phase 3 PALOMA-2 trial of palbociclib (P) with letrozole (L) compared with placebo (PLB) plus L in postmenopausal women with ER + /HER2- advanced breast cancer (ABC). *Annals of Oncology* 2016; 27.
129. Arnedos M, Cheaib B, Bayar MA et al. Abstract CT041: Anti-proliferative response and predictive biomarkers to palbociclib in early breast cancer: The Preoperative Palbociclib (POP) randomized trial. *Cancer Research* 2016; 76: CT041.
130. Campbell RA, Bhat-Nakshatri P, Patel NM et al. Phosphatidylinositol 3-kinase/AKT-mediated activation of estrogen receptor alpha: a new model for anti-estrogen resistance. *J Biol Chem* 2001; 276: 9817-9824.
131. Creighton CJ, Fu X, Hennessy BT et al. Proteomic and transcriptomic profiling reveals a link between the PI3K pathway and lower estrogen-receptor (ER) levels and activity in ER+ breast cancer. *Breast Cancer Res* 2010; 12: R40.
132. Fu X, Creighton CJ, Biswal NC et al. Overcoming endocrine resistance due to reduced PTEN levels in estrogen receptor-positive breast cancer by co-targeting mammalian target of rapamycin, protein kinase B, or mitogen-activated protein kinase kinase. *Breast Cancer Res* 2014; 16: 430.

Appendix 1. RMH200 panel design

ABL1	all; CNV	IKZF1	all; CNV
ACVR1	3 to 11	IL3RA	CNV only
AKT1	all; CNV	IRF4	all; CNV
AKT2	exon3 (E17K) + CNV	JAK1	all
ALK	19 to 29 +CNV	JAK2	all; CNV
AMER1	all	JAK3	all
ANTXR2	all	KDR	ex6-26
APC		KIT	all; CNV
ARAF	all	KLF2	all
ARID1A	all	KMT2A	all; CNV
ASXL1	all; CNV	KMT2C	all; CNV
ATM	all; CNV	KMT2D	all; CNV
ATRX	all; CNV	KRAS	all; CNV
AURKA	all; CNV	MAP2K1	all
B2M	all	MAP2K4	all
BAP1	all	MAP3K1	all
BCL2	all	MCL1	all
BCOR	all; CNV	MDM2	all; CNV
BIRC3	all; CNV	MEF2B	all
BRAF	all (inc introns8910 tx); CNV	MET	all; CNV
BRCA1	all	MLH1	all
BRCA2	all	MPL	all; CNV
BRIP1	all	MSH2	all
BTK	exon 15 (C481S)	MSH6	all
C19MC	all; CNV	MTOR	exons 28-58
CALR	exon 9	MYC	all; CNV
CARD11	all	MYCL1	all; CNV
CASP8	all	MYCN	all; CNV
CBL	all; CNV	MYD88	exon 5 (L265)
CCND1	all; CNV	NF1	all; CNV
CCND2	all; CNV	NF2	all
CCND3	CNV only	NFE2	all; CNV
CCNE1	all; CNV	NOTCH1	all
CCNE2	all; CNV	NOTCH2	exon 1,2,5,20,30; CNV
CD274	all; CNV	NPM1	exon 10, 11; CNV
CD79b	all; CNV	NRAS	all; CNV
CDH1	all; CNV	NSD1	all; CNV
CDK12	all	PALB2	all; CNV
CDK2	all	PAX5	all; CNV
CDK4	all; CNV	PBRM1	all
CDK6	all; CNV	PDCD1LG2	all; CNV

CDKN2A	all; CNV	PDGFRA	all; CNV
CDKN2B	all; CNV	PHOX2B	all
CDKN2C	all; CNV	PIK3CA	all
CEBPA	all; CNV	PIK3CD	all
CHEK2	all	PIK3R1	all
CIC	all	PLCG2	all
CKDN1B	all; CNV	PMS1	all
CKS1B	all; CNV	PMS2	all
CREBBP	all	POLE	all
CRLF1	CNV only	POT1	all
CSF3R	all; CNV	PRKAR1A	all
CTNNB1	all	PTCH1	all
CUX1	all; CNV	PTCH2	all
CXCR4	all	PTEN	all; CNV
DAXX	all	PTPN11	all; CNV
DDR2	CNV only	RAD21	all; CNV
DDX3X	all	RAD51C	all
DICER1	all	RAD51D	all
DIS3	all; CNV	RAF1	all
DNMT3A	all; CNV	RB1	all; CNV
DROSHA	all	RET	all
EBF1	CNV only	RFN43	all
EGFR	all; CNV	RHOA	all
EP300	all; CNV	RICTOR	CNV only
ERBB2	all; CNV	ROS1	exons 32-43
ERBB3	all; CNV	RUNX1	all; CNV
ESR1	all	SETBP1	all; CNV
ETNK1	all; CNV	SETD2	all
ETV6	all; CNV	SF3B1	all; CNV
EZH2	all; CNV	SH2B3	all
F2R	all; CNV	SMAD2	all; CNV
FADD	all; CNV	SMAD3	all
FAM46C	all; CNV	SMAD4	all
FAT1	all	SMARCA4	all
FBXW7	all; CNV	SMARCB1	all
FGF10	all; CNV	SMARCE1	all
FGFR1	all; CNV	SMO	all
FGFR2	all; CNV	SOX2	all; CNV
FGFR3	all; CNV	SRSF2	all; CNV
FGFR4	all; CNV	STAG2	all; CNV
FLT3	all; CNV	STAT3	all
FOXL2	all; CNV	STAT5B	all
FOXO1	all; CNV	SUFU	all
GATA1	all; CNV	TCF3	all

GATA3	all; CNV	TERT	all; CNV; promoter (-800)
GNA11	exon 5	TET2	all; CNV
GNAQ	exon 5	TFE3	all
GNAS	exon 5	TG	CNV only
H3F3A	all	TP53	all; CNV
H3F3B	all	TP63	CNV only
HIST1H3B	all	TSC1	all
HIST1H3C	all	TSC2	all
HIST2H3C	all	U2AF1	all; CNV
HRAS	all	VHL	all
ID3	all	WT1	all; CNV
IDH1	all; CNV	YAP1	all; CNV
IDH2	all; CNV	YES1	CNV only
IGF1R	all; CNV	ZRSR2	all; CNV

Thanks to

Nick for giving me the opportunity to undertake this work and for being such an inspirational leader, both as a clinician and as a scientist.

The patients and their families who participated in the PIPA trial for their never-dying contribution.

My parents, brother, and sister for their love and for supporting me in this adventure.

Eli, Martín and Julia for making it possible.